




5-2015

Elucidating the Impact of Roseophage on Roseobacter Metabolism and Marine Nutrient Cycles

Nana Yaw Darko Ankrah

University of Tennessee - Knoxville, nankrah@vols.utk.edu

Follow this and additional works at: https://trace.tennessee.edu/utk_graddiss

 Part of the [Bioinformatics Commons](#), [Environmental Microbiology and Microbial Ecology Commons](#), [Marine Biology Commons](#), [Microbial Physiology Commons](#), [Oceanography Commons](#), and the [Virology Commons](#)

Recommended Citation

Ankrah, Nana Yaw Darko, "Elucidating the Impact of Roseophage on Roseobacter Metabolism and Marine Nutrient Cycles. " PhD diss., University of Tennessee, 2015.
https://trace.tennessee.edu/utk_graddiss/3289

This Dissertation is brought to you for free and open access by the Graduate School at TRACE: Tennessee Research and Creative Exchange. It has been accepted for inclusion in Doctoral Dissertations by an authorized administrator of TRACE: Tennessee Research and Creative Exchange. For more information, please contact trace@utk.edu.

To the Graduate Council:

I am submitting herewith a dissertation written by Nana Yaw Darko Ankrah entitled "Elucidating the Impact of Roseophage on Roseobacter Metabolism and Marine Nutrient Cycles." I have examined the final electronic copy of this dissertation for form and content and recommend that it be accepted in partial fulfillment of the requirements for the degree of Doctor of Philosophy, with a major in Microbiology.

Alison Buchan, Major Professor

We have read this dissertation and recommend its acceptance:

Steven W. Wilhelm, Erik R. Zinser, Shawn R. Campagna, Mark A. Radosevich

Accepted for the Council:

Carolyn R. Hodges

Vice Provost and Dean of the Graduate School

(Original signatures are on file with official student records.)

**Elucidating the Impact of Roseophage on Roseobacter Metabolism and Marine Nutrient
Cycles**

**A Dissertation Presented for the
Doctor of Philosophy
Degree
The University of Tennessee, Knoxville**

**Nana Yaw Darko Ankrah
May 2015**

Copyright © 2015 by Nana Yaw Darko Ankrah

All rights reserved.

Dedication

This dissertation is dedicated to my mom, Jemima Olivia Karley Pappoe; daughter, Olivia Karley Ankrah; wife, Victoria Ankrah and Grandma Harriet. This dissertation is also dedicated to the rest of my family, to Nii Oto, Nii Darku, Christopher, Olivia Kotey, Mr. Quarshie, Unlce James, Sis Nana, Ivy, Kuuku, Stephen, Emmanuel, Gloria and all the cousins, nephews and nieces.

Acknowledgements

First of all, I would like to express my strongest gratitude to my advisor, Dr. Alison Buchan, for giving me the opportunity join her lab and for all the personal and professional development I have attained under her tutelage. I would also like to thank all my committee members, Professor Steven Wilhelm, Dr. Erik Zinser, Professor Mark Radosevich and Dr. Shawn Campagna for their intellectual guidance throughout my doctoral degree.

In addition, I would like to extend thanks to lab members, both past and present, for their help and support. I'd like to thank Dr. Charles Budinoff for introducing me to various techniques in microbiology and virology during my first years as a PhD student. I'd also like to thank our lab manager, Mary Hadden, for her assistance with all qPCR assays associated with this dissertation. I'd also like to thank all Buchan lab members; Dr. Chris Gulvik, Dr. Nathan Cude, Ashley Frank, Lauren Mach Quigley, Jonelle Basso, and April Mitchell for being awesome people to work with. I'd also like to thank all the wonderful undergraduates who have contributed immensely to this dissertation in numerous ways: Dan Jones, Chelsi Short (née White), Nikki Szayni, Nathan Bendrieum, Drew Garrone, Kattie Moccia, Will Brading and Yi-Ting Huang.

And last, but in no way the least, I'd like thank my family, my daughter Olivia for staying up with me every night to get this dissertation done, and my wife, Victoria, for being a strong support base and an awesome wife.

Abstract

As the most abundant biological entities in marine environments, viruses are an important component of marine food webs. The activity of viruses contributes significantly to the mortality of marine microorganisms, ultimately influencing biological function and chemical composition of aquatic systems by impacting species composition and flow of carbon, nitrogen and other nutrients. Despite the growing recognition that viral activity contributes to marine biogeochemical cycles, the extent to which virus infection reshapes host metabolism and the effect of this alteration on the composition of host lysate remains poorly understood. Additionally, the degree to which natural bacterioplankton communities metabolise the released lysate material remains an open question. In this study, we use a *Roseobacter* lysogen, *Sulfitobacter* sp. CB2047, and its infecting phage as models to examine phage-host interactions in the marine environment. Specifically, this dissertation investigates the effect of superinfection of *Sulfitobacter* lysogens on resident prophage induction and its effect on accelerating the transfer of genetic material and increasing microbial genetic diversity. This work also characterizes the effect that phage infection has on reshaping host metabolic processes to provide building blocks for the synthesis of new virion particles and how this redirection of host metabolism affects the composition of material released as virus lysate after cell lysis. Finally, this dissertation examines how virus-derived lysates are metabolised by members of the natural bacterioplankton community and how this affects the consuming population's metabolism. Results from our studies indicate that superinfection of *Sulfitobacter* lysogens increases prophage induction ~24-fold and increases *Sulfitobacter* diversity by up to 2%. Our results also indicate that phage infection significantly elevates host metabolism, redirecting ~75% of host resources from energy production to the production of new phage virions. Additionally, our

results demonstrate that viral lysates are rich in small, labile nutrients that are readily utilized by natural bacterioplankton communities, significantly increasing their metabolite pools and nutrient turnover. Overall, this research provides an enhanced framework for understanding the role of marine viruses in shaping microbial genetic diversity and characterizes the impact that virus infections have on redirecting host metabolism as well as the availability and metabolism of nutrients to natural bacterioplankton communities.

Table of Contents

| | |
|--|-----------|
| Chapter 1 Introduction..... | 1 |
| References | 8 |
| Chapter 2 Genomic analysis of the marine bacterium <i>Sulfitobacter</i> sp. CB2047 and its infecting phages ΦCB2047A, B & C | 14 |
| Abstract..... | 16 |
| Introduction..... | 16 |
| Materials and Methods..... | 18 |
| Results and Discussion..... | 19 |
| Acknowledgement | 23 |
| References | 24 |
| Chapter 3 Polylysogeny and prophage induction by superinfection in a member of the Roseobacter clade..... | 27 |
| Abstract..... | 28 |
| Introduction..... | 28 |
| Materials and Methods..... | 30 |
| Results | 35 |
| Discussion..... | 41 |
| Acknowledgement | 48 |
| References | 49 |
| Appendix..... | 57 |
| Chapter 4 Phage infection of an environmentally relevant marine bacterium alters host metabolism and lysate composition..... | 67 |
| Abstract..... | 69 |
| Introduction..... | 70 |
| Materials and Methods..... | 72 |
| Results | 79 |
| Discussion..... | 83 |
| Acknowledgement | 88 |
| References | 89 |
| Appendix..... | 98 |
| Chapter 5 Metabolism of viral lysates by marine bacterioplankton communities. 106 | |
| Abstract..... | 107 |
| Introduction..... | 108 |
| Materials and Methods..... | 110 |
| Results | 113 |
| Discussion..... | 121 |
| Acknowledgement | 128 |
| References | 129 |
| Appendix..... | 135 |

| | |
|-----------------------------------|------------|
| Chapter 6 Conclusion | 155 |
| References | 160 |
| | |
| Vita | 163 |

List of Tables

| | |
|---|------------|
| Table 3.1. List of oligonucleotide primers used in study | 57 |
| Table 3.2: Frequency of Φ CB2047-A & ΦNYA integration into <i>Sulfitobacter</i> genome | 58 |
| Table 3.3: Frequency of phage integration into <i>Sulfitobacter</i> genome | 58 |
| Table 3.4: <i>Sulfitobacter</i> genomes with conserved putative phage attachment site .. | 59 |
| Table 3.5: <i>Sulfitobacter</i> strains tested for prophage integration | 59 |
| Table 4.1. Relative flux measurements of glutamate and glutamine. | 98 |
| Table 4.2: Metabolite content of cell free filtrates from phage infected <i>Sulfitobacter</i> sp. CB2047 | 99 |
| Table 4.3. Virus gene copies in <i>Sulfitobacter</i> sp. CB2047 infected culture | 100 |
| Table 4.4: List of metabolites quantified in metabolite flux analyses | 100 |
| Table 5.1: Site description of sampling stations..... | 135 |
| Table 5.2. Metabolites with conserved responses across all stations 24 h after incubation on virus lysates..... | 136 |

| | |
|---|------------|
| Table 5.3. ^{15}N incorporation into community metabolites | 137 |
| Table 5.4. ^{13}C incorporation into community metabolites..... | 139 |
| Table 5.5. Relative flux measurements of aspartate and guanine..... | 142 |
| Table 5.6: Relative flux measurements of malate | 143 |
| Table 5.7. Relative flux measurements of glutamate..... | 144 |

List of Figures

| | |
|--|-----------|
| Figure 3.1. Superinfecting phage and resident prophage and host population dynamics in superinfected culture. | 60 |
| Figure 3.2. Growth dynamics of <i>Sulfitobacter</i> lysogens independently infected with ΦCB2047-A and ΦNYA. | 61 |
| Figure 3.3. Phage replication dynamics in <i>Sulfitobacter</i> lysogens superinfected with a secondary phage. | 62 |
| Figure 3.4. Identification of putative phage integration site(s) in <i>Sulfitobacter</i> lysogens. | 63 |
| Figure 3.5. Gene organization around the putative prophage insertion site (<i>attB</i>) in members of the <i>Sulfitobacter</i> genus. | 64 |
| Figure 3.6. Host and resident prophage (ΦNYA) gene expression in infected <i>Sulfitobacter</i> cells. | 65 |
| Figure 3.7. Phage repressor and endolysin gene expression in infected <i>Sulfitobacter</i> cells. | 65 |
| Figure 3.8. Phage and host population dynamics in mitomycin C induced of <i>Sulfitobacter</i> sp. CB2047. | 66 |

| | |
|---|------------|
| Figure 4.1. <i>Sulfitobacter</i> and phage population dynamics in infected culture and carbon and nitrogen estimates content of infected and uninfected cells..... | 101 |
| Figure 4.2. Heatmap of intracellular metabolites of phage-infected and control <i>Sulfitobacter</i> sp. CB2047 populations. | 102 |
| Figure 4.3. Variation in intracellular metabolite concentrations between phage-infected and control populations during the infection cycle..... | 103 |
| Figure 4.4. Absolute concentrations of glutamate and glutamine in control and phage-infected <i>Sulfitobacter</i> sp. CB2047 populations. | 104 |
| Figure 4.5. Incorporation of acetate-derived ¹³C into glutamate and glutamine in phage-infected and control populations during two distinct phases of infection. | 105 |
| Figure 5.1. Changes in microbial abundance at each sampling station..... | 145 |
| Figure 5.2. Principal component analysis (PCA) scores plots of community metabolite profiles for all treatments at 0 and 24 h of incubation. | 146 |
| Figure 5.3. Principal component analysis (PCA) scores plots of community metabolite profiles displaying variation within treatments at 0 and 24 h of sample collection. | 147 |

| | |
|---|------------|
| Figure 5.4. Heatmap of intracellular metabolites of nutrient amended and non-amended microbial communities. | 148 |
| Figure 5.5. Variation in intracellular metabolite concentrations between lysate amended and C+N amended populations during the 24h incubation period. | 149 |
| Figure 5.6. Metabolic pathways significantly altered in lysate amended communities C+N amended communities. | 150 |
| Figure 5.7. Incorporation of ¹³C label into bacterioplankton community malate pools. | 151 |
| Figure 5.8. Incorporation of ¹⁵N label into bacterioplankton community guanine pools. | 152 |
| Figure 5.9. Incorporation of ¹⁵N and ¹³C label into bacterioplankton community aspartate pools. | 153 |
| Figure 5.9. Incorporation of ¹⁵N and ¹³C label into bacterioplankton community glutamate pools. | 154 |

Chapter 1

Introduction

The world's oceans, covering approximately 70% of the Earth's surface, are the primary sink for CO₂ sequestering about a third of all global carbon emissions (Sabine *et al.* 2004). The oceans also harbor photosynthetic marine microbes that produce half of the world's oxygen and are host to numerous food webs that support human populations worldwide (Behrenfeld *et al.* 2006). Changes in marine biogeochemical cycles affect the ocean's capability to support the ever-increasing human reliance on its resources. With an estimated half of the world's population living in coastal areas and relying both directly and indirectly on the oceans as a source of food, energy and transportation, it is imperative that we understand the processes that drive changes in marine biogeochemical cycles so that we can better predict oceanic response to changing environmental factors.

Microbes are the major drivers of ocean biogeochemical cycles (Suttle 2005, Suttle 2007b, Wilhelm and Suttle 1999). Among all marine biological entities, viruses have been shown to contribute most significantly to the flow of carbon, nitrogen and other nutrients (Suttle 2005). Viruses are also the most abundant biological entities in the world's oceans with recent estimates citing 10³⁰ total marine virus particles globally (Breitbart 2012). Although marine viruses are known to infect organisms from all domains of life, the majority of viruses in the ocean are thought to be bacteriophage (viruses that infect bacteria) (Breitbart 2012). Bacteriophage (phage) have been demonstrated to play important ecological roles in the marine environment, including regulating the flow of nutrients, such carbon, nitrogen and phosphorus (Jover *et al.* 2014, Suttle 2007a, Wilhelm and Suttle 1999), and shaping microbial genetic diversity through the horizontal transfer of genetic material (Paul 2008, Weinbauer 2004).

Phage-host interactions occur in various forms with lytic, lysogenic, pseudolysogenic and chronic phage infections being the most commonly documented phage lifestyles (Weinbauer

2004). Pseudolysogenic infections occur mostly in nutrient starved infected cells where there is insufficient energy for the phage to express genes to establish lysogeny or to convert to a lytic state, rendering the phage unstable and inactive (Łoś and Węgrzyn 2012, Ripp and Miller 1997). Chronic infections are characterized by the constant release of new virion progeny from the host cell by budding or extrusion without any associated host cell lysis (Ackermann and DuBow 1987).

Phages undergoing lytic infections redirect host metabolism towards the creation of new virion particles that are released during host cell lysis. It has been estimated that up to 20% of the marine bacterial community is subject to viral-induced lysis at any given time (Suttle 2007a). In fact, an estimated 3Gt of carbon is sequestered in the world's oceans each year as a result of virus-mediated lysis of microorganisms (Suttle 2007a). Via cell lysis, viruses have also been shown to accelerate the transfer of nutrients from the particulate form (in living organisms) to a dissolved state (dissolved organic matter [DOM]), the latter being more accessible to microbial communities (Wilhelm and Suttle 1999). Prior studies that have characterized the effect of virus DOM on bacterioplankton communities in natural systems have mostly focused on the impact of virus lysates on natural bacterioplankton population dynamics and diversity. These studies reported general increases in microbial population and diversity in response to virus DOM amendment (Brussaard *et al.* 2005, Middelboe *et al.* 1996, Middelboe *et al.* 2003). Other studies that have characterized the fate of virus DOM in natural systems have monitored the uptake and/or metabolism of bulk virus DOM by tracking specific elements, principally total C, N and P or measured uptake rates of certain compound classes (e.g. amino acids) (Haaber and Middelboe 2009, Middelboe *et al.* 2003, Sheik *et al.* 2013, Shelford *et al.* 2014). In addition to showing that up to 62% of lysis products from one organism can readily be metabolized and used to support

the growth of other organisms (Middelboe *et al.* 2003), these studies point to the metabolism of viral lysates by microbial communities as contributing significantly to the remineralization of N and P in the environment with estimates of up to 78% and 26% of lysate N and P being mineralized to NH_4^+ and PO_4^{3-} , respectively, by lysate consuming heterotrophic populations (Haaber and Middelboe 2009). Additionally, these studies have shown that the uptake rates of certain compound classes (e.g. amino acids) from viral lysates was concentration dependent, with no observable differences in uptake rates between different isoforms (D and L) of amino acids in virus lysates (Shelford *et al.* 2014).

Despite the growing literature showing that viral lysates are an important source of labile organic nutrients that shape microbial diversity and marine nutrient cycles, (Rohwer and Thurber 2009, Suttle 2007b, Weinbauer *et al.* 2011, Wilhelm and Suttle 1999), we know relatively little of the distinct chemical character of viral-derived dissolved organic matter (v-DOM) or how this material is metabolized by natural bacterioplankton communities. Furthermore, the extent to which viral redirection of host metabolism impacts the cellular material released as a result of viral lysis remains an open question. Thus, there remain significant knowledge gaps in our understanding of the role viruses play in mediating nutrient fluxes in the environment. Elucidating the role of lytic viruses in marine biogeochemical cycles is of critical importance to our understanding of global nutrient cycles that affect climate change and microbial food webs.

In lysogenic infections, lysogenic (temperate) phages integrate their DNA into the host genome, remain in a dormant stage as prophage and replicate along with the host until external cues trigger induction of the prophage into the lytic cycle (Lwoff 1953, Paul 2008, Weinbauer 2004). Some well-characterized agents that have been demonstrated to induce prophage include antibiotics, UV light, acyl-homoserine lactones and environmental pollutants, such as

polychlorinated biphenyls (Ghosh *et al.* 2009, Jiang and Paul 1996, Maiques *et al.* 2006, Zhang *et al.* 2000). These agents generally damage host cell DNA and trigger a RecA-mediated bacterial stress (SOS) response that triggers prophage induction (Maiques *et al.* 2006, Úbeda *et al.* 2005). Most prophage rely on the host SOS response to escape from potentially damaged hosts (Baluch *et al.* 1980, Castellazzi *et al.* 1972, Higashitani *et al.* 1992, Jiang and Paul 1996). The SOS response is utilized by cells to tolerate and respond to DNA damage by upregulating genes involved in cell survival and DNA repair (Kuzminov 1999, Little and Gellert 1983, Radman 1975, Walker 1984). This has been best studied in bacteria such as *Escherichia coli* (Little 1982). In these characterized systems, LexA and RecA proteins have been found to be the main regulators of the host SOS response (Horii *et al.* 1981, Little and Mount 1982). Under normal growth conditions, phage repressors and host LexA proteins bind to specific phage and host operators to prevent the expression of phage lytic genes and host SOS-regulated genes respectively (Little and Mount 1982). Adverse conditions, e.g. DNA damage, activate RecA which induces the auto-cleavage of phage repressors and host LexA proteins (Little 1984, Sauer *et al.* 1982). Cleaved phage repressors and LexA proteins are unable to bind to their specific operators leading to the expression of phage lytic genes (prophage induction) and host SOS-response genes respectively (Little 1993). Phage repressors generally have a lower affinity to host RecA proteins leading to a generally slower cleavage of phage repressors than host LexA proteins and this ensures that prophage induction only occurs in cells that have undergone extensive damage and are unlikely to survive rather than in cells undergoing minimal DNA damage (Friedman *et al.* 1984, Little 1993).

Superinfection (infection of an already infected cell with another phage) has also been demonstrated to induce prophage conversion (Campos *et al.* 2003, Espeland *et al.* 2004). The

exact mechanism of this induction, however, remains poorly understood and understudied in ecologically relevant marine bacteria. We also know very little about the fate of prophage in superinfected cells. In the absence of external triggers, prophages are stably maintained in the host cell and have been shown, in select model host-phage systems, to offer benefits to their host, including resistance to superinfection and increasing host fitness under nutrient-limiting conditions by silencing non-essential gene functions (Brüssow *et al.* 2004, Paul 2008). Prophages have also been shown to play various beneficial ecological roles, including toxic cyanobacterial bloom termination by prophage induction (Hewson *et al.* 2001), and increasing microbial genetic diversity by serving as important reservoirs for genes and mediating the transfer of genetic material between microbes (Paul 2008). With an estimated 50% of marine bacterial isolates containing prophages (Paul 2008) and with their documented ecological relevance, a better understanding of the relationship between temperate phage, their hosts and the environment is needed to fully comprehend the ecological role of lysogenic phage in the environment.

Bacteria belonging to the Roseobacter lineage are abundant in marine systems and carry out critical biogeochemical transformations (Buchan *et al.* 2005, Buchan *et al.* 2014, Gulvik and Buchan 2013). Their abundance and amenability to culturing make Roseobacters both an environmentally relevant and tractable model for investigating the influence of bacteriophage on both host metabolism and DOM release. For this dissertation, we developed a model host-phage system using the bacterium *Sulfitobacter* sp. 2047, a member of the Roseobacter lineage, and its infecting phages Φ CB2047-A, Φ CB2047-B and Φ NYA. This system was used to address the overall objectives of this research, which were to:

(i) examine the virus-mediated induction of a resident prophage in a Roseobacter-phage system, (ii) assess the extent to which virus infection reshapes host cell metabolism and the effect of this alteration on the cellular organic matter released following viral lysis, and (iii) track the subsequent uptake and metabolism of host-derived organic matter in marine surface water microbial communities in response to virus derived DOM addition.

The scientific research of this dissertation is addressed in four chapters (Chapter 2-5). Chapter 2 is a genomic analysis of the model marine bacterium and phages used in this study. Chapter 3 examines the establishment of polylysogeny and induction of a resident prophage in a Roseobacter-phage system in order to gain insights into the biological factors that affect prophage conversion and the transfer of genetic material in the marine environment. Chapter 4 examines the extent to which virus infection reshapes host cell metabolism and the effect of this alteration on the cellular organic matter released following viral lysis. Finally, Chapter 5 tracks the subsequent uptake and metabolism of virus derived organic matter in marine surface water microbial communities by comparing the uptake and metabolism of viral lysates across various sampling stations in the North Pacific. Collectively, the work presented in this dissertation contributes to the growing knowledge of the role of viruses as global drivers of nutrient flow and microbial genetic diversity.

References

- Ackermann HW, DuBow MS (1987). Viruses of Prokaryotes. *General Properties of Bacteriophages*. CRC Press: Boca Raton. p 202.
- Baluch J, Chase J, Sussman R (1980). Synthesis of recA protein and induction of bacteriophage lambda in single-strand deoxyribonucleic acid-binding protein mutants of *Escherichia coli*. *J Bacteriol* **144**: 489-498.
- Behrenfeld MJ, O'Malley RT, Siegel DA, McClain CR, Sarmiento JL, Feldman GC *et al.* (2006). Climate-driven trends in contemporary ocean productivity. *Nature* **444**: 752-755.
- Breitbart M (2012). Marine viruses: truth or dare. *Annual Review of Marine Science* **4**: 425-448.
- Brussaard C, Mari X, Van Bleijswijk J, Veldhuis M (2005). A mesocosm study of *Phaeocystis globosa* (Prymnesiophyceae) population dynamics: II. Significance for the microbial community. *Harmful algae* **4**: 875-893.
- Brüssow H, Canchaya C, Hardt W-D (2004). Phages and the evolution of bacterial pathogens: from genomic rearrangements to lysogenic conversion. *Microbiology and Molecular Biology Reviews* **68**: 560-602.
- Buchan A, Gonzalez JM, Moran MA (2005). Overview of the marine Roseobacter lineage. *Applied and Environmental Microbiology* **71**: 5665-5677.
- Buchan A, LeCleir GR, Gulvik CA, Gonzalez JM (2014). Master recyclers: features and functions of bacteria associated with phytoplankton blooms. *Nat Rev Micro* **12**: 686-698.

- Campos J, Martínez E, Marrero K, Silva Y, Rodríguez BL, Suzarte E *et al.* (2003). Novel type of specialized transduction for CTX ϕ or its satellite phage RS1 mediated by filamentous phage VGJ ϕ in *Vibrio cholerae*. *J Bacteriol* **185**: 7231-7240.
- Castellazzi M, George J, Buttin G (1972). Prophage induction and cell division in *E. coli*. *Molecular and General Genetics MGG* **119**: 153-174.
- Espeland EM, Lipp EK, Huq A, Colwell RR (2004). Polylysogeny and prophage induction by secondary infection in *Vibrio cholerae*. *Environmental Microbiology* **6**: 760-763.
- Friedman DI, Olson ER, Georgopoulos C, Tilly K, Herskowitz I, Banuett F (1984). Interactions of bacteriophage and host macromolecules in the growth of bacteriophage-lambda. *Microbiological Reviews* **48**: 299-325.
- Ghosh D, Roy K, Williamson KE, Srinivasiah S, Wommack KE, Radosevich M (2009). Acyl-homoserine lactones can induce virus production in lysogenic bacteria: an alternative paradigm for prophage induction. *Applied and environmental microbiology* **75**: 7142-7152.
- Gulvik CA, Buchan A (2013). Simultaneous catabolism of plant-derived aromatic compounds results in enhanced growth for members of the Roseobacter lineage. *Applied and environmental microbiology* **79**: 3716-3723.
- Haaber J, Middelboe M (2009). Viral lysis of *Phaeocystis pouchetii*: implications for algal population dynamics and heterotrophic C, N and P cycling. *The ISME journal* **3**: 430-441.

- Hewson I, O'Neil JM, Dennison WC (2001). Virus-like particles associated with *Lyngbya majuscula* (Cyanophyta; Oscillatoriaceae) bloom decline in Moreton Bay, Australia. *Aquatic Microbial Ecology* **25**: 207-213.
- Higashitani N, Higashitani A, Roth A, Horiuchi K (1992). SOS induction in *Escherichia coli* by infection with mutant filamentous phage that are defective in initiation of complementary-strand DNA synthesis. *J Bacteriol* **174**: 1612-1618.
- Horii T, Ogawa T, Nakatani T, Hase T, Matsubara H, Ogawa H (1981). Regulation of SOS functions: purification of *E. coli* LexA protein and determination of its specific site cleaved by the RecA protein. *Cell* **27**: 515-522.
- Jiang SC, Paul JH (1996). Occurrence of lysogenic bacteria in marine microbial communities as determined by prophage induction. *Marine Ecology-Progress Series* **142**: 27.
- Jover LF, Effler TC, Buchan A, Wilhelm SW, Weitz JS (2014). The elemental composition of virus particles: implications for marine biogeochemical cycles. *Nature Reviews Microbiology* **12**: 519-528.
- Kuzminov A (1999). Recombinational Repair of DNA Damage in *Escherichia coli* and Bacteriophage λ . *Microbiology and Molecular Biology Reviews* **63**: 751-813.
- Little J (1993). LexA cleavage and other self-processing reactions. *J Bacteriol* **175**: 4943.
- Little JW, Mount DW (1982). The SOS regulatory system of *Escherichia coli*. *Cell* **29**: 11-22.
- Little JW, Gellert M (1983). The SOS regulatory system: control of its state by the level of RecA protease. *Journal of molecular biology* **167**: 791-808.

- Little JW (1984). Autodigestion of *lexA* and phage lambda repressors. *Proceedings of the National Academy of Sciences* **81**: 1375-1379.
- Łoś M, Węgrzyn G (2012). Pseudolysogeny. *Advances in Virus Research* **82**: 339-349.
- Lwoff A (1953). Lysogeny. *Bacteriological Reviews* **17**: 269.
- Maiques E, Úbeda C, Campoy S, Salvador N, Lasa Í, Novick RP *et al.* (2006). β -Lactam antibiotics induce the SOS response and horizontal transfer of virulence factors in *Staphylococcus aureus*. *J Bacteriol* **188**: 2726-2729.
- Middelboe M, Jorgensen N, Kroer N (1996). Effects of viruses on nutrient turnover and growth efficiency of noninfected marine bacterioplankton. *Applied and Environmental Microbiology* **62**: 1991-1997.
- Middelboe M, Riemann L, Steward GF, Hansen V, Nybroe O (2003). Virus-induced transfer of organic carbon between marine bacteria in a model community. *Aquatic microbial ecology* **33**: 1-10.
- Paul JH (2008). Prophages in marine bacteria: dangerous molecular time bombs or the key to survival in the seas? *The ISME journal* **2**: 579-589.
- Radman M (1975). SOS repair hypothesis: phenomenology of an inducible DNA repair which is accompanied by mutagenesis. *Molecular mechanisms for repair of DNA*. Springer. pp 355-367.
- Ripp S, Miller RV (1997). The role of pseudolysogeny in bacteriophage-host interactions in a natural freshwater environment. *Microbiology* **143**: 2065-2070.

- Rohwer F, Thurber RV (2009). Viruses manipulate the marine environment. *Nature* **459**: 207-212.
- Sabine CL, Feely RA, Gruber N, Key RM, Lee K, Bullister JL *et al.* (2004). The oceanic sink for anthropogenic CO₂. *science* **305**: 367-371.
- Sauer R, Ross M, Ptashne M (1982). Cleavage of the lambda and P22 repressors by recA protein. *Journal of Biological Chemistry* **257**: 4458-4462.
- Sheik AR, Brussaard CP, Lavik G, Lam P, Musat N, Krupke A *et al.* (2013). Responses of the coastal bacterial community to viral infection of the algae *Phaeocystis globosa*. *The ISME journal*.
- Shelford EJ, Jørgensen NO, Rasmussen S, Suttle CA, Middelboe M (2014). Dissecting the role of viruses in marine nutrient cycling: bacterial uptake of D-and L-amino acids released by viral lysis. *Aquatic Microbial Ecology* **73**.
- Suttle CA (2005). Viruses in the sea. *Nature* **437**: 356-361.
- Suttle CA (2007). Marine viruses: major players in the global ecosystem. *Nat Rev Micro* **5**: 801-812.
- Úbeda C, Maiques E, Knecht E, Lasa Í, Novick RP, Penadés JR (2005). Antibiotic-induced SOS response promotes horizontal dissemination of pathogenicity island-encoded virulence factors in staphylococci. *Molecular microbiology* **56**: 836-844.
- Walker GC (1984). Mutagenesis and inducible responses to deoxyribonucleic acid damage in *Escherichia coli*. *Microbiological Reviews* **48**: 60.

- Weinbauer M, Chen F, Wilhelm S (2011). Microbial Carbon Pump in the Ocean. In: Jiao N, Azam F, Sanders S (eds). Science/AAAS Business Office.
- Weinbauer MG (2004). Ecology of prokaryotic viruses. *FEMS Microbiology Reviews* **28**: 127-181.
- Wilhelm SW, Suttle CA (1999). Viruses and Nutrient Cycles in the Sea - Viruses play critical roles in the structure and function of aquatic food webs. *BioScience* **49**: 781-788.
- Zhang X, McDaniel AD, Wolf LE, Keusch GT, Waldor MK, Acheson DW (2000). Quinolone antibiotics induce Shiga toxin-encoding bacteriophages, toxin production, and death in mice. *Journal of Infectious Diseases* **181**: 664-670.

Chapter 2

Genomic analysis of the marine bacterium *Sulfitobacter* sp. CB2047 and its infecting phages Φ CB2047-A, -B & -C

Versions of this chapter were originally published by Ankrah NYD, Budinoff CR, Lane TR Hadden MK, Wilhelm SW, and Buchan A.

Ankrah NYD, Lane T, Budinoff CR, Hadden MK, Buchan A. 2014. Draft genome sequence of *Sulfitobacter* sp. CB2047, a member of the Roseobacter clade of marine bacteria, isolated from an *Emiliana huxleyi* bloom. *Genome Announc.* 2(6):e01125-14. doi:10.1128/genomeA.01125-14.

Ankrah NYD, Budinoff CR, Wilson WH, Wilhelm SW, Buchan A. 2014. Genome sequences of two temperate phages, Φ CB2047-A and Φ CB2047-C, infecting *Sulfitobacter* sp. strain 2047. *Genome Announc.* 2(3):e00108-14. doi:10.1128/genomeA.00108-14.

Ankrah NYD, Budinoff CR, Wilson WH, Wilhelm SW, Buchan A. 2014. Genome sequence of the *Sulfitobacter* sp. strain 2047-infecting lytic phage Φ CB2047-B. *Genome Announc.* 2(1):e00945-13. doi:10.1128/genomeA.00945-13.

NYDA participated in sample processing, interpreted the data and drafted the manuscript. CRM, MH & TL participated in data collection, sample processing, and data analysis. WW & SWW participated in the design of the study and helped to draft the manuscript. AB participated in the design and coordination of the study, aided in the interpretation of the data, and helped to draft the manuscript. All authors read and approved the final manuscript(s).

Abstract

Members of the Roseobacter lineage and their infecting phage play important roles in various marine biogeochemical cycles and provide valuable models for studying the role of marine viruses in aquatic environments. We report here the draft genome sequence of *Sulfitobacter* sp. strain CB2047, a marine bacterium of the Roseobacter clade, isolated from a phytoplankton bloom. The genome encodes pathways for the catabolism of aromatic compounds as well as transformations of carbon monoxide and sulfur species. The strain also encodes a prophage (Φ NYA) as well as the gene transfer agent (GTA), both of which are prevalent among members of the Rhodobacterales order. We also report here the complete genome sequences of two temperate Podoviridae, *Sulfitobacter* phages Φ CB2047-A and Φ CB2047-C, and the N4-like podophage Φ CB2047-B all of which infect *Sulfitobacter* sp. strain CB2047. This is the first report of temperate podophage infecting members of the *Sulfitobacter* genus of the Roseobacter clade.

Introduction

Viruses are important components of marine food webs where they contribute significantly to the mortality of microorganisms and consequently alter species composition and influence the flow of carbon, nitrogen and other nutrients (Wilhelm and Suttle 1999). Viruses are also known to increase microbial genetic diversity through the horizontal transfer of genes (Paul 2008). Despite the growing literature on the ecological role of viruses in the marine environment there remain major gaps in understanding the host range of marine viruses, the effect of virus

infection on host metabolism and the effects of these changes in metabolism in the material released post cell lysis. Relevant host-phage model systems are needed to better understand the relationship between viruses, their hosts and the environment. The majority of viruses found in aquatic systems are phages (viruses that infect bacteria) (Breitbart 2012), but relatively few environmentally relevant marine phage-host systems have been described to date.

Bacteria of the Roseobacter lineage, which includes the genus *Sulfitobacter*, are abundant marine heterotrophs and constitute upwards of 30% of coastal marine bacteria (Buchan *et al.* 2005). Members of this lineage also process a significant portion of the total carbon in the marine environment and mediate several key biogeochemical processes, including the transformation of organic and inorganic sulfur compounds, the oxidation of carbon monoxide, and the degradation of vascular plant material (Buchan *et al.* 2005, Buchan *et al.* 2014, González *et al.* 1999, Gulvik and Buchan 2013). Dimethylsulfoniopropionate (DMSP)-producing phytoplankton species, such as the coccolithophorid *Emiliana huxleyi*, are important sources of organic sulfur in marine waters and documented Roseobacter niches (Buchan *et al.* 2014). Their abundance and amenability to cultivation make Roseobacters, along with their infecting phages, excellent models for studying how microbial activities shape biogeochemical cycles (Ankrah *et al.* 2014c, Buchan *et al.* 2005). We describe here the genome sequences of a recently established Roseobacter-phage system (Ankrah *et al.* 2014c): *Sulfitobacter* sp. strain CB2047, a marine bacterium of the Roseobacter clade and its infecting phages Φ CB2047-A, Φ CB2047-B and Φ CB2047-C.

Materials and methods

***Sulfitobacter* sp. CB2047 isolation, sequencing and genomic analysis**

Sulfitobacter sp. CB2047 was isolated during an induced *Emiliana huxleyi* bloom in Raunefjorden, Norway, by direct plating onto 0.22- μ m filtered fjord seawater agar plates supplemented with dimethylsulfoniopropionate (DMSP) as the sole carbon source (Ankrah *et al.* 2014c). The genome was sequenced using Illumina technology with an average sequencing coverage of approximately 600 \times . The genome was assembled into 12 contigs, ranging in size from 18 kb to 2.3 Mb, using CLC Assembly Cell (CLC bio, Cambridge, MA, USA). The genome of CB2047 was annotated using the NCBI Prokaryotic Genome Annotation Pipeline (http://www.ncbi.nlm.nih.gov/genome/annotation_prok/) and the KAAS genome annotation and pathway reconstruction server (Moriya *et al.* 2007).

***Sulfitobacter* phage isolation, sequencing and genomic analysis**

The three podophages were isolated from an induced algal bloom mesocosm study in Raunefjorden, Norway, using standard plaque assay techniques (Ankrah *et al.* 2014c, Budinoff 2012), and were sequenced by the Broad Institute under the Gordon and Betty Moore Foundation's Marine Phage, Virus, and Virome Sequencing Project. An average sequencing coverage of $\approx 30\times$ was obtained for both phages. Genome annotations were done using the RAST annotation server (Aziz *et al.* 2008) and tRNAscan-SE search server (Lowe and Eddy 1997). Translated peptides from the phage genomes were used as BLASTp queries to the NCBI non-redundant protein sequence database to manually curate possible gene functions and identify the nearest phage or prophage relatives. The CoreGenesUniqueGenes (CGUG) genome analysis tool

(Mahadevan *et al.* 2009) was used to identify gene homologues and assign core genes that are shared with other closely related phages.

Results and Discussion

Sulfitobacter sp. CB2047 genomic analysis

The draft genome sequence of *Sulfitobacter* sp. CB2047 is 3,767,790 bp (3.76 Mb) with a G+C content of 60.3%. The genome contains 3,563 coding sequences and 37 predicted tRNAs. Based on 16S rRNA gene sequence similarity, CB2047 is 99.93, 99.93, 98.31, and 100% identical to *Sulfitobacter* strains EE36 (AALV01000001), 3SOLIMAR09 (AXZR00000000), FIGIMAR09 (JEMU00000000), and NAS-14.1 (AALZ01000001), respectively. The genome of CB2047 is lysogenized by a mitomycin-inducible 42 kb prophage (KM233261) that has high sequence homology to other *Sulfitobacter* sp. CB2047 infecting phages: Φ CB2047-A and Φ CB2047-C (Ankrah *et al.* 2014a). Genome-wide nucleotide similarity alignments with the Φ CB2047-A and Φ CB2047-C genomes showed that the prophage shares 79 and 74% nucleotide identity, respectively. The genome also possesses the gene transfer agent (GTA) gene cluster, including the diagnostic capsid protein gene, g5 (KFC25944.1) (Zhao *et al.* 2008).

Sulfitobacter sp. CB2047 harbors several central carbon metabolic pathways, including glycolysis, the tricarboxylic acid cycle (TCA), and the pentose phosphate pathway. Furthermore, pathways for aromatic compound catabolism are present, including the protocatechuate branch of the β -keto adipate pathway (pcaGH [KFC25619.1, KFC25620.1]) and the phenylacetate catabolic pathway (paaABX [KFC27335.1, KFC27336.1, KFC27331.1]). Also present are genes for sulfur

metabolism, including the DMSP-cleavage enzyme (dddL [KFC25711.1]) and the Sox enzyme system (soxXYZABCD [KFC25464.1 to KFC25470.1]), which oxidizes thiosulfate to sulfate (Friedrich *et al.* 2001) Carbon monoxide dehydrogenase (coxSLM [KFC25996.1 to KFC25998.1]), which mediates the reversible conversion between carbon monoxide and carbon dioxide (King and Weber 2007), is present in this genome. Also present is an N-acyl-L-homoserine lactone (AHL) synthetase homolog (luxI [KFC28110.1]), indicating the strain may be capable of utilizing AHL-based quorum sensing. However, no genes with homology to AHL binding response regulators (luxR) were identified. Indeed, the presence of “orphan” luxI genes appears common among *Sulfitobacter* species (Cude and Buchan 2013). The genome also encodes for a type IV secretion system (virB1,2,3,4,6,8,9,10 [KFC27915.1 to KFC27903.1]), that may facilitate interactions with other organisms, including eukaryotic phytoplankton. The whole-genome sequence of *Sulfitobacter* sp. CB2047 was deposited in GenBank under the accession no. JPOY00000000. The version described in this paper is JPOY01000000, and consists of contig sequences JPOY01000001 to JPOY01000012.

Temperate phages Φ CB2047-A and Φ CB2047-C genomic analysis

We report here the genomes of two lysogenic Podoviridae, phages Φ CB2047-A and Φ CB2047-C, infecting *Sulfitobacter* sp. strain 2047, a member of the Roseobacter clade of marine bacteria. This is the first report of temperate Podoviridae infecting members of the *Sulfitobacter* genus of the Roseobacter clade. Phage Φ CB2047-A is 40,929 bp, with a G+C content of 58.8%. A total of 73 open reading frames (ORFs) were identified in phage Φ CB2047-A. Phage Φ CB2047-C is 40,931 bp, with a G+C content of 59%. A total of 73 ORFs were identified in phage Φ CB2047-C. Phages Φ CB2047-A and Φ CB2047-C are nearly identical at the

nucleotide level, except for a ~2,000-bp region encoding a T5orf172 domain-containing protein (PF10544) and RusA-like endodeoxyribonuclease in Φ CB2047-A and five hypothetical proteins in Φ CB2047-C, where they share no sequence similarity. Φ CB2047-A and Φ CB2047-C share greatest sequence similarity to Φ EBPR podovirus 2, an uncultured phage from an enhanced biological phosphorus removal reactor (Skennerton *et al.* 2011). CGUG analysis identified 17 highly homologous genes (BLASTp threshold score, 85) between Φ CB2047-A and Φ CB2047-C and Φ EBPR podovirus 2. Both Φ CB2047-A and Φ CB2047-C have a DNA Bre-C like integrase to integrate in the host genome and lysis/lysozyme proteins with glycosyl hydrolase and peptidoglycan binding domains predicted to be involved in host cell lysis. Phages Φ CB2047-A and Φ CB2047-C also show relatedness to the temperate Myxococcus phage Mx8 (accession no. NC_003085), with protein homology existing within the terminase gene and several putative tail-fiber genes.

In contrast to other known roseophages, the genomes of Φ CB2047-A and Φ CB2047-C do not contain genes showing strong homology to currently described DNA polymerases, thymidylate synthases, ribonucleotide reductases, and deoxycytidine deaminases (Ankrah *et al.* 2014b). The absence of well-characterized replication/nucleotide metabolism genes indicates that Φ CB2047-A and Φ CB2047-C may rely heavily on host resources for nucleotide production to generate new virions or possibly use novel replication and nucleotide metabolism proteins. Also absent from the genomes of Φ CB2047-A and Φ CB2047-C are homologs to known DNA methylases, which are frequently present in other temperate relatives (Murphy *et al.* 2013), including Φ EBPR podovirus 2 (accession no. AEI70896.1). The genomes of Φ CB2047-A and Φ CB2047-C encode homing endonucleases (HNH_3 domain [Pfam13392]), which may be beneficial to the host and/or offer a competitive advantage to the phage by cleaving the DNA of

other closely related competing phages during mixed infections (Goodrich-Blair and Shub 1996). The whole-genome sequences of *Sulfitobacter* phages Φ CB2047-A and Φ CB2047-C were deposited in GenBank under the accession no. HQ332142 and HQ317384, respectively.

Lytic N4-like phage Φ CB2047-B genomic analysis

Phage Φ CB2047-B is 74,480 bp (74.5 kb) with a G+C content of 43% and 92 identified open reading frames. The genome sequence indicates this is an N4-like bacteriophage that is highly similar to but genetically distinct from other recently described roseophages (Zhao *et al.* 2009). Morphological analysis by transmission electron microscopy confirmed that phage Φ CB2047-B belongs to the family Podoviridae. The genome content and architecture of Φ CB2047-B are similar to those of other N4 phages. Consistent with most other N4-like phages, the genome possesses 437-bp direct terminal repeat sequences on its distal ends. A CGUG analysis identified 20 highly homologous genes (BLASTp threshold score, 85) between phage Φ CB2047-B and these previously reported N4-like phages: the enterobacterium phage N4 (accession no. NC_008720), *Pseudomonas* sp. phages LUZ7 (accession no. FN422398) and LIT1 (accession no. FN422399), and N4-like roseophages Φ DSS3P2 (accession no. FJ591093) and Φ EE36P1 (accession no. FJ591094). An analysis focused exclusively on N4-like roseophages (Φ DSS3P2 and Φ EE36P1) identified 41 genes with high homology. Genome-wide nucleotide similarity alignments with the Φ DSS3P2 and Φ EE36P1 genomes showed that phage Φ CB2047-B shares 43.9 and 44.4% nucleotide identity, respectively. Unlike other N4-like phages, Φ CB2047-B contains a deoxycytidine triphosphate (dCTP) deaminase instead of a deoxycytidine monophosphate deaminase, indicating a preference for an alternative route for the generation of dUMP for thymidine biosynthesis. The closest homolog in the NCBI database to

the phage dCTP deaminase is from a coliphage, EC1-UPM (accession no. AGC31535), which has 37% identity. The host genome also contains a homolog to this protein that shares 29% identity to the phage gene and suggests genetic divergence. The complete sequence of the *Sulfitobacter* phage Φ CB2047-B genome can be accessed under the GenBank accession no. HQ317387.

Acknowledgements

This work was supported by an NSF grant (OCE-1061352) to A.B and S. W.W.

References

- Ankrah NYD, Budinoff CR, Wilson WH, Wilhelm SW, Buchan A (2014a). Genome Sequences of Two Temperate Phages, Φ CB2047-A and Φ CB2047-C, Infecting *Sulfitobacter* sp. Strain 2047. *Genome Announcements* **2**.
- Ankrah NYD, Budinoff CR, Wilson WH, Wilhelm SW, Buchan A (2014b). Genome Sequence of the *Sulfitobacter* sp. Strain 2047-Infecting Lytic Phage Φ CB2047-B. *Genome Announcements* **2**.
- Ankrah NYD, May AL, Middleton JL, Jones DR, Hadden MK, Gooding JR *et al.* (2014c). Phage infection of an environmentally relevant marine bacterium alters host metabolism and lysate composition. *ISME J* **8**: 1089-1100.
- Aziz RK, Bartels D, Best AA, DeJongh M, Disz T, Edwards RA *et al.* (2008). The RAST Server: rapid annotations using subsystems technology. *BMC genomics* **9**: 75.
- Breitbart M (2012). Marine viruses: truth or dare. *Annual Review of Marine Science* **4**: 425-448.
- Buchan A, González JM, Moran MA (2005). Overview of the marine *Roseobacter* lineage. *Applied and environmental microbiology* **71**: 5665-5677.
- Buchan A, LeCleir GR, Gulvik CA, Gonzalez JM (2014). Master recyclers: features and functions of bacteria associated with phytoplankton blooms. *Nat Rev Micro* **12**: 686-698.
- Budinoff CR (2012). Diversity and activity of *Roseobacters* and roseophage.
- Cude WN, Buchan A (2013). Acyl-homoserine lactone-based quorum sensing in the *Roseobacter* clade: complex cell-to-cell communication controls multiple physiologies. *Frontiers in microbiology* **4**: 336.

- Friedrich CG, Rother D, Bardischewsky F, Quentmeier A, Fischer J (2001). Oxidation of reduced inorganic sulfur compounds by bacteria: emergence of a common mechanism? *Applied and Environmental Microbiology* **67**: 2873-2882.
- González JM, Kiene RP, Moran MA (1999). Transformation of Sulfur Compounds by an Abundant Lineage of Marine Bacteria in the α -Subclass of the Class Proteobacteria. *Applied and environmental microbiology* **65**: 3810-3819.
- Goodrich-Blair H, Shub DA (1996). Beyond homing: competition between intron endonucleases confers a selective advantage on flanking genetic markers. *Cell* **84**: 211-221.
- Gulvik CA, Buchan A (2013). Simultaneous catabolism of plant-derived aromatic compounds results in enhanced growth for members of the Roseobacter lineage. *Applied and environmental microbiology* **79**: 3716-3723.
- King GM, Weber CF (2007). Distribution, diversity and ecology of aerobic CO-oxidizing bacteria. *Nature Reviews Microbiology* **5**: 107-118.
- Lowe TM, Eddy SR (1997). tRNAscan-SE: a program for improved detection of transfer RNA genes in genomic sequence. *Nucleic acids research* **25**: 0955-0964.
- Mahadevan P, King JF, Seto D (2009). CGUG: in silico proteome and genome parsing tool for the determination of. *BMC research notes* **2**: 168.
- Moriya Y, Itoh M, Okuda S, Yoshizawa AC, Kanehisa M (2007). KAAS: an automatic genome annotation and pathway reconstruction server. *Nucleic acids research* **35**: W182-W185.

- Murphy J, Mahony J, Ainsworth S, Nauta A, van Sinderen D (2013). Bacteriophage orphan DNA methyltransferases: insights from their bacterial origin, function, and occurrence. *Applied and environmental microbiology* **79**: 7547-7555.
- Paul JH (2008). Prophages in marine bacteria: dangerous molecular time bombs or the key to survival in the seas? *The ISME journal* **2**: 579-589.
- Skenneron CT, Angly FE, Breitbart M, Bragg L, He S, McMahon KD *et al.* (2011). Phage encoded H-NS: a potential achilles heel in the bacterial defence system. *PloS one* **6**: e20095.
- Wilhelm SW, Suttle CA (1999). Viruses and Nutrient Cycles in the Sea Viruses play critical roles in the structure and function of aquatic food webs. *Bioscience* **49**: 781-788.
- Zhao Y, Wang K, Budinoff C, Buchan A, Lang A, Jiao N *et al.* (2008). Gene transfer agent (GTA) genes reveal diverse and dynamic Roseobacter and Rhodobacter populations in the Chesapeake Bay. *The ISME journal* **3**: 364-373.
- Zhao Y, Wang K, Jiao N, Chen F (2009). Genome sequences of two novel phages infecting marine Roseobacters. *Environmental microbiology* **11**: 2055-2064.

Chapter 3

Polylysogeny and prophage induction by superinfection in a member of the Roseobacter clade

Abstract

Lysogeny has been hypothesized to be prevalent in marine environments with an estimated 50% of marine bacterial isolates containing prophages. Prophages have been shown to provide benefits to host cells, including protection from secondary phage infection (i.e. superinfection inhibition) and an increase in fitness under nutrient-limiting conditions. While the abiotic factors that stimulate prophage induction have been well studied, the biotic factors that mediate this process are less understood. To fill this knowledge gap and to better understand the biotic factors that affect prophage induction in marine environments a lysogenized bacterium belonging to the Roseobacter clade of marine bacteria, *Sulfitobacter* sp. CB2047, was infected with a temperate phage (Φ CB2047-A) and the effect of secondary phage infection on prophage induction monitored over the infection cycle. Our results indicate that superinfection of the lysogenized cell induces prophage conversion by a RecA-mediated mechanism and the establishment of polylysogeny in some members of the population. Integration of Φ CB2047-A is a site-specific DNA recombination event between a 15bp attachment site (*attP*) on Φ CB2047-A and a homologous 15bp target (*attB*) on the bacterial chromosome. These data increase our understanding of the biotic factors that stimulate prophage induction and provide an ecologically relevant mechanism by which genetic information is transferred in the marine environment.

Introduction

Temperate bacteriophage can reproduce via one of two replication modes: a lytic mode where the phage immediately creates new virion particles after infecting the cell and subsequently lyses the cell to release newly formed virions or a lysogenic mode where the phage

integrates its DNA into the host genome, where it is subsequently termed a prophage, and is stably maintained (Calendar 2006, Lwoff 1953). Prophages have been shown, in select model host-phage systems, to offer benefits to their host, including resistance to superinfection and increasing host fitness under nutrient-limiting conditions by silencing non-essential gene functions (Brüssow *et al.* 2004, Paul 2008). Under lysogenic conditions, prophage replication occurs when the host cell divides and this only changes once external cues trigger the induction of the prophage to enter into the lytic cycle and subsequently lyse the host. Some well characterized agents that induce prophage induction include antibiotics (Maiques *et al.* 2006), acyl-homoserine lactones (Ghosh *et al.* 2009), UV light and environmental pollutants like polychlorinated biphenyls (Jiang and Paul 1996). These agents generally damage host cell DNA, triggering a RecA-mediated bacterial stress response that results in prophage induction (Maiques *et al.* 2006, Úbeda *et al.* 2005).

While the abiotic mechanisms by which the lysogenic to lytic switch occurs are well characterized in model bacterial-phage systems, the biological mechanisms by which prophage are naturally induced in the marine environment remains poorly understood. A few studies have documented the induction of resident prophage in lysogenized cells after superinfection with new phage. These studies have mostly focused on the relevance of these inductions on disease dissemination and remain limited to members of the *Vibrio* and *Escherichia* genera (e.g. Campos *et al.* 2003, Espeland *et al.* 2004, Refardt 2011).

Lysogeny has been hypothesized to be prevalent in marine environments (Leitet *et al.* 2006, Paul 2008, Stopar *et al.* 2004) with an estimated 50% of marine bacterial isolates containing prophages (Paul 2008). Prophage induction in marine systems has been demonstrated to play various beneficial ecological roles, including mediating the collapse of harmful algal

blooms (Hewson *et al.* 2001) and increasing microbial genetic diversity through the horizontal transfer of genes (Weinbauer 2004). The prevalence of lysogenized cells in the marine environment (Paul 2008) and the importance of prophage in the transfer of genetic material and shaping microbial diversity and population dynamics warrant a better understanding of the relationship between prophages, their hosts and the environment.

Members of the Roseobacter lineage of marine bacteria are very abundant in the world's oceans, are metabolically versatile and have been demonstrated to play important roles in various marine biogeochemical cycles (Buchan *et al.* 2005, Buchan *et al.* 2014, Gulvik and Buchan 2013). Recent reports (Chen *et al.* 2006, Zhao *et al.* 2010b) also indicate a high prevalence of lysogeny among Roseobacter isolates making them relevant models to study prophage induction in marine environments and potential sources to isolate and characterize transducing phage for genetic manipulations of marine bacteria. In this study, we examine the establishment of polylysogeny and induction of a resident prophage in a recently established Roseobacter-phage system (Ankrah *et al.* 2014c) in order to gain insights into the biological factors that affect prophage conversion and the transfer of genetic material in the marine environment.

Materials and Methods

Isolation and induction of *Sulfitobacter* sp. CB2047 with mitomycin C

Lysogenized *Sulfitobacter* sp. CB2047 and its infecting phage Φ CB2047-A were isolated from a mesocosm study in Raunefjorden, Norway by enrichment with dimethylsulfoniopropionate and standard bacteriophage enrichment techniques as previously described (Ankrah *et al.* 2014a, Ankrah *et al.* 2014b). *Sulfitobacter* sp. CB2047 was grown in

artificial sea water (Budinoff and Hollibaugh 2007) supplemented with 0.25% yeast extract and 0.4% tryptone at 25 °C in the dark with 200 r.p.m. agitation. Once cultures reached an optical density (OD₅₄₀) of ca. 0.1, mitomycin C was added at a final concentration of 0.5µg/mL and incubated for 22h at 25 °C in the dark with 200 r.p.m. agitation. Triplicate control cultures with no mitomycin C added were maintained and sampled in parallel. Under these conditions, a difference in growth between control and mitomycin C cultures was evident at ~4 h post mitomycin C addition. One milliliter samples were collected at the time of phage addition (t=0) and then at 22 h post mitomycin C addition for enumeration of prophage (ΦNYA) using qPCR assays specific for ΦNYA. Samples collected at 22 h were centrifuged at 5000 g for 30 mins to remove intact cells and cell debris and the supernatant used for ΦNYA enumeration.

Experimental design for prophage induction and gene expression analysis

To determine if superinfection induces conversion of the *Sulfitobacter* sp. CB2047 prophage (ΦNYA) and to characterize the transcriptional changes associated with this induction event, the host bacterium was grown on artificial sea water (Budinoff and Hollibaugh 2007) supplemented with 0.25% yeast extract and 0.4% tryptone at 25 °C in the dark with 200 r.p.m. agitation. Once cultures reached an optical density (OD₅₄₀) of ca. 0.17, phages were added at a multiplicity of infection of 0.06. Under these conditions, cell lysis is evident at ~6 h post infection (p.i.). To monitor prophage induction dynamics, 1mL samples were collected at the time of phage addition (t=0 h) and then at 1, 2, 3, 4, 6, 8 and 10 h post virus addition. These samples were stored at -20°C for enumeration of the resident prophage (ΦNYA) and the superinfecting phage (ΦCB2047-A) using qPCR assays specific for each phage. One milliliter samples were also collected on 0.2µm Supor membrane filters (Pall, Ann Arbor, MI) via vacuum

filtration and washed twice using a buffered saline solution (230 mm NaCl, 5.3 mm KCl, 3.9 mm CaCl₂, 0.1 mm H₃BO₃, 11.8 mm MgSO₄, 11.2 mm MgCl₂, 0.8 mm NaHCO₃, 5 mm NH₄Cl, 75 μM K₂HPO₄ and 10 mm Tris-HCl (pH 7.5)) at the same timepoints for transcript analysis. Samples for quantitative polymerase chain reaction (qPCR) were flash frozen and stored at -20 °C until processing, whereas samples for plaque assays were immediately processed. At each sampling point, production of new virions was determined by qPCR. Control cultures (without added phage) were maintained and sampled in parallel. All experiments were performed in triplicate.

Phage and prophage enumeration

Phage (ΦCB2047-A) and prophage (ΦNYA) were enumerated using qPCR assays specific for each phage (see Table 3.1). Collected samples were thawed on ice and lysed at 95 °C for 15min. Samples were spun to remove cell debris, diluted in 10 mm Tris-HCl pH 8.0 and qPCR performed on an Opticon 2 real-time PCR detector with the Opticon Monitor 3.1.32 software package (Bio-Rad Laboratories, Inc., Hercules, CA). Quantitative PCR reactions were performed in a 25 μL volume with 12.5 μL SYBR Premix Ex Taq cocktail RR041 (Perfect Real Time; Takara Bio, Inc., Shiga, Japan), 500 nM forward and reverse primers and 10 μL of template dilutions. The amplification programs for each primer set are as follows: 95°C for 3 min, 40 cycles of: 95 °C for 20 s, 56 °C or 55 °C (for ΦCB2047-A or ΦNYA respectively) for 20 s, 72 °C for 20 s, followed by 5 min at 72 °C. Fluorescence measurements were conducted at the end of each cycle at 72 °C. Melt curves were generated after each assay to verify the specificity of the amplification by heating from 50 to 100 °C, read every 1 °C. Standards were developed from plasmids containing cloned sequences (TOPO TA cloning kit for sequencing [Invitrogen,

Carlsbad, CA]) and 10-fold serial dilutions of these samples in 10 mM Tris-HCl were used in the reactions. Standard curves were determined as the correlation between the log of gene copy numbers and the Ct. In all cases, correlation coefficients for standard curves were ≥ 0.99 .

Identification of single and polylysogens and putative phage integration site

A 110-bp fragment containing part of Φ CB2047-A endolysin gene amplified by PCR with the primer pair 2047A-C_for/2047A-C_rev (Table 3.1) was used as a diagnostic assay for Φ CB2047-A lysogenized cells. A 128-bp fragment containing part of Φ NYA endolysin gene amplified by PCR with the primer pair 2047PP1_for/2047PP1_rev (Table 3.1) was used as the Φ NYA-specific probe to identify cells lysogenized by Φ NYA. A 1279-bp and 484-bp fragment amplified by primer pairs jxn761U_for/int937_rev and jxn1105D_for/jxn1105D_rev (Table 3.1) were used to identify the putative integration sites for each phage, respectively.

RNA extraction, reverse transcription and quantitative PCR

Filters were thawed on ice and RNA and DNA were co-extracted using the AllPrep DNA/RNA Mini Kit (Qiagen, Valencia, CA) following the manufacturer's instructions. After extraction of the RNA, DNA was removed from RNA using the TURBO DNA-free Kit (Ambion, Austin, TX). The resulting RNA sample was converted to cDNA using M-MLV Reverse Transcriptase and random hexamers (Invitrogen, Carlsbad, CA). 0.5 μ L of the random hexamers (500 ng/ μ L), 1.0 μ L dNTPs (10 mM), and 10.5 μ L of the RNA sample (6 ng/ μ L) were heated to 65°C for 5 min and then chilled on ice. Four μ L 5X First Strand Buffer [250 mM Tris-HCl (pH 8.3), 375 mM KCl, 15 mM MgCl₂], 2 μ L 0.1 M dithiothreitol, and 1 μ L Rnase Out (Invitrogen) was then added. The solution was mixed and incubated at 37°C for 2 min. One μ L

M-MLV RT (200 units/ μ L) was added to the solution and incubated 10 min at 25°C followed by 50 min at 37°C. The enzyme was inactivated by heating 15 min at 70°C.

Transcripts diagnostic of the host SOS response (*recA* and *lexA*), phage DNA replication/repair (*ssb*, Rad52/22), phage excision/cell lysis (endolysin) and prophage integration (*int*, *cro/cI* like repressors) were measured and normalized to the expression of three host reference genes (*alaS*, *map*, and *rpoC*). Primers were designed for each gene and are shown in Table 3.1. The three host reference genes (*map*, *rpoC*, and *alaS*) were selected using previously described criteria (Nieto *et al.* 2009). Primers were designed using the Primer3 online software tool (<http://frodo.wi.mit.edu/>) and the genome sequences of the host and Φ CB2047-A and are listed in Table 1. All primer sets were tested on genomic DNA or purified phage and yielded a single band of the expected size (range of amplicons from 160-203bp).

The PCR was done in a Bio-Rad DNA Engine Opticon 2 real-time PCR detector (Bio-Rad, Hercules, CA) with SYBR Green PCR reagents (Invitrogen, Carlsbad, CA). Twenty-five microliter reactions were prepared in 0.2 ml skirted 96-well qPCR plates (Thermo Scientific, Waltham, MA) with 12.5 μ L SYBR Green Pre-Mix 2X, 7.5 μ L dH₂O, 1.25 μ L forward primer, 1.25 μ L reverse primer, and 2.5 μ L of the sample cDNA. Plates were heated for 95°C for 3 min, followed by 40 cycles of 95°C for 20 s, 55°C for 20 s, 72°C for 20 s. At the conclusion of the cycling conditions, the reactions were held at 72°C for 5 min. Melting curves were generated after each assay to verify the specificity of the amplification by heating the samples from 50°C to 100°C at 1°C/s and taking fluorescence measurements every 1°C. These melt curves consistently showed a single peak per primer set indicating high specificity of the primer sets.

Statistical analysis ANOVA mean separations were done using the Tukey's Honestly Significant Difference test in SigmaPlot 11.0 (Systat Software, Inc., Chicago, IL). RT-qPCR data analysis and the normalized relative transcript quantity was calculated using the qBASE method which permits the use of multiple reference genes to guarantee reference gene stability as well as the use of biological replicates to guarantee experiment reproducibility (Hellemans *et al.* 2007). These data were normalized to the three reference genes and expressed relative to the T₀ values for each sample set.

Results

Sulfitobacter sp. CB2047 and its infecting phage ΦCB2047-B (an N4-like lytic phage) and ΦCB2047-A and -C (temperate phages) were isolated for use as model phage-host systems to characterize the role viruses play in reshaping host metabolism and marine biogeochemical cycles (Budinoff 2012). Plaque assays using the newly purified ΦCB2047-B phage stocks and *Sulfitobacter* sp. CB2047 as a host organism always revealed two distinct plaque morphologies: one clear in appearance (characteristic of a lytic phage like ΦCB2047-B) and the other “bull's-eye” in appearance (Φ2047A), indicative of temperate phage.

Initially attributing the observation of the different plaque morphologies to contamination of lytic phage (ΦCB2047-B) stocks with either of temperate phage (ΦCB2047-A or -C) multiple attempts were made to produce new phage stocks and avoid cross contamination during infections. However, the dual plaque morphologies were always observed on agar overlay plates. We, therefore, hypothesized that our host organism may be lysogenized by a prophage that is induced upon superinfection with a secondary phage. Sequencing of the host bacterium

Sulfitobacter sp. CB2047 identified a prophage, Φ NYA, in the host genome that is distinct, yet highly similar to both Φ CB2047-A and -C at the nucleotide level, adding further complexity to the system. Genome-wide nucleotide similarity alignments of Φ CB2047-A and Φ NYA showed that phage Φ CB2047-A shares 85.65 % identity with Φ NYA. A CoreGenesUniqueGenes (CGUG) (Mahadevan *et al.* 2009) analysis identified 58 highly homologous genes (BLASTp threshold score, 75) between Φ CB2047-A and Φ NYA.

Superinfection induces conversion of the prophage

As a first approach to investigate the effect of superinfection on lysogenized *Sulfitobacter* cells, we infected *Sulfitobacter* sp. CB2047 with Φ CB2047-A and monitored the population dynamics of the resident prophage, Φ NYA, and the superinfecting phage, Φ CB2047-A, over a 10 h infection cycle. By the end of the 10 hour experiment, superinfection of *Sulfitobacter* sp. CB2047 resulted in a 1600-fold increase in the superinfecting phage Φ CB2047-A (from 5×10^8 [$\pm 5 \times 10^7$] to 7×10^{11} [$\pm 2 \times 10^{11}$] virions/mL compared to a 50-fold increase in the resident prophage Φ NYA (from 9×10^8 [$\pm 1 \times 10^8$] to 5×10^{10} [$\pm 6 \times 10^9$] virions/mL (Figure 3.1a).

Compared to the uninfected controls, there was a significant increase (24-fold, $p < 0.05$) in Φ NYA gene copy numbers in Φ CB2047-A infected cultures relative to the uninfected controls by 10 hrs post-infection (Figure 3.1b). The increase in prophage induction resulted in the production of c.a. $5 \times 10^{10} \text{ mL}^{-1}$ new Φ NYA virions in the infected cultures compared to an increase of c.a. $1 \times 10^8 \text{ mL}^{-1}$ Φ NYA virions in the uninfected cultures by 10 hrs. The latter is consistent with host growth and, thus predicted to represent integrated prophage rather than induced phage (i.e. virions) (Figure 3.1b). The growth of Φ CB2047-A superinfected (MOI=0.06) *Sulfitobacter* cultures was nearly identical to that of the uninfected controls until the onset of cell

lysis at ~5 hrs p.i., when significant ($p < 0.05$) differences in growth between Φ CB2047-A superinfected and uninfected control cultures were observed (Figure 3.1c). By 10 hrs p.i., cell densities in the superinfected cultures were approximately 40% of the uninfected controls.

Prophage substitution and the establishment of polylysogeny

In order to assess the integration profiles of Φ CB2047-A in *Sulfitobacter* sp. CB2047, the host was infected with Φ CB2047-A at an MOI of 0.06 and at 4 and 8h p.i. aliquots of the infected culture were plated onto complex medium and the resulting colonies probed for the presence/absence of the resident prophage, Φ NYA, and the superinfecting phage, Φ CB2047-A, using PCR assays targeting diagnostic regions of each phage (see methods). Our results show that ~8% of the recovered *Sulfitobacter* colonies were no longer PCR-positive for Φ NYA and instead were PCR-positive for Φ CB2047-A. Furthermore, ~18% of the colonies appeared polylysogenized as they were PCR-positive for both Φ CB2047-A and Φ NYA. The remaining colonies that were screened resembled the parent host strain (i.e. PCR-positive for Φ NYA) (Table 3.2 & b).

Integration-dependent bacteriophage immunity

To determine if *Sulfitobacter* lysogens or polylysogens possessed immunity or superinfection inhibition, we independently infected single and polylysogenized *Sulfitobacter* strains with Φ NYA and Φ CB2047-A and monitored cell lysis (Figure 3.2) and phage production (Figure 3.3) across an infection cycle. Our results show that strains lysogenized by Φ NYA (CB2047 wild type) were resistant to cell lysis by Φ NYA but were susceptible to lysis by Φ CB2047-A (Figure 3.2a). Superinfection with Φ CB2047-A resulted in a $\sim 10^4$ fold -increase in

production of new Φ CB2047-A virions (Figure 3.3a) and a ~100-fold increase in Φ NYA induction in these cultures (Figure 3.3b). Superinfection with Φ NYA yielded no increase in prophage induction (Figure 3.3a&b). A *Sulfitobacter* Φ NYA/ Φ CB2047-A double lysogen (designated as strain YM2AD) was resistant to cell lysis when superinfected with either Φ NYA or Φ CB2047-A (Figure 3.2b). Superinfection of the double lysogens also produced no new phage (Figure 3.3c-d). Strains lysogenized with Φ CB2047-A alone (designated as YM3A) were resistant to cell lysis by Φ CB2047-A but were susceptible to cell lysis by Φ NYA (Figure 3.2c). Superinfection with Φ NYA resulted in a ~100-fold increase in production of new Φ NYA virions (Figure 3.3e) and a ~100-fold increase in Φ CB2047-A induction in these cultures (Figure 3.3f). Superinfection with Φ CB2047-A yielded no increase in resident prophage induction (Figure 3.3e-f).

Phage integration site

The genome of Φ NYA is flanked by a 15 bp GC rich direct terminal repeat (designated *attP*) that is homologous to the 3' end of the host tRNA-Leu gene (designated *attB*). Genome sequence analysis of Φ CB2047-A revealed a homologous 15bp *attP* sequence within the Φ CB2047-A genome. As most phage and other genetic elements tend to have a high affinity for integration into tRNA genes (Fouts 2006), we hypothesized that Φ NYA and Φ CB2047-A share a common integration site on the *Sulfitobacter* sp. CB2047 genome. To determine if the tRNA-Leu gene, used by Φ NYA for integration, was also target for Φ CB2047-A integration, we amplified fragments from two locations flanking the bacterial and prophage attachment sites (see Figure 3.4a). Our results indicate that Φ CB2047-A and Φ NYA share a common integration site during prophage substitution events, with both phage utilizing the tRNA-Leu gene as a putative

insertion site (Figure 3.4a). To determine if polylysogenic *Sulfitobacter* strains, that is strains that are PCR-positive for both Φ NYA and Φ CB2047-A, share a similar integration site, we amplified the junction fragments between host DNA, the 15 bp integration site and the head and tail regions of Φ NYA and Φ CB2047-A (see Figure 3.4b). We also amplified the Φ NYA tail- Φ CB2047-A -head region to determine the integration orientation for both phages (Figure 3.4b). Our results indicate that both phages share a common integration site with the head of Φ CB2047-A attached to the tail end of Φ NYA in the host chromosome (Figure 3.4b).

Integration site conserved in other *Sulfitobacter*

To determine the prevalence of the putative bacterial attachment site (*attB*) among other members of the *Sulfitobacter* genus, a BLASTN analysis of the 13 publicly available *Sulfitobacter* genomes was conducted. The 15 bp putative bacterial attachment site (*attB*) sequence was identified (BLASTN E-value cutoff, 5) in 62% (8 out of 13) of the *Sulfitobacter* genomes queried (Table 3.4). With our data confirming the presence of a common putative integration site among a majority of the *Sulfitobacter* strains probed, we sought to determine if the presence of the putative integration site in a *Sulfitobacter* genome could be indicative of a potential susceptibility to infection by our two phage. To determine if Φ NYA and Φ CB2047-A can infect and integrate into the genomes of *Sulfitobacter* strains with the putative bacterial attachment site (*attB*) present in their genomes, we attempted to infect five *Sulfitobacter* strains with Φ NYA and Φ CB2047-A and then probed individual colonies for integration using primers specific for each phage. After c.a. 10h post infection, cells were plated onto a complex medium and individual colonies screened for the integration of either phage by PCR assay. Our results show both Φ NYA and Φ CB2047-A infect and lysogenize all five *Sulfitobacter* strains

tested (Table 3.5). Yet, unlike *Sulfitobacter* strain CB2047, no evidence of culture lysis is observed at any time during the infection process. An analysis of the genomes of the five *Sulfitobacter* strains showed a conservation of the genes flanking the 3' end of the *attB* site among all five strains (Figure 3.6).

Host and phage gene expression during induction

To characterize the changes in gene expression associated with prophage induction by superinfection and to identify a putative mechanism by which the resident prophage Φ NYA is induced in *Sulfitobacter* cells as a result of superinfection, we monitored the expression of the host SOS genes, *recA* and *lexA*, as well as select phage genes involved in the establishment of lysogeny (integrase [*int*], *cro/cI* like repressor [*rep*]), phage DNA replication and repair (single stranded DNA binding protein gene [*ssb*], double stranded DNA break repair gene [*rad52*]) and cell lysis (endolysin [*lys*]) over an infection cycle.

Our results from the gene expression assays indicate that relative to the uninfected controls, gene expression in the superinfected cells was significantly ($p < 0.05$) elevated for all host and phage genes monitored 3 and 6 hours post infection (Figure 3.6). Superinfection resulted in an initial 5-fold increase and 2-fold increase in *lexA* expression 3 and 6h post-infection, respectively. For *recA* transcripts a 2- and 3-fold increase in gene expression 3 and 6h post-infection, respectively, was observed (Figure 3.6a). Superinfection also resulted in an upregulation of Φ NYA lysogeny genes, with a ~19- and 5-fold increase in expression of Φ NYA integrase and repressor genes being observed 3h post superinfection, respectively (Figure 3.6b). Φ NYA DNA replication and repair genes *ssb* and *rad52* were upregulated by 74- and 50-fold,

respectively, 3 h post infection (Figure 3.6b). Φ NYA endolysin genes were upregulated 12-fold 3h post infection (Figure 3.6b).

Gene expression of the superinfecting phage, Φ CB2047-A, was also upregulated during superinfection. Since Φ CB2047-A is not present in our host genome prior to infection, changes in Φ CB2047-A gene expression are reported relative to transcript numbers measured at our initial sampling timepoint, T=0h, immediately following addition of phage (Figure 3.7). Repressor gene expression of the superinfecting phage, Φ CB2047-A, was upregulated 66-fold at 6h post-infection compared to an 8-fold increase in resident prophage Φ NYA repressor gene expression at the same timepoint (Figure 3.7a). Similarly, endolysin gene expression of the superinfecting phage, Φ CB2047-A, was upregulated-2700 fold 6h post-infection while the resident prophage, Φ NYA, endolysin gene expression was upregulated 44-fold at the same timepoint relative to expression levels at the start of superinfection (Figure 3.7b). It should be noted that 6h after superinfection Φ CB2047-A virion concentration in the infected cultures was 10-fold higher than the concentration of Φ NYA virions, and by 10 hrs post-infection Φ CB2047-A virions outnumbered Φ NYA virions by 16 to 1 (see Figure 3.1a).

Discussion

In this study we infected *Sulfitobacter* lysogens with a secondary phage and monitored resident prophage induction dynamics and the associated changes in lysogen and phage gene expression that occurs during superinfection. Superinfecting lysogenized *Sulfitobacter* cells with secondary phage yielded three distinct outcomes which might be reflective of events that are common in nature; a) induction and conversion to the lytic cycle of the resident prophage

resulting in cell lysis b) excision of the resident prophage and the subsequent integration of the superinfecting phage without cell lysis and c) the co-integration of both resident prophage and superinfecting phage in the same cell thereby establishing polylysogeny. Prophages serve as genetic reservoirs and mediate the transfer of genetic information from one bacterium to another when induced, thereby increasing microbial metabolic capabilities and microbial genetic diversity (Breitbart 2012, Paul 2008, Sime-Ngando 2014). Any environmental or biological factors that increase the rates at which prophage are induced in the environment will inadvertently increase the rate at which genetic information is transferred from one organism to another. While a strong emphasis has been made in the past to characterize the physical and chemical factors that induce prophage in the marine environment (Chen *et al.* 2006, Jiang and Paul 1996, Maiques *et al.* 2006, Úbeda *et al.* 2005, Zhao *et al.* 2010a), there is very little data about the biological means by which prophage can be induced in the environment (Espeland *et al.* 2004). Our data strongly points to superinfection as a mechanism for increasing the transfer of genetic material in the environment and also as a mechanism for enhancing genetic diversity of microbial populations. For the phage-host system used in this study superinfection increased induction of the resident prophage ~24 fold and increased the genetic diversity of 10% of the infected population by introducing new genes into the host genome through the establishment of lysogeny and/or polylysogeny. Lysogeny or polylysogeny introduced new genes that made up 1 and 2% of the host genome, respectively. Polylysogeny establishment by our superinfecting phage Φ CB2047-A, also provided other benefits for both resident phage, Φ NYA, and the host bacterium. The host bacterium benefited from the upregulation of superinfection exclusion and repressor genes of both prophage that provided the host with immunity against subsequent infections and excluded the superinfecting phage, Φ CB2047-A, DNA from competing with the

resident prophage, Φ NYA, DNA for the same host which may have ended in the destruction of the host and resident phage as described in other systems (Berngruber *et al.* 2010, Canchaya *et al.* 2003). Our experiments infecting *Sulfitobacter* single and polylysogens with homoimmune phage supports this observation as no new phage virions were produced from our infections and no cell lysis was observed in any of our homoimmune infection experiments.

To characterize the changes in gene expression associated with prophage induction by superinfection and to identify a putative mechanism by which the resident prophage are induced from *Sulfitobacter* lysogens due to superinfection, we monitored the expression of select host and phage genes. Monitoring the transcriptional changes that occur during superinfection allowed us to characterize the putative life style (lytic/lysogenic) preferences of both superinfecting phage and resident prophage during superinfection events.

Phage integrases are site-specific recombinases that mediate insertion of the phage into the host genome during lysogeny (Groth *et al.* 2000). Phage repressors, which are mostly host RecA-dependent auto-cleavable proteins, bind to specific operators to prevent expression of phage genes involved in lytic development (Echols and Green 1971). Single-stranded DNA [ssDNA] binding proteins (ssb) remove secondary structures from ssDNA allowing host recombinases, such as RecA, more direct access to ssDNA during DNA repair (Baluch *et al.* 1980, Chase and Williams 1986). SSB-deficient mutants have been demonstrated to be defective in SOS repair (Lieberman and Witkin 1983, Whittier and Chase 1983) and prophage induction (Vales *et al.* 1980). The double-stranded DNA [dsDNA] break repair gene *rad52/22* which encodes for an exonuclease expands DNA nicks into gaps, to allow joint molecules to form during DNA break repair (Hosoda 1976). Rad52 is required for most recombination and repair processes and also for the production of viable virion progeny (Chen and Bernstein 1988). Rad52

mutants have been demonstrated to produce non-viable phage with incomplete genomes (Chen and Bernstein 1988). Bacteriophage encoded endolysin are peptidoglycan hydrolases produced towards the end of phage lytic cycles to cleave host cell peptidoglycan to allow virion progeny to be released (Loessner 2005).

The significant upregulation of prophage DNA replication and repair genes *rad52* and *ssb* observed in our superinfected cultures is suggestive of a conversion to the lytic cycle by our resident prophage and an active replication of prophage virions in preparation for cell lysis, evidence for which we see in the significant upregulation in expression of phage lysis genes as superinfection progresses. Transcriptional analysis of the superinfecting phage and resident prophage endolysin genes also allowed us to make comparative assessments of both phages to decipher which phage was mainly responsible for cell lysis in the superinfected cultures. Our data clearly points to the superinfecting phage Φ CB2047-A, as the main driver for cell lysis in the superinfected cultures with endolysin gene expression levels increasing 2700-fold for Φ CB2047-A compared to a 44-fold increase in endolysin gene expression for Φ NYA. This may be suggestive of the superinfecting phage, Φ CB2047-A, utilizing the lytic cycle as its main lifestyle during superinfections while the resident prophage maintains lysogeny as a preferred lifestyle with the lytic phase occurring in only a small fraction of the Φ NYA lysogenized cells. The lytic cycle of phages has been demonstrated to an effective mechanism of controlling microbial populations (Hewson *et al.* 2001) and shaping marine biogeochemical cycles (Wilhelm and Suttle 1999). Superinfection of our *Sulfitobacter* lysogens resulted in significant lysis of the infected population compared to the uninfected controls and may suggestive of superinfection as an important mechanism for microbial population control and the production of bioavailable

nutrients for microbes in nutrient-limiting environments where prophage inductions will not normally occur (Paul 2008).

Our data also provides evidence for the establishment/maintenance of lysogeny in our superinfected populations. Φ CB2047-A repressor expression levels increased 65-fold post-infection while Φ NYA expression levels increased 8-fold 6h after infection with Φ CB2047-A. Since Φ NYA was already in a lysogenic state, we anticipated very little upregulation in repressor transcription levels as lysogeny had been established. On the other hand, we expected Φ CB2047-A repressor expression levels to be significantly upregulated as more Φ CB2047-A integrated into *Sulfitobacter* cell chromosomes. The observed increase in Φ NYA repressor expression might be indicative of attempts by Φ NYA to prevent conversion to the lytic cycle thereby protecting itself from being destroyed by superinfection and also protecting the host cell from lysis. The increase in integrase transcription also supports the observed increase in prophage integration rates in our superinfected cultures. Integrase transcription increased by 19-fold by the third hour after infection and this also coincided with an 8% increase in lysogeny in our superinfected cultures (Figure 3.6b and Table 3.2). It should be noted that the primers used for our integrase expression analysis do not discriminate between Φ NYA and Φ CB2047-A so quantitative estimates cannot be made about contributions of each phage towards the total increase in integrase transcripts observed.

Most well studied prophage utilize the host SOS response to escape from potentially damaged cells by converting to the lytic phase (Baluch *et al.* 1980, Castellazzi *et al.* 1972, Higashitani *et al.* 1992, Jiang and Paul 1996). The SOS response is utilized by cells to tolerate and respond to DNA damage by upregulating genes involved in cell survival and DNA repair (Kuzminov 1999, Little and Gellert 1983, Radman 1975, Walker 1984). LexA and RecA

proteins are the main regulators of the host SOS response (Horii *et al.* 1981, Little and Mount 1982). Under normal growth conditions phage repressors and host LexA proteins bind to specific phage and host operators to prevent the expression of phage lytic genes and host SOS-regulated genes respectively (Little and Mount 1982). Adverse conditions *e.g.* DNA damage, activate RecA which induces the auto-cleavage of phage repressors and host LexA proteins (Little 1984, Sauer *et al.* 1982). Cleaved phage repressors and LexA proteins are unable to bind to their specific operators leading to the expression of phage lytic genes (prophage induction) and host SOS-response genes respectively (Little 1993). Phage repressors generally have a lower affinity to host RecA proteins leading to a generally slower cleavage of phage repressors than host LexA proteins and this ensures that prophage induction only occurs in cells that have undergone extensive damage are unlikely to survive and not in cells undergoing minimal DNA damage (Friedman *et al.* 1984, Little 1993).

Previous studies in our lab have indicated that *Sulfitobacter* sp. CB2047 resident prophage, Φ NYA, is mitomycin C inducible (see Figure 3.8). It is well established that the a large proportion of chemical agents (including mitomycin c) that induce prophage induction in cells generally damage host cell DNA and illicit an SOS response characterized by the activation of the RecA and LexA proteins (Frye *et al.* 2005, Hare *et al.* 2014, Roberts and Roberts 1975). It is also well established that virus infection results in host DNA damage and the subsequent accumulation of single-stranded DNA, which activates the host cell SOS response (Friedman *et al.* 1984, Higashitani *et al.* 1992). We, therefore, hypothesized that the switch to the lytic phase by the resident prophage is a result of the activation of the host SOS response due to virus-mediated DNA damage during infection. To address this hypothesis we monitored the

expression of host SOS response genes *recA* and *lexA* and phage genes involved in the establishment of lysogeny.

Superinfection of *Sulfitobacter* lysogens resulted in an upregulation in transcription of both *lexA* and *recA* genes similar to other reported studies monitoring gene expression during prophage induction with chemical and physical agents (Courcelle *et al.* 2001, Frye *et al.* 2005, Hare *et al.* 2014, Maiques *et al.* 2006). In *E. coli* cells undergoing DNA damage due to UV exposure, LexA cleavage was shown to occur within minutes after exposure with a subsequent increase in LexA expression and accumulation occurring after 20 minutes as DNA damage is repaired or the damaging agent disappears (Sassanfar and Roberts 1990). LexA along with other genes (*e.g.* one strand repair genes *uvrA,B,D*) are among the first genes to be induced during SOS response and the increase in expression of these genes is usually less than 10 times that of their constitutive expression (Kuzminov 1999). As the concentration of LexA in the cell diminishes, genes suppressed by LexA (including the *lexA* gene) are more frequently transcribed (Courcelle *et al.* 2001, Sassanfar and Roberts 1990). Upregulation of *lexA* transcription during SOS responses has been documented in studies using mitomycin C and H₂O₂ as inducing agents to study *Salmonella* phage and host gene expression during prophage induction (Frye *et al.* 2005) and studies monitoring the SOS gene expression profiles in UV exposed *E. coli* cells (Courcelle *et al.* 2001).

We propose the following model of prophage induction in *Sulfitobacter* sp. 2047. A) Secondary phage infection results in DNA damage and the accumulation of single stranded DNA B) Host DNA damage elicits SOS response with an increased production of RecA proteins C) RecA proteins cleave phage repressors inactivating them and resulting in a switch to the lytic cycle by the resident prophage. This model is consistent with observations of our study, and

provides direction for future investigations using *recA* and *lexA* *Sulfitobacter* mutants to characterize the mechanisms behind this temperate to lytic switch.

We acknowledge that as we were looking at the bulk phage induction properties of a bacterial population, we do not know if each of these scenarios (induction, lysogeny, lysis) are occurring independently in multiple cells or whether a combination of these scenarios occurs in individual cells. For instance, it is impossible to tell using our current methods if induction occurs in a subset of the cells that are superinfected by secondary phage, or whether the superinfected cells cause adjacent uninfected cells to induce their resident prophage to convert to the lytic cycle. Although we did not investigate which of these alternative scenarios might be occurring in our infected cultures, we have shown here a significant increase in resident prophage induction as a result of superinfection by a secondary phage and provide an environmentally relevant biological mechanism by which prophage in lysogenized cells can be induced to go in the lytic cycle in nature. Altogether, our data points to superinfection as an environmentally relevant mechanism by which the transfer of genetic information is accelerated in the environment and mechanism by which phage and host can prolong their survival in the environment.

Acknowledgement

We would like to thank all the wonderful undergraduates who contributed to this chapter in numerous ways: Andrew Garrone, Katherine Moccia, William Brading and Yi-Ting Huang. We are grateful to Dr. Balbina Nogales for providing *Sulfitobacter* strains 3SOLIMAR09 and 1FIGIMAR09 used in this study. This work was supported by NSF grant OCE-1061352 to A.B.

References

- Ankrah NY, Budinoff CR, Wilson WH, Wilhelm SW, Buchan A (2014a). Genome Sequences of Two Temperate Phages, Φ CB2047-A and Φ CB2047-C, Infecting *Sulfitobacter* sp. Strain 2047. *Genome Announcements* **2**: e00108-00114.
- Ankrah NYD, Lane T, Budinoff CR, Hadden MK, Buchan A (2014b). Draft Genome Sequence of *Sulfitobacter* sp. CB2047, a Member of the Roseobacter Clade of Marine Bacteria, Isolated from an *Emiliana huxleyi* Bloom. *Genome Announcements* **2**.
- Ankrah NYD, May AL, Middleton JL, Jones DR, Hadden MK, Gooding JR *et al.* (2014c). Phage infection of an environmentally relevant marine bacterium alters host metabolism and lysate composition. *ISME J* **8**: 1089-1100.
- Baluch J, Chase J, Sussman R (1980). Synthesis of recA protein and induction of bacteriophage lambda in single-strand deoxyribonucleic acid-binding protein mutants of *Escherichia coli*. *J Bacteriol* **144**: 489-498.
- Berngruber TW, Weissing FJ, Gandon S (2010). Inhibition of superinfection and the evolution of viral latency. *J Virol* **84**: 10200-10208.
- Breitbart M (2012). Marine viruses: truth or dare. *Annual Review of Marine Science* **4**: 425-448.
- Brüssow H, Canchaya C, Hardt W-D (2004). Phages and the evolution of bacterial pathogens: from genomic rearrangements to lysogenic conversion. *Microbiology and Molecular Biology Reviews* **68**: 560-602.
- Buchan A, González JM, Moran MA (2005). Overview of the marine Roseobacter lineage. *Applied and environmental microbiology* **71**: 5665-5677.

- Buchan A, LeCleir GR, Gulvik CA, Gonzalez JM (2014). Master recyclers: features and functions of bacteria associated with phytoplankton blooms. *Nat Rev Micro* **12**: 686-698.
- Budinoff CR, Hollibaugh JT (2007). Ecophysiology of a Mono Lake Picocyanobacterium. *Limnology and Oceanography* **52**: 2484-2495.
- Budinoff CR (2012). Diversity and activity of Roseobacters and roseophage.
- Calendar R (2006). *The Bacteriophages*. Oxford University Press: New York.
- Campos J, Martínez E, Marrero K, Silva Y, Rodríguez BL, Suzarte E *et al.* (2003). Novel type of specialized transduction for CTX ϕ or its satellite phage RS1 mediated by filamentous phage VGJ ϕ in *Vibrio cholerae*. *J Bacteriol* **185**: 7231-7240.
- Canchaya C, Proux C, Fournous G, Bruttin A, Brüssow H (2003). Prophage genomics. *Microbiology and Molecular Biology Reviews* **67**: 238-276.
- Castellazzi M, George J, Buttin G (1972). Prophage induction and cell division in *E. coli*. *Molecular and General Genetics MGG* **119**: 153-174.
- Chase JW, Williams KR (1986). Single-stranded DNA binding proteins required for DNA replication. *Annu Rev Biochem* **55**: 103-136.
- Chen DS, Bernstein H (1988). Yeast gene RAD52 can substitute for phage T4 gene 46 or 47 in carrying out recombination and DNA repair. *Proceedings of the National Academy of Sciences* **85**: 6821-6825.
- Chen F, Wang K, Stewart J, Belas R (2006). Induction of multiple prophages from a marine bacterium: a genomic approach. *Applied and Environmental Microbiology* **72**: 4995-5001.

- Courcelle J, Khodursky A, Peter B, Brown PO, Hanawalt PC (2001). Comparative gene expression profiles following UV exposure in wild-type and SOS-deficient *Escherichia coli*. *Genetics* **158**: 41-64.
- Echols H, Green L (1971). Establishment and maintenance of repression by bacteriophage lambda: the role of the cI, cII, and cIII proteins. *Proceedings of the National Academy of Sciences* **68**: 2190-2194.
- Espeland EM, Lipp EK, Huq A, Colwell RR (2004). Polylysogeny and prophage induction by secondary infection in *Vibrio cholerae*. *Environmental Microbiology* **6**: 760-763.
- Fouts DE (2006). Phage_Finder: automated identification and classification of prophage regions in complete bacterial genome sequences. *Nucleic acids research* **34**: 5839-5851.
- Friedman DI, Olson ER, Georgopoulos C, Tilly K, Herskowitz I, Banuett F (1984). Interactions of bacteriophage and host macromolecules in the growth of bacteriophage-lambda. *Microbiological Reviews* **48**: 299-325.
- Frye JG, Porwollik S, Blackmer F, Cheng P, McClelland M (2005). Host gene expression changes and DNA amplification during temperate phage induction. *J Bacteriol* **187**: 1485-1492.
- Ghosh D, Roy K, Williamson KE, Srinivasiah S, Wommack KE, Radosevich M (2009). Acyl-homoserine lactones can induce virus production in lysogenic bacteria: an alternative paradigm for prophage induction. *Applied and environmental microbiology* **75**: 7142-7152.

- Groth AC, Olivares EC, Thyagarajan B, Calos MP (2000). A phage integrase directs efficient site-specific integration in human cells. *Proceedings of the National Academy of Sciences* **97**: 5995-6000.
- Gulvik CA, Buchan A (2013). Simultaneous catabolism of plant-derived aromatic compounds results in enhanced growth for members of the Roseobacter lineage. *Applied and environmental microbiology* **79**: 3716-3723.
- Hare JM, Ferrell JC, Witkowski TA, Grice AN (2014). Prophage Induction and Differential RecA and UmuDAb Transcriptome Regulation in the DNA Damage Responses of *Acinetobacter baumannii* and *Acinetobacter baylyi*. *PloS one* **9**: e93861.
- Hellemans J, Mortier G, De Paepe A, Speleman F, Vandesompele J (2007). qBase relative quantification framework and software for management and automated analysis of real-time quantitative PCR data. *Genome biology* **8**: R19.
- Hewson I, O'Neil JM, Dennison WC (2001). Virus-like particles associated with *Lyngbya majuscula* (Cyanophyta; Oscillatoriaceae) bloom decline in Moreton Bay, Australia. *Aquatic Microbial Ecology* **25**: 207-213.
- Higashitani N, Higashitani A, Roth A, Horiuchi K (1992). SOS induction in *Escherichia coli* by infection with mutant filamentous phage that are defective in initiation of complementary-strand DNA synthesis. *J Bacteriol* **174**: 1612-1618.
- Horii T, Ogawa T, Nakatani T, Hase T, Matsubara H, Ogawa H (1981). Regulation of SOS functions: purification of *E. coli* LexA protein and determination of its specific site cleaved by the RecA protein. *Cell* **27**: 515-522.

- Hosoda J (1976). Role of genes 46 and 47 in bacteriophage T4 reproduction: III. Formation of joint molecules in biparental recombination. *Journal of molecular biology* **106**: 277-284.
- Jiang SC, Paul JH (1996). Occurrence of lysogenic bacteria in marine microbial communities as determined by prophage induction. *Marine Ecology-Progress Series* **142**: 27.
- Kuzminov A (1999). Recombinational Repair of DNA Damage in *Escherichia coli* and Bacteriophage λ . *Microbiology and Molecular Biology Reviews* **63**: 751-813.
- Leitet C, Riemann L, Hagström Å (2006). Plasmids and prophages in Baltic Sea bacterioplankton isolates. *Journal of the Marine Biological Association of the United Kingdom* **86**: 567-575.
- Lieberman HB, Witkin EM (1983). DNA degradation, UV sensitivity and SOS-mediated mutagenesis in strains of *Escherichia coli* deficient in single-strand DNA binding protein: effects of mutations and treatments that alter levels of exonuclease V or RecA protein. *Molecular and General Genetics MGG* **190**: 92-100.
- Little J (1993). LexA cleavage and other self-processing reactions. *J Bacteriol* **175**: 4943.
- Little JW, Mount DW (1982). The SOS regulatory system of *Escherichia coli*. *Cell* **29**: 11-22.
- Little JW, Gellert M (1983). The SOS regulatory system: control of its state by the level of RecA protease. *Journal of molecular biology* **167**: 791-808.
- Little JW (1984). Autodigestion of lexA and phage lambda repressors. *Proceedings of the National Academy of Sciences* **81**: 1375-1379.
- Loessner MJ (2005). Bacteriophage endolysins—current state of research and applications. *Curr Opin Microbiol* **8**: 480-487.

- Lwoff A (1953). Lysogeny. *Bacteriological Reviews* **17**: 269.
- Mahadevan P, King JF, Seto D (2009). CGUG: in silico proteome and genome parsing tool for the determination of. *BMC research notes* **2**: 168.
- Maiques E, Úbeda C, Campoy S, Salvador N, Lasa Í, Novick RP *et al.* (2006). β -Lactam antibiotics induce the SOS response and horizontal transfer of virulence factors in *Staphylococcus aureus*. *J Bacteriol* **188**: 2726-2729.
- Nieto PA, Covarrubias PC, Jedlicki E, Holmes DS, Quatrini R (2009). Selection and evaluation of reference genes for improved interrogation of microbial transcriptomes: case study with the extremophile *Acidithiobacillus ferrooxidans*. *BMC Molecular Biology* **10**: 63.
- Paul JH (2008). Prophages in marine bacteria: dangerous molecular time bombs or the key to survival in the seas? *The ISME journal* **2**: 579-589.
- Radman M (1975). SOS repair hypothesis: phenomenology of an inducible DNA repair which is accompanied by mutagenesis. *Molecular mechanisms for repair of DNA*. Springer. pp 355-367.
- Refardt D (2011). Within-host competition determines reproductive success of temperate bacteriophages. *The ISME journal* **5**: 1451-1460.
- Roberts JW, Roberts CW (1975). Proteolytic cleavage of bacteriophage lambda repressor in induction. *Proceedings of the National Academy of Sciences* **72**: 147-151.
- Sassanfar M, Roberts JW (1990). Nature of the SOS-inducing signal in *Escherichia coli*: The involvement of DNA replication. *Journal of molecular biology* **212**: 79-96.

- Sauer R, Ross M, Ptashne M (1982). Cleavage of the lambda and P22 repressors by recA protein. *Journal of Biological Chemistry* **257**: 4458-4462.
- Sime-Ngando T (2014). Environmental bacteriophages: viruses of microbes in aquatic ecosystems. *Frontiers in microbiology* **5**.
- Stopar D, Černe A, Žigman M, Poljšak-Prijatelj M, Turk V (2004). Viral abundance and a high proportion of lysogens suggest that viruses are important members of the microbial community in the Gulf of Trieste. *Microbial ecology* **47**: 1-8.
- Úbeda C, Maiques E, Knecht E, Lasa Í, Novick RP, Penadés JR (2005). Antibiotic-induced SOS response promotes horizontal dissemination of pathogenicity island-encoded virulence factors in staphylococci. *Molecular microbiology* **56**: 836-844.
- Vales LD, Chase JW, Murphy JB (1980). Effect of ssbA1 and lexC113 mutations on lambda prophage induction, bacteriophage growth, and cell survival. *J Bacteriol* **143**: 887-896.
- Walker GC (1984). Mutagenesis and inducible responses to deoxyribonucleic acid damage in *Escherichia coli*. *Microbiological Reviews* **48**: 60.
- Weinbauer MG (2004). Ecology of prokaryotic viruses. *FEMS Microbiology Reviews* **28**: 127-181.
- Whittier RF, Chase JW (1983). DNA repair properties of *Escherichia coli* tif-1, recA_o281 and lexA1 strains deficient in single-strand DNA binding protein. *Molecular and General Genetics MGG* **190**: 101-111.
- Wilhelm SW, Suttle CA (1999). Viruses and Nutrient Cycles in the Sea - Viruses play critical roles in the structure and function of aquatic food webs. *BioScience* **49**: 781-788.

Zhao Y, Wang K, Ackermann H-W, Halden RU, Jiao N, Chen F (2010a). Searching for a "Hidden" Prophage in a Marine Bacterium. *Applied and Environmental Microbiology* **76**: 589-595.

Zhao Y, Wang K, Ackermann H-W, Halden RU, Jiao N, Chen F (2010b). Searching for a "hidden" prophage in a marine bacterium. *Appl Environ Microbiol* **76**: 589-595.

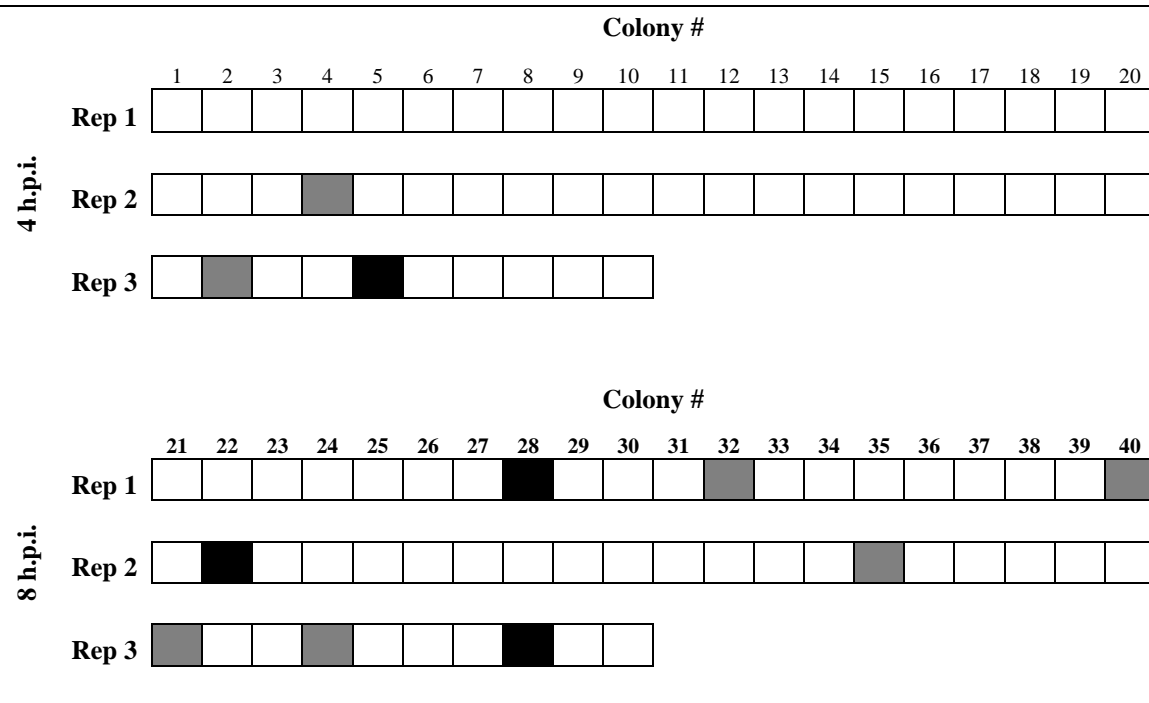
Appendix

Tables

Table 3.1. Oligonucleotides used in this study

| Primer name | Primer sequence (5'-3') | Gene target | Purpose/experiment |
|----------------|-------------------------|---------------------------------------|---------------------------------------|
| alaS_577for | GGAGAGAGTGACGCATGGAT | alanine tRNA hydrolase | Host reference gene |
| alaS_719rev | CAGCTGTCGAGATGGACGTA | alanine tRNA hydrolase | Host reference gene |
| map_164for | TCACGCAGATGATCGAAGAC | methionine aminopeptidase | Host reference gene |
| map_334rev | CATCGACAATTACGGTGACG | methionine aminopeptidase | Host reference gene |
| rpoC_3196for | AAAAAGTCCGTCGTGGTGAC | RNA polymerase | Host reference gene |
| rpoC_3356rev | AACGGCATGTCTTCCATAGG | RNA polymerase | Host reference gene |
| 2047LexA_for | ACTCGATCTGCTGGCCTTTA | <i>lexA</i> transcriptional regulator | Host SOS response |
| 2047LexA_rev | TCGGGCAGTTTCACTACCTC | <i>lexA</i> transcriptional regulator | Host SOS response |
| 2047RecA_for | CTGATTTCCCAGCCTGACAC | recombinase <i>recA</i> | Host SOS response |
| 2047RecA_rev | AGCCTGTCTAGCTTACGCATT | recombinase <i>recA</i> | Host SOS response |
| Pro PEPG_for | CTATGAAGGCATGGGCGATA | endolysin | ΦNYA Induction |
| Pro PEPG_rev | GGCGATCGATCCAACACT | endolysin | ΦNYA Induction |
| Pro Rad_for | TGGCCCTCTACGACAAAGAC | Rad52/22 dsDNA break repair | ΦNYA Induction |
| Pro Rad_rev | TCGTTTAGTTCGTGCTGCAT | Rad52/22 dsDNA break repair | ΦNYA Induction |
| Pro SSB_for | GCCTTGGAACGTCAATTCAT | ssDNA binding protein (<i>ssb</i>) | ΦNYA Induction |
| Pro SSB_rev | ACAACGGCAAGGACAAGAAC | ssDNA binding protein (<i>ssb</i>) | ΦNYA Induction |
| Pro rep_rev | CCGTGCCATTATTTGGCTAT | phage repressor | ΦNYA Induction |
| Pro rep_rev | GCTAATGTGCTGGGCCTTAG | phage repressor | ΦNYA Induction |
| int772_for | TGGGTCATTCTAACGCTGGT | integrase | Phage lysogeny establishment |
| int937_rev | ATTCCACAATCTCAAGCGCC | integrase | Phage lysogeny establishment |
| 47AHTH_XRE_for | CAAAAGCTGACGCAGACTCA | phage repressor | Φ47A lysogeny establishment |
| 47AHTH_XRE_rev | ATATCCCGCATCAGCTCAAC | phage repressor | Φ47A lysogeny establishment |
| 47A PEPG_for | GTGTTTGCATAATCGGCAAG | endolysin | Φ47A replication |
| 47A PEPG_rev | CGGATCTGGAAAACCAGCTT | endolysin | Φ47A replication |
| 2047PP1_for | TATTCATAGCGAGGCGCAGT | endolysin | ΦNYA enumeration |
| 2047PP1_rev | ATACCTGCCCAACGTACAG | endolysin | ΦNYA enumeration |
| 2047A-C_for | CCCATGTGTATGTCGCCTCT | endolysin | Φ47A enumeration |
| 2047A-C_rev | CAGCGTTGAAAAAGGCTCTG | endolysin | Φ47A enumeration |
| jxn761U_for | GGCCAGCATAACCGTTTCC | histidine kinase | Phage Integration site identification |
| int937_rev | ATTCCACAATCTCAAGCGCC | integrase | Phage Integration site identification |
| jxn1105D_rev | TGTCGCCAACACCTCTACC | HTH transcriptional regulator | Phage Integration site identification |
| jxn1105D_for | GGGAGGCATGAGCGTAGAA | hypothetical protein | Phage Integration site identification |

Table 3.2. Integration frequency of single and polylysogens



Resident prophage, Φ NYA only
 Prophage substitution, Φ CB2047-A replaces Φ NYA
 Double lysogen, both identified

Table 3.3. Frequency of Φ CB2047-A & Φ NYA integration into *Sulfitobacter* genome, % (MOI 0.06)

| Time (h.p.i.) | Rep 1 | Rep 2 | Rep 3 | Average |
|---------------|-------|-------|-------|---------|
| 4 | 0 | 5 | 20 | 8 |
| 8 | 15 | 10 | 30 | 18 |

Table 3.4. *Sulfitobacter* genomes with conserved putative phage attachment site sequence

| Accession number | Organism name | <i>attB</i> sequence |
|------------------|---|----------------------|
| JPOY01000011 | <i>Sulfitobacter</i> sp. CB2047 | + |
| NZ_CH959310 | <i>Sulfitobacter</i> sp. EE-36 | + |
| AXZR01000001 | <i>Sulfitobacter pontiacus</i> 3SOLIMAR09 | + |
| NZ_CH959312 | <i>Sulfitobacter</i> sp. NAS-14.1 | + |
| JEMU01000011 | <i>Sulfitobacter mediterraneus</i> 1FIGIMAR09 | + |
| JASC01000014 | <i>Sulfitobacter</i> sp. NB-68 | + |
| JAMD01000001 | <i>Sulfitobacter</i> sp. H3 | + |
| JIBC01000006 | <i>Sulfitobacter</i> sp. 20_GPM-1509m | + |
| JASH01000011 | <i>Sulfitobacter mediterraneus</i> KCTC 32188 | - |
| JASD01000008 | <i>Sulfitobacter</i> sp. NB-77 | - |
| JASG00000000.1 | <i>Sulfitobacter guttiformis</i> KCTC 32187 | - |
| JASF00000000.1 | <i>Sulfitobacter donghicola</i> DSW-25 | - |
| JASE00000000.1 | <i>Sulfitobacter</i> sp. MM-124 | - |

+ sequence present in genome, - sequence not present

Table 3.5 *Sulfitobacter* strains tested for prophage integration

| Accession number | Organism name | Φ NYA | Φ CB2047A |
|------------------|---|------------|----------------|
| JPOY01000011 | <i>Sulfitobacter</i> sp. CB2047 | + | + |
| NZ_CH959310 | <i>Sulfitobacter</i> sp. EE-36 | + | + |
| AXZR01000001 | <i>Sulfitobacter pontiacus</i> 3SOLIMAR09 | + | + |
| NZ_CH959312 | <i>Sulfitobacter</i> sp. NAS-14.1 | + | + |
| JEMU01000011 | <i>Sulfitobacter mediterraneus</i> 1FIGIMAR09 | + | + |

Plus sign indicates positive PCR reaction.

Figures

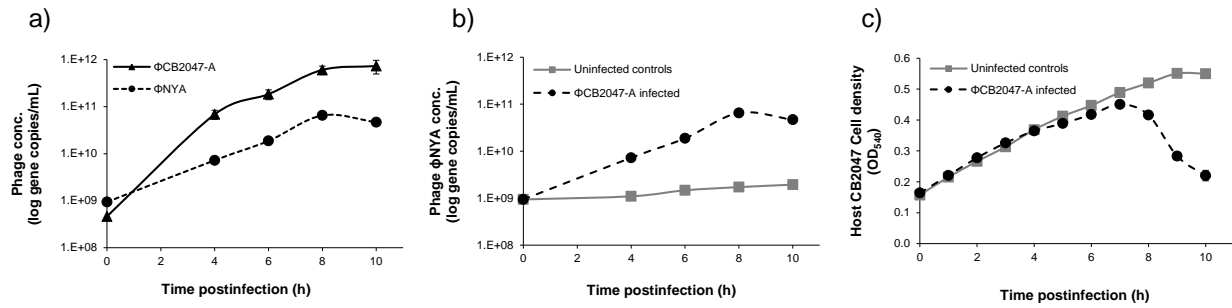


Figure 3.1. (a) Superinfecting phage and resident prophage population dynamics in superinfected culture (b) Prophage (Φ NYA) induction dynamics in Φ CB2047-A superinfected and uninfected control cultures. (c) Host (CB2047) population dynamics in Φ CB2047-A superinfected and uninfected control cultures. Error bars represent the standard error of the mean and are obscured by the data markers, in some cases.

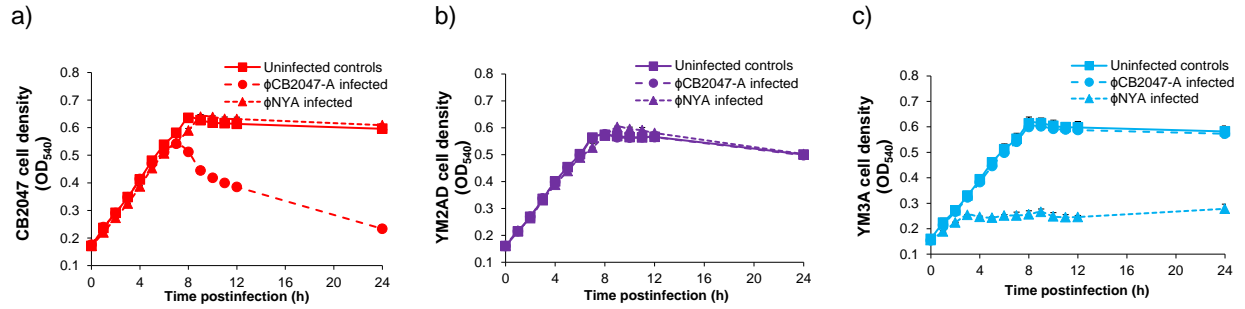


Figure 3.2. Growth dynamics of *Sulfitobacter* strains independently infected with ϕ CB2047-A and ϕ NYA. (a) *Sulfitobacter* sp. CB2047 (ϕ NYA single lysogen) (b) *Sulfitobacter* sp. YM2AD (ϕ CB2047-A / ϕ NYA double lysogen) (c) *Sulfitobacter* sp. YM3A (ϕ CB2047-A single lysogen). Error bars represent the standard error of the mean and are obscured by the data markers, in some cases.

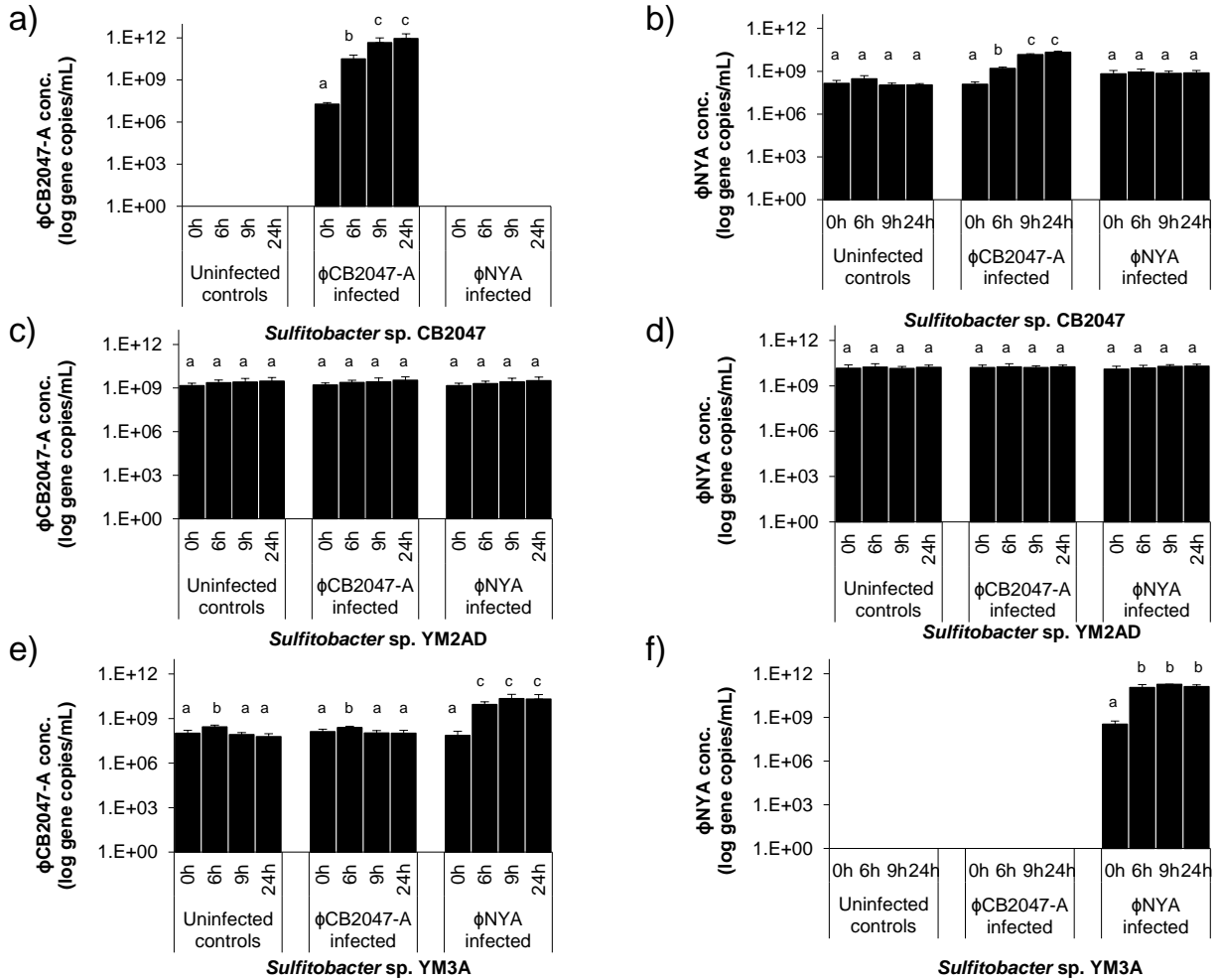


Figure 3.3. Phage replication dynamics in *Sulfitobacter* lysogens superinfected by a secondary phage. Error bars represent the standard error of the mean. Different letters denote columns with significantly different ($p < 0.1$) phage gene copy numbers within a given plot.

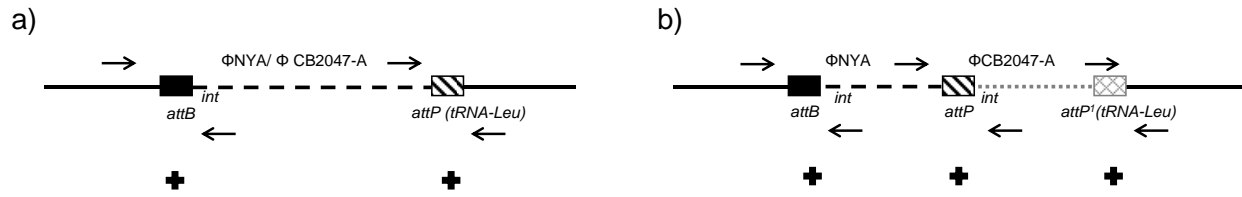


Figure 3.4. Identification of putative phage integration sites in *Sulfitobacter* (a) single lysogens (b) polylysogens. Plus sign indicates positive PCR reaction.

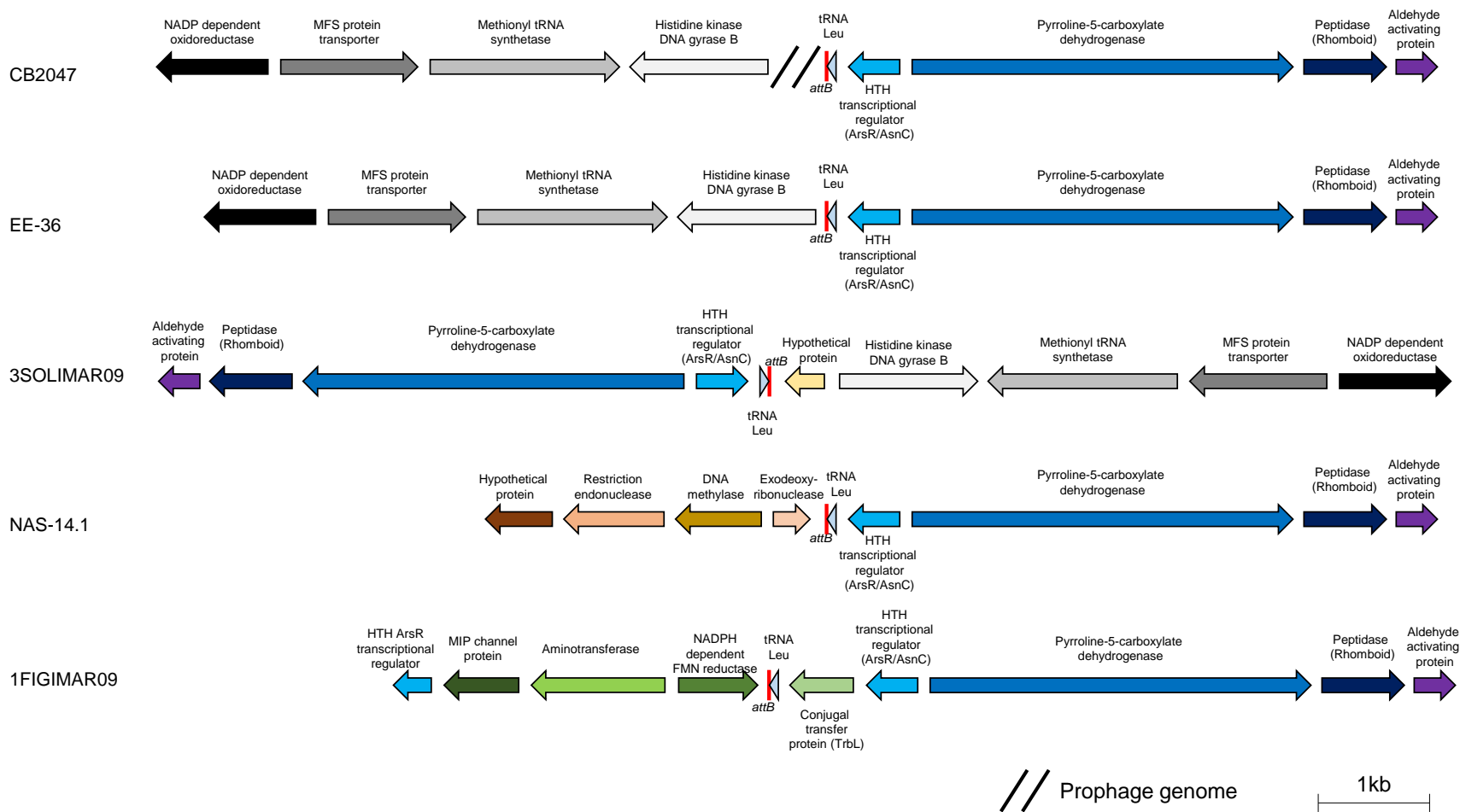


Figure 3.5. Gene organization around the putative prophage insertion site (*attB*) in members of the *Sulfitobacter* genus.

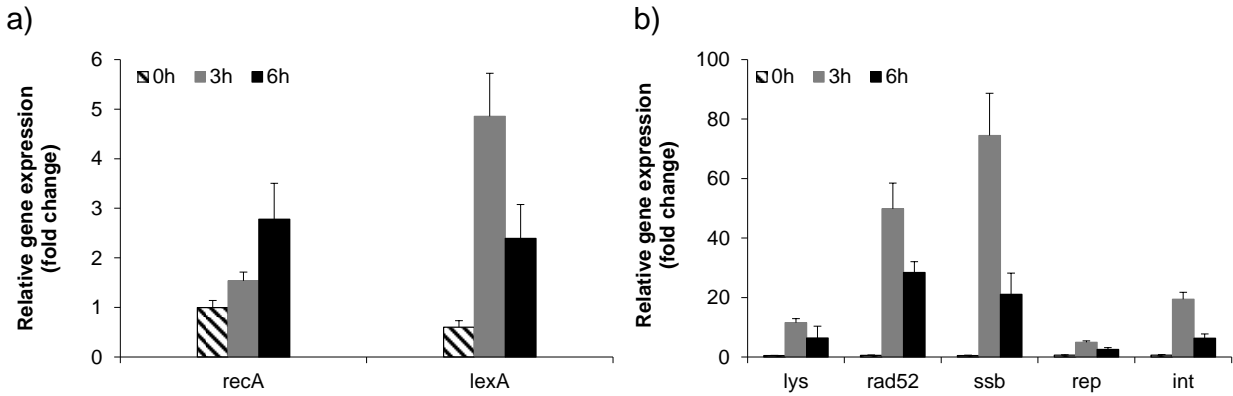


Figure 3.6. Normalized (a) host and (b) resident prophage (Φ NYA) gene expression in infected *Sulfitobacter* cells. Expression levels are normalized to three reference genes (see methods) and relative to uninfected cell gene expression at the same timepoint. Error bars represent the standard error of the mean. Gene expression values were significantly different ($p < 0.01$) at all times for each gene analyzed.

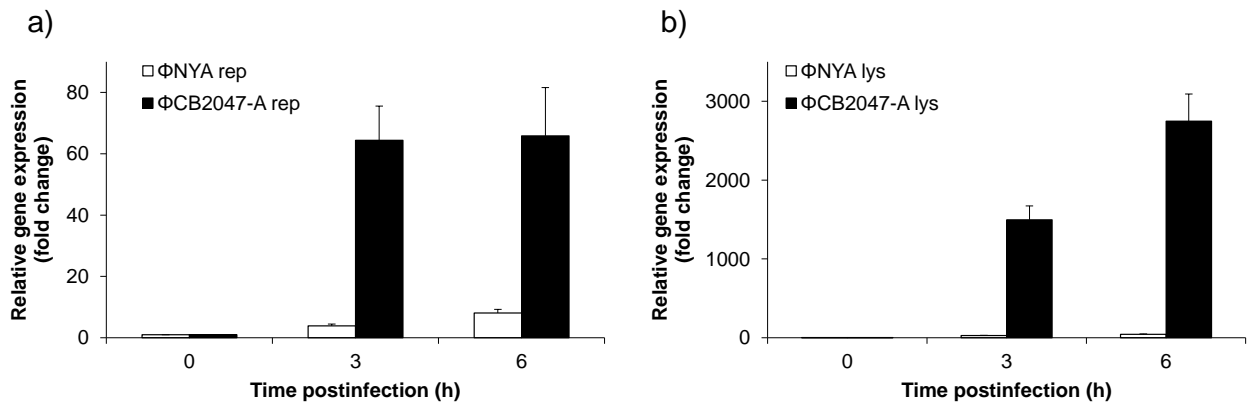


Figure 3.7. Phage (a) repressor and (b) endolysin gene expression in infected *Sulfitobacter* cells. Expression levels are normalized to three reference genes (see methods) and relative to phage gene expression at timepoint T=0 of the same treatment. Error bars represent the standard error of the mean. Gene expression values were significantly different ($p < 0.001$) at all times (except $t=0h$) for each gene analyzed.

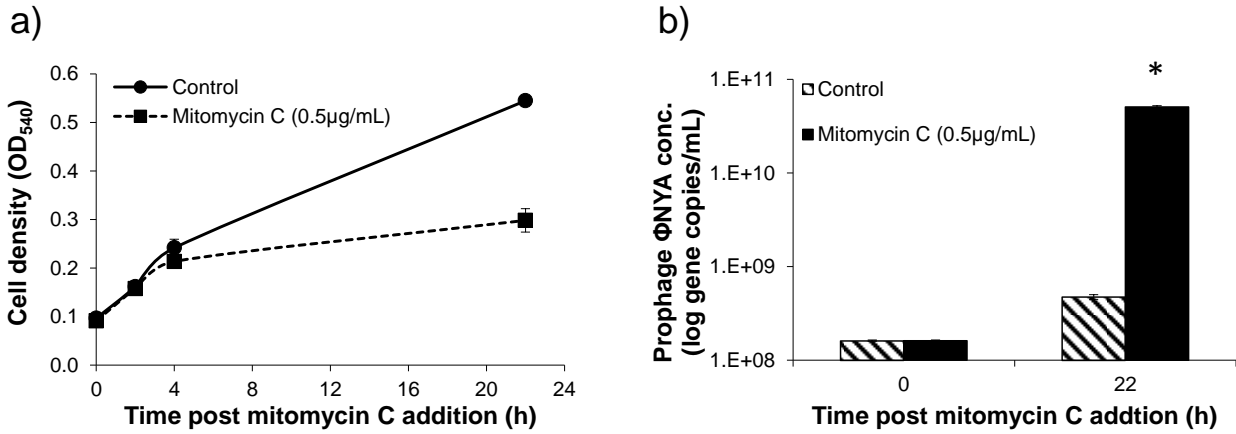


Figure 3.8. Mitomycin C induction of *Sulfitobacter* sp. CB2047. **(a)** Host growth dynamics in control and induced cultures. **(b)** Phage concentration in control and induced cultures. Error bars represent the standard error of the mean and are obscured by the data markers, in some cases. Asterisk indicates significant difference ($p < 0.001$) between treatments.

Chapter 4

Phage infection of an environmentally relevant marine bacterium alters host metabolism and lysate composition

A version of this chapter was originally published by Ankrah NYD, May AL, Middleton JL, Jones DR, Hadden MK, Gooding JR, LeCleur GR, Wilhelm SW, Campagna SR and Buchan A.

Ankrah NYD, May AL, Middleton JL, Jones DR, Hadden MK, Gooding JR, LeCleur GR, Wilhelm SW, Campagna SR, Buchan A. 2014. Phage infection of an environmentally relevant marine bacterium alters host metabolism and lysate composition. *ISME J.* **8**: 1089–1100.
<http://dx.doi.org/10.1038/ismej.2013.216>.

NYDA participated in the design and coordination of the study, participated in the experiment, interpreted the data and drafted the manuscript. ALM & JM participated in the experiment, sample processing, data collection, data analysis and helped to draft the manuscript. DRJ, MKH & JRG participated in the experiment and aided in sample processing. SWW participated in the design of the study and helped to draft the manuscript. SRC participated in the design and coordination of the study, aided in the interpretation of the data, and helped to draft the manuscript. AB participated in the design and coordination of the study, participated in the experiment, aided in the interpretation of the data, and helped to draft the manuscript. All authors read and approved the final manuscript.

Abstract

Viruses contribute to the mortality of marine microbes, consequentially altering biological species composition and system biogeochemistry. While it is well established that host cells provide metabolic resources for virus replication, the extent to which infection reshapes host metabolism at a global level and the effect of this alteration on the cellular material released following viral lysis is less understood. To address this knowledge gap, the growth dynamics, metabolism and extracellular lysate of roseophage infected *Sulfitobacter* sp. 2047 was studied using a variety of techniques, including liquid chromatography–tandem mass spectrometry (LC-MS/MS)-based metabolomics. Quantitative estimates of the total amount of carbon and nitrogen sequestered into particulate biomass indicate that phage infection redirects ~75% of nutrients into virions. Intracellular concentrations for 82 metabolites were measured at seven time points over the infection cycle. By the end of this period, 71% of the detected metabolites were significantly elevated in infected populations, and stable-isotope based flux measurements showed that these cells had elevated metabolic activity. In contrast to simple hypothetical models that assume that extracellular compounds increase due to lysis, a profile of metabolites from infected cultures showed that >70% of the 56 quantified compounds had decreased concentrations in the lysate relative to uninfected controls, suggesting that these small, labile nutrients were being utilized by surviving cells. These results indicate that virus-infected cells are physiologically distinct from their uninfected counterparts, which has implications for microbial community ecology and biogeochemistry.

Introduction

It is estimated that 20-30% of the marine microbial community is infected by viruses at any given time. This contributes to an estimated 3 gigatons of carbon that are released in the world's oceans each year as a result of virus-mediated lysis (Suttle 2007). The released dissolved organic matter (DOM) is a major contributor to marine microbial activity (Weinbauer *et al.* 2011), stimulating both primary and secondary productivity *e.g.* (Middelboe and Lyck 2002, Middelboe and Jorgensen 2006, Riemann and Middelboe 2002). Through their lytic activities, viruses influence the flow of carbon, nitrogen and other nutrients in the marine environment (Brussaard *et al.* 2008).

To better define the role of viruses as global drivers of nutrient flow, we need an improved understanding of the impact of infection on host metabolic processes. Presently, little is known of the influences of bacteriophage infection on global host metabolism beyond isolated model systems. A few marine phage-host systems appear to sequester sufficient resources for nucleic acid synthesis entirely from degradation of host DNA (Wikner *et al.* 1993), although the sources of other macromolecular building blocks are unknown. Much of the knowledge concerning phage-host interactions comes from studies in *Escherichia coli*. Both lysogenic and lytic coliphages initially promote similar alterations in host metabolism (Calendar 2006) that halt host cell DNA synthesis (Kazmierczak and Rothman-Denes 2006), degrade host DNA (Miller *et al.* 2003), and assemble the machinery for viral production (Taylor 1995). These activities drastically alter aspects of host metabolism in a specific manner that favors virus replication *e.g.* (Poranen *et al.* 2006). In fact, a number of viruses contain auxiliary metabolic genes (AMGs) to overcome rate-limiting steps in host biosynthesis (Breitbart 2012). A dramatic example of host manipulation has been demonstrated in marine cyanophage that encode and express

photosynthesis proteins homologous to those found in their hosts (Thompson *et al.* 2011). However, the extent to which pathway-specific alterations of host metabolism is a universal strategy among phages remains unknown. Further, the hijacking of host metabolic processes may not be fully sufficient to supply the demand for rapid virus production, necessitating the acquisition of resources from the environment. For example, the breakdown of host DNA does not fully supply precursors needed for coliphage DNA synthesis. Thus, an initial lag in *E. coli* metabolism is followed by rapid uptake of nutrients to be used for *de novo* synthesis of macromolecular building blocks (Friedman and Gots 1953). Similarly, it has been found that thymidine uptake by infected *Pseudoalteromonas* sp. SKA18 occurred at rates similar to uninfected cells during the early stages of infection, yet became markedly enhanced just prior to onset of cell lysis (Middelboe 2000). These observations suggest an interplay between the viral life cycle and environmental nutrient availability.

From the standpoint of characterizing the influence of virus activity on ocean biogeochemistry, most studies and have largely focused on characterizing the bulk material properties of lysate DOM (*e.g.* total C, N, Fe, Se; *e.g.* (Bratbak *et al.* 1998, Gobler *et al.* 1997, Lønborg *et al.* 2013, Poorvin *et al.* 2004) or monitoring a few select molecules (*e.g.* dimethyl sulfide, acrylate) or compound classes, such as amino acids and carbohydrates (*e.g.* (Middelboe and Jorgensen 2006, Shelford *et al.* 2012, Weinbauer and Peduzzi 1995). In general, these studies reported increases in these molecules in lysates (*e.g.* (Lønborg *et al.* 2013, Poorvin *et al.* 2004) and have hypothesized that viral lysates are rich in free and combined amino acids (Middelboe and Jorgensen 2006) and may be an important source of labile organic nitrogen (Shelford *et al.* 2012). Only recently has the technology necessary to monitor metabolism at the systems level become available via NMR (Fiehn 2002) or liquid chromatography—mass

spectrometry (LC-MS/MS) based metabolomics (Bajad *et al.* 2006, Coon *et al.* 2005, Siuzdak 1994), and these same tools can be used to help characterize the chemical composition of DOM.

Bacteria belonging to the Roseobacter lineage, which includes *Sulfitobacter* species, are abundant in marine systems and carry out critical biogeochemical transformations (Buchan *et al.* 2005, Buchan *et al.* 2014). Herein we report the study of a *Sulfitobacter* sp. 2047-roseophage infection system in which LC-MS/MS-based metabolomics techniques were employed to both compare the metabolism of an infected population with an uninfected control and to gain insight into the interaction between active infection and small metabolites within the DOM pool. As non-lipid containing phages are comprised primarily of nucleic acid and protein, typically in an equal mass ratio *e.g.* (Bancroft and Freifelder 1970), we hypothesized that any influences of viral infection on host metabolism would be manifested in pathways that contribute to the synthesis of the biochemical building blocks for these macromolecules and that this would be reflected in the suite of metabolites released from lysed cells.

Materials and Methods

Isolation of bacterial and phage strains

Sulfitobacter sp. 2047 was isolated from a mesocosm study in Raunefjorden, Norway in 2008 by enrichment with dimethylsulfoniopropionate (DMSP) (Budinoff 2012, Pagarete *et al.* 2011). Agar plates (0.8% *w/v* Noble Agar [Difco, Sparks, MD, USA]) were made using 0.22 μm filtered fjord water and 10 mM DMSP (kindly provided by J. Henrikson and W. Whitman, UGA). The strain was subsequently maintained on Artificial Seawater (ASW): 1.0% agar plates [230 mM NaCl, 5.3 mM KCl, 3.9 mM CaCl₂, 0.1 mM H₃BO₃, 11.8 mM MgSO₄, 11.2 mM MgCl₂, 0.8 mM

NaHCO₃, 5 mM NH₄Cl, 75 μM K₂HPO₄, and 10 mM Tris-HCl (pH 7.5)] supplemented with 0.25% yeast extract and 0.4% tryptone at 20 °C. Filter-sterilized (0.22 μm) stock solutions were added to the autoclaved basal salt solution along with vitamins, iron, and trace metals prepared as previously described (Budinoff and Hollibaugh 2007). A lytic phage (Φ2047B) (Ankrah *et al.* 2014, Budinoff 2012) was isolated from viral concentrates of Raunefjorden seawater using standard bacteriophage enrichment (Van Twest and Kropinski 2009, Wommack *et al.* 2009). Plaque purification and preparation of phage stocks were based on previously described methods (Kropinski *et al.* 2009). Concentrated lysates were made by gently washing soft agar from plaque assay plates with MSB buffer. The final purified phage concentrate was 0.22 μm filtered and stored at 4 °C in the dark. All growth experiments with the bacterium, including infections, were performed in ASW at 20 °C. All chemicals were obtained from Fisher Scientific (Fair Lawn, NJ, USA). Genome analysis of *Sulfitobacter* sp. 2047 revealed it is lysogenized by a prophage that is genetically distinct from Φ2047B.

Microscopy

For microscopic direct counts, *Sulfitobacter* sp. 2047 cells were stained with SYBR Gold stain (25 X concentration, Invitrogen, Carlsbad, CA, USA) and enumeration was performed on a Leica DMRXA microscope using filter cube L5 (excitation filter BP 480/40, suppression filter BP 527/30) according to protocols previously described (Patel *et al.* 2007). For each slide, 10 fields were counted.

Bacterial culture conditions and metabolite measurements

To determine whether phage infection shifts the metabolite repertoire of *Sulfitobacter* sp. 2047, the bacterium was grown in ASW supplemented with 10 mM sodium acetate at 25 °C in the dark with 200 rpm agitation. Once cultures reached an OD₅₄₀ of *ca.* 0.17, phage were added at a multiplicity of infection of 4 (4 phage cell⁻¹). Under these conditions, cell lysis is evident at approximately 240 min post infection. To monitor host metabolites during all phases of infection, samples were collected prior to phage addition ($t = 0$) and then 15, 30, 60, 120, 240, 360 and 480 min post phage addition. Extracellular metabolites were measured in cell-free filtrates of the populations at 480 min. Control cultures (without added phage) were maintained and sampled in parallel. Samples taken for microscopic analyses were fixed with gluteraldehyde (0.5%), stored at -80 °C and processed using standard techniques. Samples for qPCR were flash frozen and stored at -80 °C until processing, while samples for metabolite analysis were immediately processed.

Following the initial experiment, a separate analysis using stable isotope labeled nutrients was performed to examine turnover rates and cellular fluxes for a subset of metabolites. For these studies, 20 mM ¹³C-labeled sodium acetate (1, 2-¹³C₂, 99%, Cambridge Isotope Laboratories, Andover, MA, USA) was added to a set of control and viral infected cultures at either 0 min or 240 min post infection. These two time points were selected to represent each of the two phases of infection that were evident from the metabolite profiles identified in the initial experiment described above. Samples for the flux analysis were taken from each culture at 0, 5, 15, 30, 60 and 120 min post-addition of ¹³C-acetate. However, isotope incorporation was complete at 60 min, and the data presented herein reflects this.

The targeted metabolomics methods employed to measure relative intracellular metabolite concentrations and turnover rates used slight modifications of a known metabolite extraction procedure (Bennett *et al.* 2008, Rabinowitz and Kimball 2007, Yuan *et al.* 2008). Briefly, 10 mL of cells were rapidly collected on Magna™ nylon filters (Millipore, Billerica, MA) via vacuum filtration and then extracted by placing the filter directly in a petri dish containing extraction solvent at 4 °C as previously described. Extracellular metabolites from both infected and control cultures were collected at 480 min by filtering 10 mL of culture as previously described and collecting the filtrate. The resulting liquids were lyophilized then re-suspended in 300 µL 40:40:20 acetonitrile: methanol: water with 0.1 M formic acid for MS analysis. Two LC-MS/MS analyses, one in each of positive and negative ion modes, were performed for each sample, and relative metabolite levels and fluxes were analyzed as previously described (Bennett *et al.* 2008, Rabinowitz and Kimball 2007, Yuan *et al.* 2008).

Chromatographic details for metabolite analysis

Compounds were separated by high performance liquid chromatography (HPLC). A quaternary pump was used to generate a gradient for elution of compounds from the stationary phase. Samples were delivered to the column after injection (10 µL) with an autosampler kept at 4 °C. The separation eluent was directly passed to the mass spectrometer.

For positive ion mode analyses, the stationary phase was aminopropyl functionalized particles (5 µm pore size, 100 Å particle size) packed into a 250 x 2 mm column (Luna NH₂ Phenomenex, Torrance, CA). The flow rate was 150 µl/min and the column was maintained at 10 °C. The mobile phases were 95% 20 mM ammonium acetate, 20 mM ammonium hydroxide (in HPLC grade water, buffered at pH 9.4) and 5% HPLC grade acetonitrile (solvent A) and

HPLC grade acetonitrile (solvent B). The solvents were used to construct a 40 min gradient elution profile as follows: t = 0 min: 15% solvent A, 85% solvent B; t = 15 min, 100% solvent A, 0% solvent B; t = 28 min, 100% solvent A, 0% solvent B; t = 30 min, 15% solvent A, 85% solvent B; t = 40 min, 15% solvent A, 85% solvent B.

For negative ion mode analyses, the stationary phase was a Synergi Hydro-RP C18 (4 μm pore size, 80 \AA particle size) packed into a 150 x 2 mm column (Phenomenex). The flow rate was 200 $\mu\text{L}/\text{min}$ and the column was maintained at 25 $^{\circ}\text{C}$. The mobile phases were 11 mM tributylamine and 15 mM acetic acid in 97% HPLC grade water with 3% HPLC grade methanol (solvent A) and HPLC grade methanol (solvent B). The solvents were used to construct a 50 min gradient elution profile as follows: t = 0 min: 100% solvent A, 0% solvent B; t = 5 min, 100% solvent A, 0% solvent B; t = 10 min, 80% solvent A, 20% solvent B; t = 15min, 80% solvent A, 20% solvent B; t = 30min, 35% solvent A, 65% solvent B; t = 33 min, 5% solvent A, 95% solvent B, t = 37 min, 5% solvent A, 95% solvent B; t = 38 min, 100% solvent A, 0% solvent B; t = 50 min, 100% solvent A, 0% solvent B.

Mass spectrometric detection parameters

Following HPLC separation, samples were delivered to the electrospray ionization (ESI) chamber of a triple quadrupole mass spectrometer via a 0.1 mm (internal diameter) fused silica capillary. The ESI source spray voltage was set to 4500 V for detection in positive ion mode and 3000 V for detection in negative ion mode. The sheath gas was nitrogen at 40 psi. Argon was used as the collision gas at 1.5 Torr and the inlet capillary temperature was maintained at 290 $^{\circ}\text{C}$. Selected reaction monitoring (SRM) technology was used for sample analysis. The scan time and

width for each SRM was 0.05 s and 1 m/z , respectively. The complete SRM detection parameters for the majority of compounds have been previously reported by Rabinowitz and colleagues (Bajad *et al.* 2006, Rabinowitz and Kimball 2007, Yuan *et al.* 2008). The SRM detection parameters for the flux analysis are shown in Table 4.4.

Metabolite data analysis

Signal intensity for all metabolites was analyzed as peak area, and each measurement was manually curated using the Xcalibur 2.0.7 Quan Browser analysis package (Thermo Fisher Scientific). Metabolite area counts were normalized to cell density to obtain per cell metabolite abundances, and a ratio of these values from each condition was used to compare relative concentrations of metabolites. All heat maps were generated using Gene Cluster 3.0 (de Hoon *et al.* 2004) and viewed using Java TreeView 1.1.5 (Saldanha 2004). Interactions among the metabolites were visualized using resources available through the Kyoto Encyclopedia of Genes and Genomes (KEGG) database (www.genome.jp/kegg/).

Metabolite stable isotope incorporation data analysis

Peak areas for all compounds detected in the ^{13}C incorporation experiments were calculated as described for the pool size data above. Once the peak areas were determined, the ratios of unlabeled, partially labeled, and fully labeled metabolites were determined for each time point. These values were then used to calculate the rate of disappearance (turnover) for the unlabeled material. The data were fit using the following equation: $y = Ae^{(-kx)} + c$, where k is the rate constant. This equation is most correct for populations that have reached steady state, which may not be the case in the experiments reported herein due to the addition of a pulse of labeled

nutrients. Therefore, the ratios of rate constants from the phage infected and control cultures were calculated and multiplied by the fold difference in metabolite concentration to determine relative fluxes.

Phage enumeration

Phages were enumerated using qPCR assays specific for each of the two phage (prophage and Φ 2047B). Genome sequences were obtained for the host and Φ 2047B, facilitating the design and optimization of phage-specific primer sets. qPCR was carried out by using a DNA Engine Opticon 2 real-time PCR detector with the Opticon Monitor 3.1.32 software package (Bio-Rad Laboratories, Inc., Hercules, CA). qPCR reactions were performed in a 25 μ L volume with 12.5 μ L SYBR Premix Ex *Taq* cocktail RR041 (Perfect Real Time; Takara Bio, Inc., Shiga, Japan), 500 nM forward and reverse primers and 10.0 μ L of template dilutions. The amplification programs for each primer set are as follows: 95 °C for 3 min, 40 cycles of: 95 °C for 20 s, 56 °C or 55 °C (prophage or Φ 2047B, respectively) for 20 s, 72 °C for 20 s, followed by 5 min at 72 °C. Fluorescence measurements were conducted at the end of each cycle at 72 °C. Melt curves were generated after each assay to verify the specificity of the amplification by heating from 50 to 100 °C, read every 1 °C. Standards were developed from plasmids containing cloned sequences and 10-fold serial dilutions of these samples in 10 mM Tris-HCl were used in the reactions. Standard curves were determined as the correlation between the log of gene copy numbers and the C_t . In all cases, correlation coefficients for standard curves assays were ≥ 0.99 .

Results

The *Sulfitobacter*-phage infection cycle

The growth of the infected *Sulfitobacter* sp. CB2047 cultures was nearly identical to that of the uninfected controls until the onset of cell lysis at 240 min post-infection (p.i.) (Figure 4.1a). Rapid production of phage occurred between 60 and 240 min p.i., at which point it plateaued. By the end of the 480 min experiment, 3.53×10^{11} new virus particles had been produced, the density of bacteria in the flasks receiving phage was approximately 30% of that present in the no-virus control cultures, and phage outnumbered bacteria approximately 2500 to 1 (Figure 4.1a). Under the growth conditions employed here, infection of the host with the lytic phage results in induction of a prophage for at least a portion of the host population, leading to the propagation of both phage in batch culture (Table 4.3).

Stoichiometric shifts in carbon and nitrogen associated with phage infection

The distributions of carbon (C) and nitrogen (N) in biological particles for the control culture and the *Sulfitobacter*-roseophage infection system were calculated based on reported estimates of the C and N content in both marine viruses and bacteria. The total masses of bacterial cellular and phage C and N were calculated using previously reported elemental estimates of 0.2 fg C and 0.076 fg N per phage and 149 fg C and 35 fg N per cell (Chan *et al.* 2012, Heldal *et al.* 1985, Jover *et al.* 2014, Vrede *et al.* 2002). At the final time point, cells in the control culture contained $76.74 (\pm 10.43)$ and $18.0 (\pm 2.45)$ mg/L of C and N, respectively (Fig 4.1b-c). During the experiment, this culture was estimated to incorporate 31.33 and 7.33 mg/L of C and N, respectively, into new cells. In comparison, phage infected cultures were found to have 95 mg/L of C in both intact bacterial cells (22.35 ± 2.98 mg/L) and viral particles (72.66 ± 2.05

mg/L) by the final time point. As for N, 29.59 mg/L had been incorporated in total with 5.25 (\pm 0.7) and 24.34 (\pm 0.7) mg/L being found in bacteria and phage, respectively (Figure 4.1b-c). These data were used to calculate the C:N ratio for infected and control populations throughout the course of the experiment. This ratio remained constant for the control populations, but decreased by 32% for the infected cultures by 480 min (Figure 4.1d).

Intracellular metabolite concentrations throughout the infection cycle

The relative concentrations of 82 central pathway metabolites (the “core metabolome”) were measured via LC-MS/MS for both infected and control populations at seven discrete time points throughout the infection cycle (Figure 4.2). During the early infection period (ending at 120 min p.i.), < 25% of the measured metabolites were significantly different between the infected and control populations (18 at $p \leq 0.05$ and ≥ 1.5 fold change). At the end of the infection cycle (480 min p.i.), ~75% of metabolite concentrations were significantly elevated (59 at $p \leq 0.05$ and ≥ 1.5 fold change) in phage-infected populations (Figure 4.3). The intracellular metabolite concentration progressively increased in the phage-infected populations for nearly every metabolite over the course of the infection cycle. In fact, almost no metabolites showed a significant decrease in concentration. For example, dramatic differences were evident in UDP-activated sugars. The relative concentration of UDP-glucose in the infected population was elevated 1.7-fold 15 min after phage addition and remained fairly constant throughout the experiment. UDP-glucuronate/galacturonate became elevated over time with a 13-fold spike in concentration at 120 min post infection, the time point preceding widespread cell lysis. Similarly, several amino acids were elevated in concentration in the late phase infected populations relative to controls by 1.6 to 6.0-fold, with an average of 2.9-fold, at 480 min p.i. (i.e. alanine,

asparagine, aspartate, cysteine, glutamate, glutamine, lysine, proline, serine, threonine, and valine). To verify that *Sulfitobacter* sp. 2047 contained high concentrations of glutamate and glutamine, their absolute concentrations were determined for this experiment and found to be 7.1×10^{-14} g/cell and 2×10^{-15} g/cell, respectively, in the infected culture at the final time point (Figures 4.4a-b).

Metabolic turnover and flux during phage infection

Complementary experiments to analyze metabolite turnover and metabolic flux were also performed using a stable-isotope labeled carbon source. ^{13}C -acetate was added to separate sets of cultures at times that matched both the early (immediately following virus addition) and late (240 min p.i.) phases that were identified from the time course used to determine growth dynamics and overall metabolite concentration (*i.e.* Figures 4.1a and 4.2). Incorporation of the label into 14 selected metabolites representing TCA cycle components, N assimilation intermediates, and amino acids was monitored via LC-MS/MS during the first 120 min following ^{13}C acetate addition in both cases. These measurements provide two useful pieces of data: (1) the rate at which the metabolite pool is converted to entirely new metabolites due to biosynthesis and (2) the total amount of nutrients that pass through a specific compound, *i.e.*, the flux through them, which is proportional to the turnover rate and metabolite pool size. With the exception of glutamate and glutamine (Table 4.1 and Figure 4.5), the turnover rates for all measured metabolites were indistinguishable between the control and viral treated cultures throughout the infection cycle. Consequently, the fluxes for these metabolites were increased in infected populations since the larger pools were being replenished at equivalent, or only slightly reduced, rates. The measured turnover rates for glutamate and glutamine are indistinguishable between the

control and viral treated cultures during the early infection period (Figure 4.5A&C), however, they are decreased in the infected cultures during the later stages of infection (Figure 4.5B & D). The calculated flux through glutamate in the infected cultures is equivalent to controls throughout both phases of the infection cycle. However, flux through glutamine is 70-100% and 200-400% higher during the early and late infection periods, respectively (Table 4.1).

Composition of extracellular small molecule components following phage-induced cell lysis

Cell-free filtrates of phage-infected and control cultures were collected at 480 min p.i., and 56 metabolites were detected in filtrates from either infected or control cultures (Table 4.2). The metabolite concentrations in the infected cultures were not uniformly higher for every molecule. Instead, there was an increase in 29%, no change in 45%, and a decrease in 27% of the metabolite concentrations detected in the virus-infected cultures (Table 4.2). For example, several components of C and N metabolism (i.e. α -ketoglutarate, phosphoenolpyruvate, lactate and erythrose-4-phosphate) as well as small-cofactors (FAD, NAD) are either decreased or not detected in the filtrates of virus-infected cultures relative to controls. In contrast, cell wall constituents, such as phosphatidylcholine and phosphatidylethanolamine, were present only in the filtrates of virus-infected cultures. In addition, several amino acids (asparagine, methionine, cysteine, and homoserine) and urea were elevated by an average of 2- and 2.8-fold, respectively. Finally, all acyl-CoAs were either elevated or only present in infected culture filtrates (Table 4.2).

Discussion

A way to view the potential metabolic burden of virion production on a host cell is to consider the elemental resources required by the virus. The C:N ratio of phage (3.00) is predicted to be lower than that of bacteria (4.25) (Chan *et al.* 2012, Jover *et al.* 2014, Vrede *et al.* 2002). Quantitative estimates indicated that phage particles represented a significant portion of redistributed C and N in our experiment, and as a result of phage production these elements were incorporated into biological particles (cells and phage) at greater, but disproportionate, amounts compared to control populations. In fact, the infected cultures had incorporated 49% more C and 148% more N than the controls by the conclusion of the experiment. Thus, partitioning of host N into phage particles represented a potential for stoichiometric disruption in the C:N of infected cells.

To assess the effect of phage production on the metabolism of the host population, we measured intracellular metabolites from both the control and infected cultures. These data highlight the distinct metabolic trajectories of these populations, as it was observed that viral infection led to a progressive and general increase in concentration for nearly all measured compounds. Dynamics in phage production and host population survival can be used to divide the time course of the experiment into two phases: an early infection period (0-120 min) and a later infection period (240-480 min). The per cell metabolite concentrations also support this division. During the second phase of the time-course, phage production had leveled off, the host population had dropped to half of its peak cell density and the variation in the core metabolome became more dramatic relative to the uninfected controls.

The 66 metabolites with significantly elevated concentrations in infected cultures clearly point to the population of infected cells being physiologically distinct from those that are

uninfected. Differences in UDP-activated sugars (UDP-glucose, UDP-glucuronate/galacturonate) may reflect alterations in cell wall integrity in phage-infected bacteria. Similarly, several amino acids were elevated in concentration in infected populations relative to controls. Of particular interest were glutamate and glutamine, which together serve as the entry points for 99% of inorganic N into biomolecules (Yan 2007), and are amongst the most abundant metabolites in *E. coli* (Bennett *et al.* 2009). We confirmed that the absolute concentrations for glutamate and glutamine in *Sulfitobacter* sp. 2047 are similar to those reported for *E. coli* (1.5×10^{-14} g cell⁻¹ and 1.1×10^{-15} g cell⁻¹, respectively) (Bennett *et al.* 2009) and thus are expected to be major components of the metabolome. The ratio of intracellular glutamate to glutamine is an indicator of N availability in many bacterial species, with an increased ratio indicating growth under N limitation (Flynn *et al.* 1989). An analysis of the trends in this ratio for both cultures indicates that the control population, which shows a progressive increase in this ratio through the growth cycle, is likely experiencing decreased N availability as the cultures reach the end of exponential phase. As sufficient ammonium was provided to supply the N required in both cultures, these data suggest that the infected cultures had access to preferred N-containing nutrient sources not available in the control cultures

Following the measurement of metabolite concentrations during the infection cycle, stable isotope labeling studies using ¹³C-acetate were performed to determine whether the general increases in metabolite concentrations were due to increased biosynthesis or decreased utilization of each molecule. The rates of label incorporation for 12 of the 14 metabolites monitored indicated that both populations were metabolically active. As metabolite concentrations and turn over were similar between infected and control populations during the early time points, these data further support the observation that host metabolism was not

dramatically altered within the first hour following phage addition. However, the flux through all metabolites at the later time points was altered since the higher cellular concentrations of these metabolites in the infected cultures results in an increased flux through these molecules as the larger pools are being replaced in the same unit time. While the glutamate and glutamine pools turned over more slowly during the later phase of the infection, the elevated concentrations of these compounds resulted in measured fluxes for these metabolites that were equal for glutamate and 200-400% greater for glutamine than those of the control population. We suggest that the apparent decrease in turnover rates for these two molecules is the result of uptake and incorporation of unlabeled nutrients from lysed kin.

The metabolites with decreased concentrations in the filtrates of the infected cultures were primarily those that are expected to be readily recycled, such as components of central C and N metabolism and small co-factors. This suggests intact cells in the virus-infected cultures remained active and were able to rapidly consume material from lysed cells to support their own metabolism, consequently depleting selected metabolites in the extracellular milieu. Metabolites with increased relative concentrations in the filtrates were those typically related to cellular stress or those that are potentially too large to be transported into the cell (*i.e.* > 600 Da, (Benz 1985, Williams 2000). The presence of bacterial cell wall constituents (*i.e.* phosphatidylcholine and phosphatidylethanolamine) in the phage-infected culture filtrates is also consistent with the degradation of cell wall material from lysed cells and with prior studies demonstrating the prevalence and recalcitrance of bacterial cell wall components (*i.e.* peptidoglycan) in marine (Jørgensen *et al.* 2003, McCarthy *et al.* 1998, Pedersen *et al.* 2001) and virus-derived DOM (Middelboe and Jorgensen 2006). Dissolved and free amino acids have also been previously identified in viral lysates, but the contribution of individual amino acids was not reported

(Middelboe and Jorgensen 2006). Of the extracellular amino acids detected here, several of those with the largest increases in concentration for the phage-infected cultures are also part of the normal cellular stress response (*e.g.* asparagine, cysteine, homoserine and methionine) (Jozefczuk *et al.* 2010). Acyl-CoAs may not be efficiently transported and assimilated due to their large size and/or low concentrations in nature, potentially explaining their relative increase in infected culture filtrates. The repertoire of metabolites remaining in the lysate may also be a reflection of the host's substrate preferences. For example, urea, a nitrogen-rich byproduct of *de novo* nucleotide biosynthesis (Berg *et al.* 2012), was also elevated in infected cultures.

The small molecule composition of the filtrates as well as the intracellular metabolite concentrations and turnover rates suggest that the phage-infected cultures were incorporating nutrients from recycled sources, *i.e.* from small molecules that were liberated during viral lysis or from breakdown of unlabeled macromolecules. The strongest evidence for this phenomenon comes from the data for glutamate and glutamine, which despite showing high intracellular concentrations in infected populations were undetectable in the culture filtrates. Given that these compounds are typically preferred sources of N (over ammonium) in bacteria (Kirchman *et al.* 1989, Middelboe *et al.* 1996, Riemann and Middelboe 2002) it is likely that these compounds were released from lysed cells and then rapidly assimilated by metabolically active cells.

Ecological implications & Conclusions

This work provides a biochemical basis from which a mechanistic understanding of the influence of phage infection on host metabolism can be developed for extension to a biogeochemical framework. In terms of how virus activity shapes host metabolism, our results show that phage infection in *Sulfitobacter* sp. 2047 does not lead to any pathway-specific

alterations in host metabolism. Instead, a general increase in net host metabolic activity is used to meet the requirements of virus propagation that is facilitated by recycling of metabolites from lysed siblings. Additional studies are necessary to determine whether this observed response is generalizable to other host-phage systems. It is relevant to highlight that in the model system used here simultaneous production of two distinct phage (one lytic and one lysogenic) occurs. Furthermore by the final sampling time point, some unknown and undistinguishable fraction of the population is resistant to infection, or at least lysis. Since lysogeny is hypothesized to be prevalent in marine bacteria in general (Leitet *et al.* 2006, Paul 2008, Stopar *et al.* 2004) and Roseobacters, in particular (Chen *et al.* 2006, Zhao *et al.* 2010), the complexity of this infection process may, in fact, be reflective of events that are common in nature.

An increased demand for N results in a stoichiometric imbalance of C:N in infected cells, which has implications for trophic transfer and stimulation of secondary production. In fact, our observations suggest that infected cells are a functionally different entity than their non-infected counterparts. In pelagic environments, the progression of the lytic cycle may thus be constrained by the availability of host-limiting nutrients due to increased cellular demands. Conversely, removal of constraints on nutrient availability may stimulate host growth thereby facilitating viral production (Higgins *et al.* 2009, Weinbauer *et al.* 2009). Indeed the interplay between nutrient demand and availability may influence the lytic-lysogeny decision (Herskowitz and Hagen 1980, Hong *et al.* 1971, Jiang and Paul 1998) that phage make when infecting a cell. This could also result in the establishment of a state that may be perceived as pseudolysogeny (Łoś and Węgrzyn 2012) where the cell is infected but there are insufficient cellular resources to propagate new virions. Alternatively, infected cells with access to sufficient nutrients may themselves be N enriched and more susceptible to grazing. To this end, the idea of the infected

cell as a unique biochemical cell type continues to gain traction while the role of viruses as vectors of biogeochemical change continues to expand.

Acknowledgements

We are grateful to Dr. Charles Budinoff for isolation of *Sulfitobacter* sp. 2047 and its infecting phage and Dr. Willie Wilson encouraging and facilitating our participation in the mesocosm experiment that yielded this bacterium and phage. We thank Thomas Lane for the analysis of the *Sulfitobacter* 2047 genome. We are indebted to Dr. Andrew Lang for insightful comments on an earlier version of this manuscript. This work was supported by NSF grants OCE-1061352 awarded to AB, SRC and SWW. JLM was supported by OCE-1208784 awarded to SRC.

References

- Ankrah NYD, Budinoff CR, Wilson WH, Wilhelm SW, Buchan A (2014). Genome Sequence of the *Sulfitobacter* sp. Strain 2047-Infecting Lytic Phage Φ CB2047-B. *Genome Announcements* **2**.
- Bajad SU, Lu W, Kimball EH, Yuan J, Peterson C, Rabinowitz JD (2006). Separation and quantitation of water soluble cellular metabolites by hydrophilic interaction chromatography-tandem mass spectrometry. *Journal of Chromatography A* **1125**: 76-88.
- Bancroft FC, Freifelder D (1970). Molecular weights of coliphages and coliphage DNA: I. Measurement of the molecular weight of bacteriophage T7 by high-speed equilibrium centrifugation. *Journal of Molecular Biology* **54**: 537-546.
- Bennett BD, Yuan J, Kimball EH, Rabinowitz JD (2008). Absolute quantitation of intracellular metabolite concentrations by an isotope ratio-based approach. *Nat Protocols* **3**: 1299-1311.
- Bennett BD, Kimball EH, Gao M, Osterhout R, Van Dien SJ, Rabinowitz JD (2009). Absolute metabolite concentrations and implied enzyme active site occupancy in *Escherichia coli*. *Nature chemical biology* **5**: 593-599.
- Benz R (1985). Porin from bacterial and mitochondrial outer membrane. *Critical Reviews in Biochemistry and Molecular Biology* **19**: 145-190.
- Berg JM, Tymoczko JL, Stryer L (2012). *Biochemistry*. W.H. Freeman: Basingstoke.
- Bratbak G, Jacobsen A, Heldal M (1998). Viral lysis of *Phaeocystis pouchetii* and bacterial secondary production. *Aquatic microbial ecology* **16**: 11-16.

- Breitbart M (2012). Marine viruses: truth or dare. *Annual Review of Marine Science* **4**: 425-448.
- Brussaard CPD, Wilhelm SW, Thingstad F, Weinbauer MG, Bratbak G, Heldal M *et al.* (2008). Global-scale processes with a nanoscale drive: the role of marine viruses. *ISME J* **2**: 575-578.
- Buchan A, Gonzalez JM, Moran MA (2005). Overview of the marine Roseobacter lineage. *Applied and Environmental Microbiology* **71**: 5665-5677.
- Buchan A, LeCleir GR, Gulvik CA, Gonzalez JM (2014). Master recyclers: features and functions of bacteria associated with phytoplankton blooms. *Nat Rev Micro* **12**: 686-698.
- Budinoff CR, Hollibaugh JT (2007). Ecophysiology of a Mono Lake Picocyanobacterium. *Limnology and Oceanography* **52**: 2484-2495.
- Budinoff CR (2012). Diversity and activity of Roseobacters and roseophage.
- Calendar R (2006). *The Bacteriophages*. Oxford University Press: New York.
- Chan LK, Newton RJ, Sharma S, Smith CB, Rayapati P, Limardo AJ *et al.* (2012). Transcriptional changes underlying elemental stoichiometry shifts in a marine heterotrophic bacterium. *Frontiers in Microbiology* **3**.
- Chen F, Wang K, Stewart J, Belas R (2006). Induction of multiple prophages from a marine bacterium: a genomic approach. *Applied and Environmental Microbiology* **72**: 4995-5001.
- Coon JJ, Ueberheide B, Syka JE, Dryhurst DD, Ausio J, Shabanowitz J *et al.* (2005). Protein identification using sequential ion/ion reactions and tandem mass spectrometry.

- Proceedings of the National Academy of Sciences of the United States of America* **102**: 9463-9468.
- de Hoon MJL, Imoto S, Nolan J, Miyano S (2004). Open source clustering software. *Bioinformatics* **20**: 1453-1454.
- Fiehn O (2002). Metabolomics—the link between genotypes and phenotypes. *Plant molecular biology* **48**: 155-171.
- Flynn KJ, Dickson DMJ, Al-Amoudi OA (1989). The ratio of glutamine: glutamate in microalgae: a biomarker for N-status suitable for use at natural cell densities. *Journal of plankton research* **11**: 165-170.
- Friedman S, Gots JS (1953). The purine and pyrimidine metabolism of normal and phage infected *Escherichia coli*. *Journal of Biological Chemistry* **201**: 125-135.
- Gobler CJ, Hutchins DA, Fisher NS, Cosper EM, Sanudo-Wilhelmy SA (1997). Release and bioavailability of C, N, P, Se, and Fe following viral lysis of a marine chrysophyte. *Limnology and Oceanography*: 1492-1504.
- Heldal M, Norland S, Tumyr O (1985). X-Ray microanalytic methods for measurement of dry matter and elemental content of individual bacteria. *Applied and Environmental Microbiology* **50**: 1251-1257.
- Herskowitz I, Hagen D (1980). The lysis-lysogeny decision of phage lambda: explicit programming and responsiveness. *Annual review of genetics* **14**: 399-445.

- Higgins JL, Kudo I, Nishioka J, Tsuda A, Wilhelm SW (2009). The response of the virus community to the SEEDS II mesoscale iron fertilization. *Deep-Sea Research Part II-Topical Studies in Oceanography* **56**: 2788-2795.
- Hong J-S, Smith GR, Ames BN (1971). Adenosine 3': 5'-cyclic monophosphate concentration in the bacterial host regulates the viral decision between lysogeny and lysis. *Proceedings of the National Academy of Sciences* **68**: 2258-2262.
- Jiang S, Paul J (1998). Significance of lysogeny in the marine environment: studies with isolates and a model of lysogenic phage production. *Microbial ecology* **35**: 235-243.
- Jørgensen NO, Stepanaukas R, Pedersen AGU, Hansen M, Nybroe O (2003). Occurrence and degradation of peptidoglycan in aquatic environments. *FEMS microbiology ecology* **46**: 269-280.
- Jover LF, Effler TC, Buchan A, Wilhelm SW, Weitz JS (2014). The elemental composition of virus particles: implications for marine biogeochemical cycles. *Nature Reviews Microbiology* **12**: 519-528.
- Jozefczuk S, Klie S, Catchpole G, Szymanski J, Cuadros-Inostroza A, Steinhauser D *et al.* (2010). Metabolomic and transcriptomic stress response of *Escherichia coli*. *Molecular systems biology* **6**.
- Kazmierczak KM, Rothman-Denes LB (2006). Bacteriophage N4. In: Calendar R (ed). *The Bacteriophages*. Oxford University Press: New York. pp 302-314.

- Kirchman DL, Keil RG, Wheeler PA (1989). The effect of amino acid on ammonium utilization and regeneration by heterotrophic bacteria in the sub-arctic pacific. *Deep-Sea Research Part a-Oceanographic Research Papers* **36**: 1763-1776.
- Kropinski AM, Mazzocco A, Waddell TE, Lingohr E, Johnson RP (2009). Enumeration of bacteriophages by double agar overlay plaque assay. *Bacteriophages*. Springer. pp 69-76.
- Leitet C, Riemann L, Hagström Å (2006). Plasmids and prophages in Baltic Sea bacterioplankton isolates. *Journal of the Marine Biological Association of the United Kingdom* **86**: 567-575.
- Lønborg C, Middelboe M, Brussaard CP (2013). Viral lysis of *Micromonas pusilla*: impacts on dissolved organic matter production and composition. *Biogeochemistry* **116**: 231-240.
- Łoś M, Węgrzyn G (2012). Pseudolysogeny. *Advances in Virus Research* **82**: 339-349.
- McCarthy MD, Hedges JI, Benner R (1998). Major bacterial contribution to marine dissolved organic nitrogen. *Science* **281**: 231-234.
- Middelboe M, Jorgensen N, Kroer N (1996). Effects of viruses on nutrient turnover and growth efficiency of noninfected marine bacterioplankton. *Applied and Environmental Microbiology* **62**: 1991-1997.
- Middelboe M (2000). Bacterial growth rate and marine virus–host dynamics. *Microbial Ecology* **40**: 114-124.
- Middelboe M, Lyck PG (2002). Regeneration of dissolved organic matter by viral lysis in marine microbial communities. *Aquatic Microbial Ecology* **27**: 187-194.

- Middelboe M, Jorgensen NOG (2006). Viral lysis of bacteria: an important source of dissolved amino acids and cell wall compounds. *Journal of the Marine Biological Association of the United Kingdom* **86**: 605-612.
- Miller ES, Kutter E, Mosig G, Arisaka F, Kunisawa T, Ruger W (2003). Bacteriophage T4 genome. *Microbiology and Molecular Biology Reviews* **67**: 86-+.
- Pagarete A, Corguillé G, Tiwari B, Ogata H, Vargas C, Wilson WH *et al.* (2011). Unveiling the transcriptional features associated with coccolithovirus infection of natural *Emiliania huxleyi* blooms. *FEMS microbiology ecology* **78**: 555-564.
- Paul JH (2008). Prophages in marine bacteria: dangerous molecular time bombs or the key to survival in the seas? *The ISME journal* **2**: 579-589.
- Pedersen A-GU, Thomsen TR, Lomstein BA, Jørgensen NO (2001). Bacterial influence on amino acid enantiomerization in a coastal marine sediment. *Limnology and oceanography* **46**: 1358-1369.
- Poorvin L, Rinta-Kanto JM, Hutchins DA, Wilhelm SW (2004). Viral Release of Iron and Its Bioavailability to Marine Plankton. *Limnology and Oceanography* **49**: 1734-1741.
- Poranen MM, Ravantti JJ, Grahn AM, Gupta R, Auvinen P, Bamford DH (2006). Global changes in cellular gene expression during bacteriophage PRD1 infection. *J Virol* **80**: 8081-8088.
- Rabinowitz JD, Kimball E (2007). Acidic acetonitrile for cellular metabolome extraction from *Escherichia coli*. *Analytical Chemistry* **79**: 6167-6173.

- Riemann L, Middelboe M (2002). Viral lysis of marine bacterioplankton: Implications for organic matter cycling and bacterial clonal composition. *Ophelia* **56**: 57-68.
- Saldanha AJ (2004). Java Treeview-extensible visualization of microarray data. *Bioinformatics* **20**: 3246-3248.
- Shelford EJ, Middelboe M, Møller EF, Suttle CA (2012). Virus-driven nitrogen cycling enhances phytoplankton growth. *Aquatic Microbial Ecology* **66**: 41-46.
- Siuzdak G (1994). The emergence of mass spectrometry in biochemical research. *Proceedings of the National Academy of Sciences* **91**: 11290-11297.
- Stopar D, Černe A, Žigman M, Poljšak-Prijatelj M, Turk V (2004). Viral abundance and a high proportion of lysogens suggest that viruses are important members of the microbial community in the Gulf of Trieste. *Microbial ecology* **47**: 1-8.
- Suttle CA (2007). Marine viruses—major players in the global ecosystem. *Nature Reviews Microbiology* **5**: 801-812.
- Taylor K (1995). Replication of coliphage lambda DNA. *FEMS microbiology reviews* **17**: 109-119.
- Thompson LR, Zeng Q, Kelly L, Huang KH, Singer AU, Stubbe J *et al.* (2011). Phage auxiliary metabolic genes and the redirection of cyanobacterial host carbon metabolism. *Proceedings of the National Academy of Sciences* **108**: E757–E764.
- Van Twest R, Kropinski AM (2009). Bacteriophage enrichment from water and soil. *Bacteriophages*. Springer. pp 15-21.

- Vrede K, Heldal M, Norland S, Bratbak G (2002). Elemental composition (C, N, P) and cell volume of exponentially growing and nutrient-limited bacterioplankton. *Applied and Environmental Microbiology* **68**: 2965-2971.
- Weinbauer M, Chen F, Wilhelm S (2011). Microbial Carbon Pump in the Ocean. In: Jiao N, Azam F, Sanders S (eds). Science/AAAS Business Office.
- Weinbauer MG, Peduzzi P (1995). Effect of virus-rich high molecular weight concentrates of seawater on the dynamics of dissolved amino acids and carbohydrates. *Marine ecology progress series Oldendorf* **127**: 245-253.
- Weinbauer MG, Arrieta J-M, Griebler C, Herndl GJ (2009). Enhanced viral production and infection of bacterioplankton during an iron-induced phytoplankton bloom in the Southern Ocean. *Limnology and Oceanography* **54**: 774-784.
- Wikner J, Vallino JJ, Steward GF, Smith DC, Azam F (1993). Nucleic acids from the host bacterium as a major source of nucleotides for three marine bacteriophages. *FEMS microbiology ecology* **12**: 237-248.
- Williams P (2000). Heterotrophic bacteria and the dynamics of dissolved organic material. In: DL K (ed). *Microbial ecology of the oceans*. Wiley-Liss: New York, NY. pp 153-200.
- Wommack KE, Williamson KE, Helton RR, Bench SR, Winget DM (2009). Methods for the isolation of viruses from environmental samples. *Bacteriophages*. Springer. pp 3-14.
- Yan D (2007). Protection of the glutamate pool concentration in enteric bacteria. *Proceedings of the National Academy of Sciences* **104**: 9475-9480.

Yuan J, Bennett BD, Rabinowitz JD (2008). Kinetic flux profiling for quantitation of cellular metabolic fluxes. *Nature protocols* **3**: 1328-1340.

Zhao Y, Wang K, Ackermann H-W, Halden RU, Jiao N, Chen F (2010). Searching for a "Hidden" Prophage in a Marine Bacterium. *Applied and Environmental Microbiology* **76**: 589-595.

Appendix

Tables

Table 4.1. Relative Flux Measurements of Glutamate and Glutamine.

| Time (min) | Glutamate | | Glutamine | | | |
|-------------|------------------------------|----------------------------------|----------------------------|------------------------------|----------------------------------|----------------------------|
| | Relative Pool ^{a,b} | Relative Turnover ^{a,c} | Relative Flux ^a | Relative Pool ^{a,b} | Relative Turnover ^{a,c} | Relative Flux ^a |
| 60 (early) | 1.40 ± 0.33 | 0.910 ± 0.001 | 1.28 ± 0.30 | 1.86 ± 0.40 | 0.914 ± 0.004 | 1.71 ± 0.36 |
| 120 (early) | 1.52 ± 0.30 | 0.910 ± 0.001 | 1.38 ± 0.27 | 2.30 ± 0.26 | 0.914 ± 0.004 | 2.10 ± 0.23 |
| 240 (late) | 1.67 ± 0.17 | 0.7961 ± 0.0002 | 1.33 ± 0.14 | 3.52 ± 0.76 | 0.720 ± 0.002 | 2.53 ± 0.55 |
| 360 (late) | 1.60 ± 0.42 | 0.7961 ± 0.0002 | 1.27 ± 0.33 | 5.68 ± 1.68 | 0.720 ± 0.002 | 4.08 ± 1.21 |

^a Relative Pool and Turnover (mean ± SD) were calculated by dividing the measured values from the infected by that of the control. Relative Flux was calculated as the product of the Relative Pool and Turnover. In each case, standard deviations were determined for measured values and then propagated through the calculations as appropriate for the mathematical operation being performed.

^b Data were obtained from the metabolite measurement experiment.

^c Data were obtained from the stable isotope incorporation experiment.

Table 4.2. Metabolite content of cell-free filtrates from phage-infected *Sulfitobacter* sp. 2047 relative to control cultures at 480 min post infection.

| Amino acids | Fold change^a | Nucleic acids, Nucleosides and Nucleotides | Fold change^a |
|--|--------------------------------|---|--------------------------------|
| Asparagine | 2.37(+) | Deoxyadenosine ^b | 4.69(+) |
| Methionine ^b | 1.83(+) | Thymine ^b | 2.62(+) |
| Cysteine | 1.74(+) | Cytosine ^b | 1.55(+) |
| Tryptophan | 0.73 | dCDP | 1.24 |
| Threonine | 0.10(-) | UDP | 1.12 |
| Homoserine | 1.87(+) | 5'-Methylthioadenosine | 1.05 |
| GABA ^b | 1.45 | Orotate | 0.95 |
| Betaine | 1.29 | Dihydroorotate | 0.87 |
| 1-Methylhistidine | 1.28 | N-Acetylglucosamine-1-Phosphate | 0.8 |
| O-Acetylserine | 0.91 | TDP | 0.57(-) |
| S-Adenosylmethionine | 0.88 | GMP | 0.42(-) |
| N-Acetylornithine ^b | 0.56(-) | 5-Methyldeoxycytidine ^b | 0.35(-) |
| TCA cycle | | Pentose phosphate | |
| Malonyl CoA ^d | 1000.00(+) | Fructose-1,6-Bisphosphate | 0.99 |
| Succinyl CoA | 1.34 | Sedoheptulose-7-Phosphate | 0.71 |
| Succinate | 0.78 | Erythrose-4-Phosphate | 0.00(-) |
| [Fumarate, Maleate, & Isoketovalerate] ^c | 0.72 | | |
| Citrate | 0.7 | Cofactors, vitamins and electron carriers | |
| 2-Oxoglutarate ^b | 0.62(-) | Acetyl CoA | 35.17(+) |
| 3-Phosphoglycerate | 1.89(+) | Pyridoxine | 4.63(+) |
| [1,3 & 2,3 Bisphosphoglycerate] | 1.1 | Nicotinate | 0.95 |
| Phosphoenolpyruvate | 0.61(-) | 5-Methyltetrahydrofolate | 0.85 |
| | | Methylmalonic Acid | 0.79 |
| Lipids | | Thiamine | 0.29(-) |
| [Phosphatidylcholine, Phosphatidylethanolamine] ^{c,d} | 1000.00(+) | FAD | 0.00(-) |
| Propionyl CoA | 79.81(+) | NAD | 0.00(-) |
| Ethanolamine | 2.93(+) | | |
| Palmitate | 0.97 | Other | |
| Farnesylpyrophosphate | 0.57(-) | Urea | 2.78(+) |
| | | DL-Pipecolic Acid | 1.89(+) |
| | | Acetyl Phosphate | 0.92 |
| | | 4-Hydroxybenzoate | 0.81 |
| | | Citraconate | 0.42(-) |
| | | Phenylpyruvate ^b | 0.37(-) |
| | | Lactate | 0.32(-) |

^aMetabolite levels in infected cultures are expressed relative to levels in control cultures at 480 min. Elevated metabolites, (+), (fold change ≥ 1.5) and depressed metabolites, (-), (fold change ≤ 0.67).

^bNot detected in intact cells, detected in filtrates only

^cMetabolites are indistinguishable with the applied method

^dMetabolite was not detected in control cultures, therefore a 1000 was used to denote a large increase in concentration in the infected cells.

Table 4.3. Virus Gene Copies

| Time post infection (min) | Virus Gene Copies (Φ2047A) Average | Range | Virus Gene Copies (Φ2047B) Average | Range |
|---------------------------|------------------------------------|------------|------------------------------------|------------|
| 15 | 1.55E+09 | ± 2.72E+08 | 4.37E+07 | ± 4.06E+06 |
| 30 | 1.48E+09 | ± 6.02E+08 | 4.08E+07 | ± 7.53E+06 |
| 60 | 1.11E+09 | ± 3.33E+08 | 3.88E+07 | ± 4.41E+06 |
| 120 | 1.27E+10 | ± 1.95E+09 | 5.25E+07 | ± 1.03E+07 |
| 240 | 1.05E+11 | ± 9.73E+09 | 6.20E+08 | ± 9.36E+07 |
| 360 | 2.18E+11 | ± 2.91E+10 | 1.82E+09 | ± 1.85E+08 |
| 480 | 3.51E+11 | ± 1.03E+10 | 3.50E+09 | ± 5.26E+08 |

Table 4.4. Flux method metabolites with ¹³C labeling pattern looked for in SRM method

| Metabolite | Molecular Formula | # of ¹³ C in Parent <i>m/z</i> | # of ¹³ C in Fragment <i>m/z</i> |
|--------------------------------------|--|---|---|
| 2-Oxoglutarate | C ₅ H ₅ O ₅ ⁻ | 0, 5 | 0, 4 |
| 5-Methylthioadenosine | C ₁₁ H ₁₆ N ₅ O ₃ S ⁺ | 0, 1, 10, 11 | 0, 0, 5, 5 |
| Acetyl CoA | C ₂₃ H ₃₉ N ₇ O ₁₇ P ₃ S ⁺ | 0, 2, 23 | 0, 2, 13 |
| Alanine | C ₃ H ₈ NO ₂ ⁺ | 0, 2, 2, 3 | 0, 1, 2, 2 |
| Aspartate | C ₄ H ₈ NO ₄ ⁺ | 0, 2, 2, 2, 4 | 0, 0, 1, 2, 2 |
| Citrate & Isocitrate | C ₆ H ₇ O ₇ ⁻ | 0, 2, 2, 6 | 0, 1, 2, 5 |
| D-glucono-δ-lactone-6-phosphate | C ₆ H ₁₀ O ₉ P ⁻ | 0, 6 | 0, 0 |
| Fumarate, Maleate, & Isoketovalerate | C ₄ H ₃ O ₄ ⁻ | 0, 4 | 0, 3 |
| Glutamate | C ₅ H ₁₀ NO ₄ ⁺ | 0, 2, 2, 4, 4, 5 | 0, 1, 2, 3, 4, 4 |
| Glutamine | C ₅ H ₁₁ N ₂ O ₃ ⁺ | 0, 2, 2, 4, 4, 5 | 0, 1, 2, 3, 4, 4 |
| Phosphoenolpyruvate | C ₃ H ₄ O ₆ P ⁻ | 0, 3 | 0, 0 |
| Proline | C ₅ H ₁₀ NO ₂ ⁺ | 0, 5 | 0, 4 |
| Serine | C ₃ H ₈ NO ₃ ⁺ | 0, 2, 2, 3 | 0, 1, 2, 2 |
| Succinate & Methylmalonate | C ₄ H ₅ O ₄ ⁻ | 0, 2, 2, 4 | 0, 0, 2, 3 |
| Threonine | C ₄ H ₁₀ NO ₃ ⁺ | 0, 4 | 0, 3 |

Metabolites are measured in Parent-Fragment *m/z* pairs, i.e. (0-0 & 5-4 for 2-oxoglutarate). Other carbons are unlabeled ¹²C.

Figures

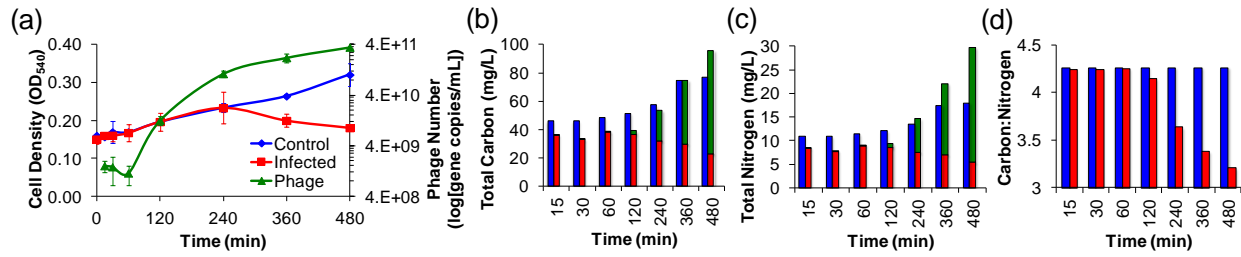


Figure legends

Figure 4.1. (a) *Sulfitobacter* sp. 2047 cell density (OD₅₄₀) and phage concentration at each metabolite sampling time point reported in Figure 4.2. Line graphs are color-coded as follows: phage-infected culture (■), control culture (◆) and phage numbers (▲). Turbidity declines are indicative of phage-induced lysis. Phage numbers were derived from qPCR assays. Averages and ranges of biological duplicates are reported. Estimates of (b) carbon and (c) nitrogen content and their (d) ratios for *Sulfitobacter* sp. 2047 cells and phage during an infection cycle. Bar graphs are color-coded as follows: phage (■), infected culture (■) and control culture (■). Bacterial cell densities were determined by microscopy. Phage numbers were determined using qPCR. Bacterial carbon (149 fg C cell⁻¹) and nitrogen (35 fg N cell⁻¹) were derived from literature values of marine bacteria as reported in text. Phage carbon (0.2 fg C phage⁻¹) and nitrogen (0.076 fg N phage⁻¹) were derived from theoretical calculations (Jover *et al.*, 2014). Values reflect the average of duplicate biological replicates.

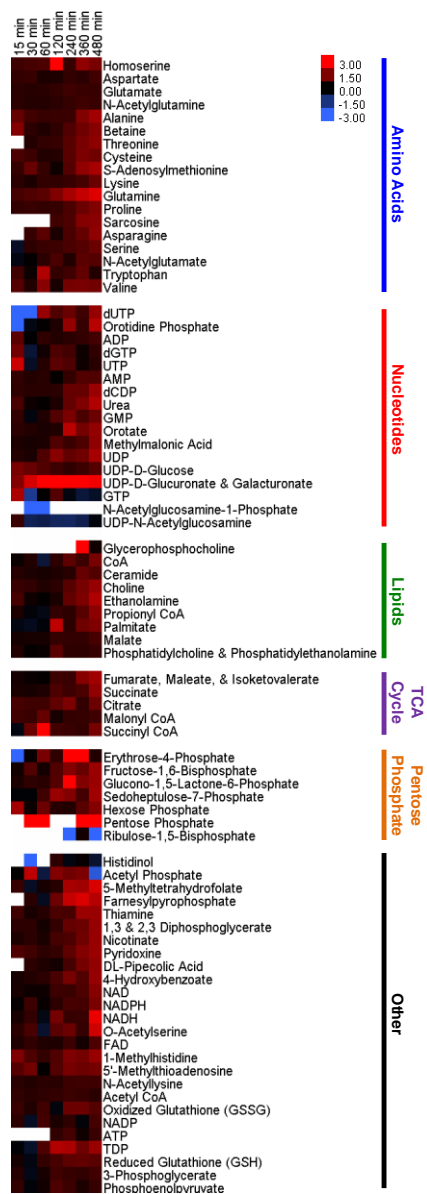


Figure 4.2. Heatmap of intracellular metabolites of phage-infected and control *Sulfitobacter* sp. 2047 populations. Metabolite concentrations are normalized to bacterial cell number and expressed relative to levels measured in the uninfected host cells at the corresponding time point. Ratios are log₂ transformed. Increases in intracellular metabolite concentrations are shown in red and decrease in blue. Columns correspond to minutes post infection, rows represent specific metabolites. Values are averages of duplicate biological and technical replicates and values.

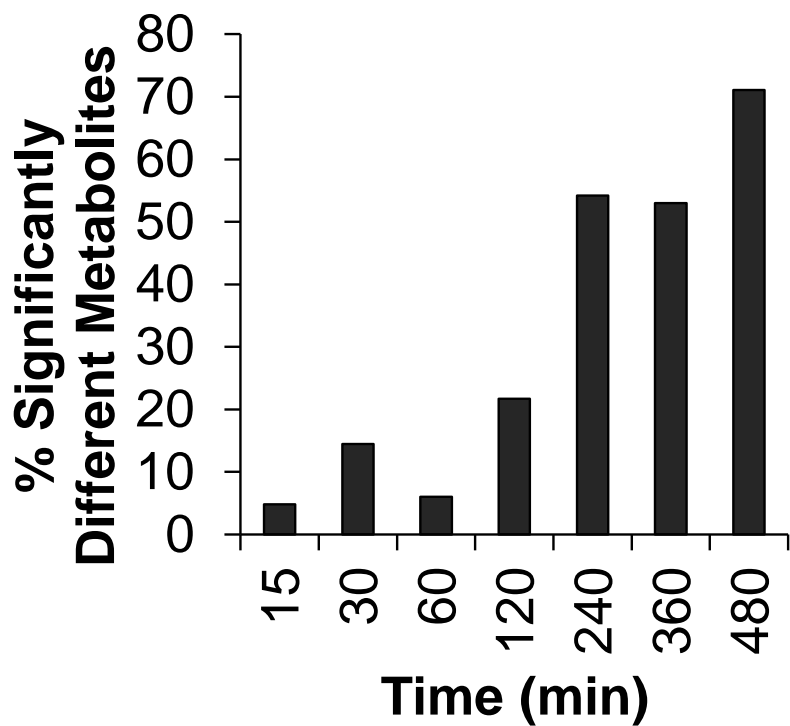


Figure 4.3. Variation in intracellular metabolite concentrations between phage-infected and control populations during the infection cycle shown in Figure 4.2. Columns indicate fold changes ≥ 1.5 and $p \leq 0.05$, all data shown in Tables S3 and S4.

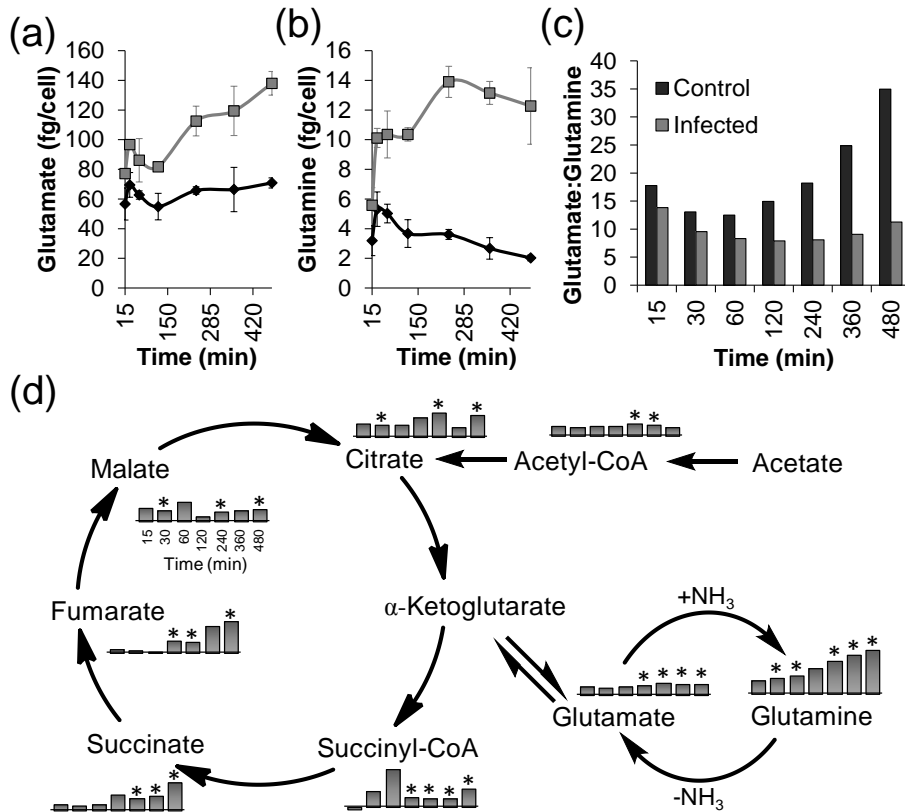


Figure 4.4. Absolute concentrations of (a) glutamate and (b) glutamine in control (■) and phage-infected (□) *Sulfitobacter* sp. 2047 populations. Values represent duplicate biological and duplicate technical replicates. Error bars show the standard error of the mean. (c) Glutamate to glutamine ratios for phage-infected and control populations throughout the experimental time course. Bar graphs are coded as indicated by the key in each figure. (d) Selected metabolites are shown to illustrate the relationship between the TCA cycle and glutamate and glutamine metabolism in *Sulfitobacter* sp. 2047. The bar graphs represent concentrations for metabolites in the phage-infected culture and are expressed as fold change relative to the control at the corresponding time point as shown for malonyl-CoA. Fold changes are \log_2 transformed and represent averages of duplicate biological and technical replicates. Asterisks designate significant fold-changes (≥ 1.5 and $p \leq 0.05$).

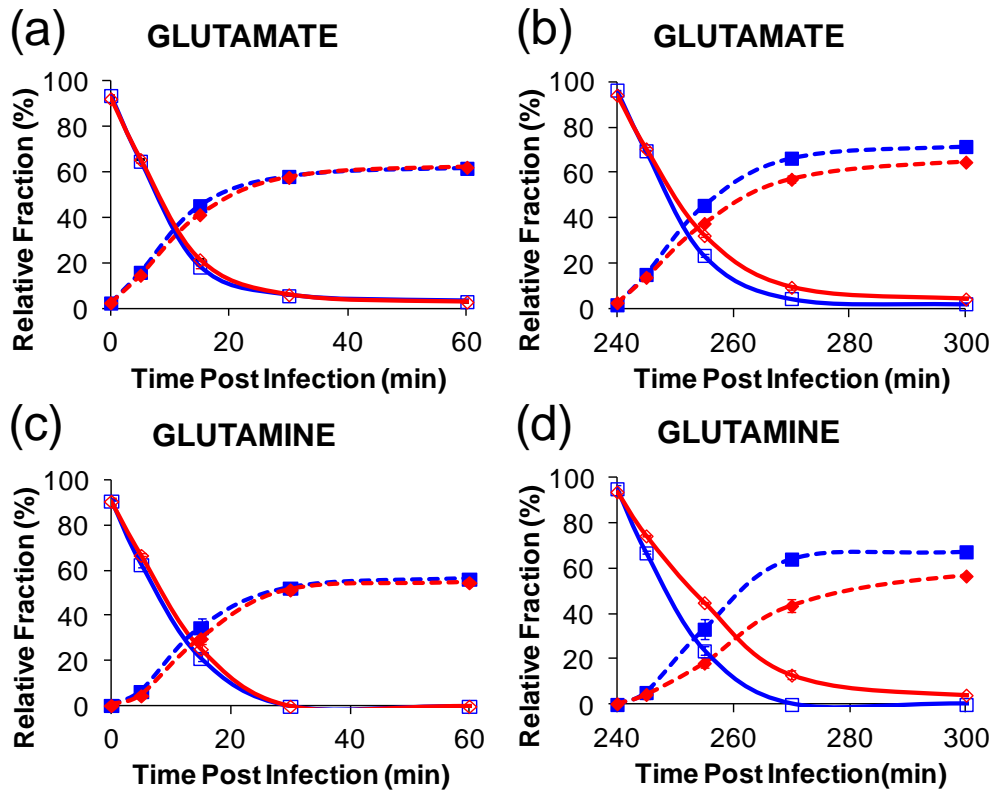


Figure 4.5. Incorporation of acetate-derived ^{13}C into (a and b) glutamate and (c and d) glutamine in phage-infected and control populations during two distinct phases of infection: (a and c) 0-60 min p.i. [early] and (b and d) 240-300 min p.i. [late]. The graphs show the disappearance of unlabeled metabolites for phage-infected (\diamond) and control (\square) populations as well as the appearance of fully ^{13}C -labeled metabolites in phage-infected (\blacklozenge) and control (\blacksquare) populations. Error bars represent range of the data and are obscured by the data markers, in some cases.

Chapter 5

Metabolism of viral lysates by marine bacterioplankton communities

Abstract

There are an estimated 10^{30} marine viruses in the world's oceans. These viruses are hypothesized to be responsible for 10^{28} viral infections that result in the lysis of ~20% of the total microbial biomass in the world's oceans every day. Viral lysis of microbes has been demonstrated to be an important source of labile organic nutrients for natural bacterioplankton communities. Despite the growing literature on the importance of marine viruses in shaping marine food webs and ocean biogeochemical cycles we know relatively little of the influence dissolved organic matter (DOM) resulting from virus-mediated cell lysis has on the metabolism of natural bacterioplankton communities. To address this knowledge gap, natural bacterioplankton communities in the North Pacific were amended with Roseobacter-derived virus lysate (containing 50 μ M C and 10 μ M N) and the change in metabolic rates and nutrient turnover in response to lysate addition were studied using ultra performance liquid chromatography–high resolution mass spectrometry (UPLC-HRMS)-based metabolomics. Intracellular metabolite pool measurements from this study reveal significant increases in ~20% of the 111 metabolites monitored compared to unamended controls. These metabolites represent pathways involved in amino acid metabolism, glycolysis, the tricarboxylic acid (TCA) cycle and nucleotide metabolism. Additionally isotope based flux measurements reveal significant increases in nutrient turnover by up to 900% in the virus lysate amended communities compared to non-amended controls. These data provide detail on the overall metabolism and specific biochemical pathways involved in the transformation of viral lysis-derived cellular components by bacterioplankton populations.

Introduction

Viruses are the most abundant predators in the marine environment with recent estimates citing 10^{30} total marine virus particles in the world's oceans (Breitbart 2012). Approximately 10^{23} virus infections are estimated to occur in the world's oceans every second (Suttle 2007) with ~20% of these infections being lytic infections where the infecting virus hijacks the host organism's metabolism and upregulates several host biosynthetic pathways towards the production of new phage virions (Ankrah *et al.* 2014). The upregulation of host biosynthetic pathways results in the accumulation of labile nutrients within infected cells that are released as dissolved organic matter (DOM) upon cell lysis. Via cell lysis, viruses have also been shown to accelerate the transfer of nutrients from the particulate form (in living organisms) to a dissolved state (dissolved organic matter [DOM]), the latter being more accessible to microbial communities (Wilhelm and Suttle 1999). In fact, virus-mediated lysis of microorganisms is estimated to sequester 3Gt of carbon in the world's oceans each year (Suttle 2007).

The quality of the released virus lysis-derived DOM (or virus lysate) has been of interest to microbial ecologists and has been the focus of numerous studies over the last few decades. For instance, virus lysates have been shown to be a rich source of amino acids (Ankrah *et al.* 2014, Middelboe and Jorgensen 2006, Weinbauer and Peduzzi 1995), Fe (Poorvin *et al.* 2004), labile organic N (Shelford *et al.* 2012) and an important source of bioavailable C, N and Se (Bratbak *et al.* 1998, Gobler *et al.* 1997, Lønborg *et al.* 2013) which is assimilated by active members of microbial communities and incorporated back into the particulate pool through the synthesis of new bacterioplankton (Wilhelm and Suttle 1999).

Prior studies have characterized the effect virus lysates have on host population dynamics and diversity (Brussaard *et al.* 2005, Middelboe *et al.* 1996, Middelboe *et al.* 2003, Weinbauer *et*

al. 2011), monitored the uptake and/or metabolism of bulk lysate by tracking specific elements, principally total C, N and P (Haaber and Middelboe 2009, Middelboe *et al.* 1996, Sheik *et al.* 2013), measured the remineralization rates of lysate-derived N and P (Haaber and Middelboe 2009) or monitored the uptake rates of a few select molecules, such as amino acids and ammonium (Shelford *et al.* 2014). In addition to reporting general increases in microbial population and phylogenetic diversity in lysate metabolizing communities (Brussaard *et al.* 2005, Middelboe *et al.* 2003, Sheik *et al.* 2013), these studies have demonstrated that up to 62% of lysis products from one organism can readily be metabolized and used to support the growth of other organisms (Middelboe *et al.* 2003); and demonstrated that the uptake rates of certain compound classes (e.g. amino acids) from viral lysates was concentration dependent with no observable differences in uptake rates between different isoforms (D and L) of amino acids in virus lysates (Shelford *et al.* 2014). Results from these studies also point to the metabolism of viral lysates by microbial communities as contributing significantly to the remineralization N and P in the environment with estimates of up to 78% and 26% of lysate N and P being mineralized to NH_4^+ and PO_4^{3-} , respectively, by lysate metabolizing communities.

In this study, to further bridge the knowledge gap on how virus lysates are metabolized in the environment, we amended natural bacterioplankton communities in the North Pacific with Roseobacter-derived virus lysate and monitored the change in metabolic rates and nutrient turnover in response to lysate addition. We hypothesized that since viral lysates are rich in labile nutrients there will be a general upregulation of microbial metabolism and flux of nutrients through diverse metabolic pathways in the recipient microbial communities.

Methods

Unlabeled lysate generation

Sulfitobacter sp. 2047 cells were grown in artificial sea water (Budinoff and Hollibaugh 2007) supplemented with 20 mM sodium acetate (Fisher Scientific, Fair Lawn, NJ, USA) and 5mM ammonium chloride (Fisher Scientific, Fair Lawn, NJ, USA) at 25 °C in the dark with 200 r.p.m. agitation. Once cultures reached an OD₅₄₀ of ca. 0.17, phages were added at a multiplicity of infection of 4 (4 phage cell⁻¹). Infected cultures were incubated for 20 h to achieve maximum cell lysis. The lysed culture was 0.22µm filtered and the filtrate frozen at -80°C. The frozen filtrate was lyophilized using a FreeZone Plus 12 Liter Cascade Console Freeze Dry System (Labconco, Kansas City, MO, USA). Lysate carbon and nitrogen concentrations were determined by elemental analysis in a commercial lab (Galbraith Laboratories Inc., Knoxville, TN, USA).

¹³C and ¹⁵N-labeled lysate generation

To generate stable isotope labeled *Roseobacter* lysates, fully labeled ¹³C or ¹⁵N *Sulfitobacter* sp. 2047 was grown in artificial sea water supplemented with 20 mM ¹³C-labeled sodium acetate (1,2-¹³C₂, 99%, Cambridge Isotope Laboratories, Andover, MA, USA) or 5mM ¹⁵N ammonium chloride (¹⁵N, 99%, Cambridge Isotope Laboratories, Andover, MA, USA) at 25 °C in the dark, with 200 r.p.m. agitation. Once cultures reached an OD₅₄₀ of ca. 0.17, phages were added at a multiplicity of infection of 4 (4 phage cell⁻¹). Infected cultures were incubated for 20 h to achieve maximum cell lysis. The lysed culture was 0.22µm filtered and the filtrate frozen at -80°C. The frozen filtrate was lyophilized using a FreeZone Plus 12 Liter Cascade Console Freeze Dry System (Labconco, Kansas City, MO, USA).

Experimental design

To examine the effects of phage derived DOM on natural bacterioplankton communities seawater samples were collected at nine locations in the North Pacific in July 2013 aboard the R/V Kilo Moana. Collecting stations represent different temperature gradients in oligotrophic ocean waters (see Table 5.1). At each station, water was collected at $\approx 3\text{m}$ depth below the surface by using 10-liter Niskin bottles.

To examine the turnover rates of phage derived *Roseobacter* lysate metabolites in natural communities, lyophilized ^{13}C and ^{15}N -labelled lysates were added to 1L natural seawater samples at final concentrations of $10\ \mu\text{M}$ N and $50\ \mu\text{M}$ C. The mesocosms were incubated at *in situ* temperatures in triplicate. At 0, 1, 2, 4, 6 and 12 hours post lysate addition, 100 mL aliquots were collected in triplicate by vacuum filtration on $0.2\ \mu\text{m}$ Magna Nylon filters and flash frozen in liquid nitrogen until processing. Additional seawater samples with $50\ \mu\text{M}$ ^{13}C -labelled sodium acetate and $10\ \mu\text{M}$ ^{15}N -labelled ammonium chloride, with no phage derived lysates, added were maintained and sampled in parallel.

For total metabolite pool analysis, lyophilized phage derived *Roseobacter* lysates were added to 2L natural seawater samples at final concentrations of $10\ \mu\text{M}$ N and $50\ \mu\text{M}$ C. The mesocosms were incubated at *in situ* temperatures in the dark. At 0, 2, 6, and 24 hours post lysate addition, 300 mL aliquots were collected and stored as indicated above. Control cultures amended with $50\ \mu\text{M}$ sodium acetate and $10\ \mu\text{M}$ ammonium chloride, with no phage derived lysates added, were maintained and sampled in parallel.

Metabolite measurement

The targeted metabolomic methods employed to measure relative intracellular metabolite concentrations and turnover rates used slight modifications of a known metabolite extraction procedure (Bennett *et al.* 2008, Rabinowitz and Kimball 2007, Yuan *et al.* 2008). Briefly, filters were thawed and metabolites extracted by placing the filters directly in a petri dish containing extraction solvent (40:40:20 acetonitrile/methanol/water with 0.1 M formic acid) at 4 °C. The filters were washed with extraction solvent, transferred to Eppendorf tubes and centrifuged to pellet cell debris. The filtrate was then dried on a nitrogen drying apparatus and re-suspended in 300 µL of HPLC grade water. A UPLC-HRMS analysis, in negative ion mode, was performed for each sample, and relative metabolite levels were analyzed as previously described (Bennett *et al.* 2008, Rabinowitz and Kimball 2007, Yuan *et al.* 2008).

Metabolite data analysis

Signal intensity for all metabolites was analyzed as peak area, and each measurement was manually curated using the Xcalibur 2.0.7 Quan Browser analysis package (Thermo Fisher Scientific, Waltham, MA, USA). Metabolite area counts were normalized to cell concentration to obtain per cell metabolite abundances, and a ratio of these values from each condition was used to compare relative concentrations of metabolites. All heat maps were generated using Gene Cluster 3.0 (de Hoon *et al.* 2004) and viewed using Java TreeView 1.1.5 (Saldanha 2004). Principal Component Analysis (PCA) was carried out using MetaboAnalyst 3.0 (Xia *et al.* 2012). Interactions among the metabolites were visualized using resources available through the Kyoto Encyclopedia of Genes and Genomes (KEGG) database (www.genome.jp/kegg/).

Data analysis for stable isotope incorporation into metabolites

Peak areas for all compounds detected in the ^{15}N and ^{13}C incorporation treatments were calculated as described for the pool size data above. Once the peak areas were determined, the ratios of unlabeled, partially labeled and fully labeled metabolites were determined for each time point. These values were then used to calculate the rate of disappearance (turnover) for the unlabeled material. The data were fit using the following equation, $y=Ae^{(-kx)}$, where k is the rate constant. The ratios of rate constants from the lysate amended and control cultures were calculated and multiplied by the fold difference in metabolite concentration to determine relative fluxes.

Cell enumeration

To monitor changes in community population dynamics in response to virus derived DOM addition, 1mL aliquots of each sample were collected at each timepoint and fixed with gluteraldehyde (0.5%) and stored at $-80\text{ }^{\circ}\text{C}$ until processing. Samples were thawed and stained with SYBR Gold (25 \times concentration, Invitrogen, Carlsbad, CA, USA) for 2 h in the dark and enumerated using a Guava easyCyteHT flow cytometer (Millipore, Billerica, MA) as previously described (Tripp *et al.* 2008).

Results

To examine the effects of phage-derived DOM on natural bacterioplankton metabolism, microbial communities in the North Pacific were amended with Roseobacter-derived unlabeled and stable-isotope labelled (^{13}C and ^{15}N) virus lysate (containing $50\text{ }\mu\text{M C}$ and $10\text{ }\mu\text{M N}$) and the change in community intracellular metabolite pools, metabolic rates and nutrient turnover

studied using ultra performance liquid chromatography–high resolution mass spectrometry (UPLC-HRMS)-based metabolomics. Studies to monitor changes in intracellular metabolite pools in response to lysate addition were conducted at four stations along a cruise transect (Stations 14, 30, 40, 46). Isotope-based flux measurements to examine changes in metabolic rates and turnover in response to lysate amendment were conducted at five stations along a cruise transect (Stations 2, 14, 44, 48, 50).

Microbial community population dynamics

Amendment of natural communities with *Roseobacter*-derived virus lysates resulted in a ~2.5-fold increase in cell concentration from an initial average concentration of 3.0×10^5 cells mL⁻¹ at the time of amendment to a final average concentration of 7.4×10^5 cells mL⁻¹ after 24h of incubation at all stations sampled (Figure 5.1). Similarly, microbial abundance also increased 1.7-fold from an average initial concentration of 3.0×10^5 cells mL⁻¹ at the time of amendment to a final average concentration of 4.9×10^5 cells mL⁻¹ after 24h of incubation in response to the addition 50 μM C and 10 μM N at all four stations sampled (Figure 5.1). In contrast to the significantly ($p < 0.0005$) increased cell abundances observed in the nutrient amended (lysate or C+N) treatments, microbial abundance stayed comparatively unchanged in the non-amended communities increasing ~1.2-fold from an initial cell average concentration of 3.0×10^5 cells mL⁻¹ at the start of incubation to a final average concentration of 3.7×10^5 cells mL⁻¹ after 24h of incubation at all stations sampled (Figure 5.1).

Changes in microbial community metabolite pools

To characterize the impact of virus-derived dissolved organic matter (v-DOM) on the metabolite pools of natural bacterioplankton communities, bacterioplankton communities in the North Pacific were amended with Roseobacter-derived virus lysate (containing 50 μM C and 10 μM N) and incubated for a period of 24h. Duplicate control cultures with no nutrient amendment or amended with 50 μM sodium acetate and 10 μM ammonium chloride were maintained and sampled in parallel. The relative intracellular concentrations of 111 central pathway metabolites were measured using ultra performance liquid chromatography–high resolution mass spectrometry (UPLC-HRMS) for lysate amended, C+N amended and non-amended microbial populations at four discrete time points.

A Principal Component Analysis (PCA) of all community intracellular metabolite concentrations was performed to determine the overall relationships and variances between our treatments at the start of incubation and at the end of the 24 h incubation period. The results of the PCA (Figure 5.2) show that at the start of incubation individual samples from different treatments cluster together indicating a similar metabolic profile for all bacterioplankton communities at the start of incubation. After 24 hours of incubation on different substrates, however, clear-cut separations are evident between treatments with the direction (geometry) and magnitude of change (distance from the median/control) varying with the type of treatment which is suggestive of a treatment dependent alteration in metabolic profiles and also highlights the diversity within individual community responses to nutrient amendment. The greatest change (geometry and magnitude) in metabolite profiles observed in all 3 treatments occurs within the lysate amended populations. Additionally, our PCA data show that after 24 h of incubation on different substrates, half of the metabolic changes occurring within the C+N controls co-cluster

with the no addition treatments and the other half co-cluster with the lysate amended communities. These data, altogether, provide direct evidence that virus lysates alter community metabolism to a greater extent than single substrate nutrient sources and highlight the metabolic differences distinct nutrient sources have on consuming microbial populations.

An additional PCA performed to determine the overall relationships and variances within individual treatments at the start of incubation and after 24 h of incubation showed a smaller cluster representing samples at 24 h within a larger cluster representing samples at the start of incubation for the unamended controls (Figure 5.3). This data is suggestive of a shrinking of the biochemical footprint in the unamended communities over time, an observation that may be attributed to the phenomenon known as ‘bottle effects’, reported in many *in situ* incubations (Fuhrman and Azam 1980, Hammes *et al.* 2010). On the other hand, samples collected at 0 and 24 h clearly separated into individual clusters for the C+N and virus lysate amended communities (Figure 5.3). In both cases the direction and magnitude of change varied with time, indicating a strong effect of nutrient amendment on the metabolic profiles of bacterioplankton communities amended with either a simple (C+N) or complex substrates (v-DOM). The spread of the samples for each treatment on each plot highlight the diversity within individual responses and may be suggestive of a site dependent response to nutrient amendment.

To highlight the specific metabolite changes that occur within microbial communities in response to lysate and C+N amendment, the fold changes of individual lysate and C+N amended community metabolite intracellular concentrations relative to intracellular metabolite concentrations in the unamended controls are displayed in a heatmap (Figure 5.4). Our data from these analysis indicate that relative to the unamended controls 14% (15 out of 111) of the metabolites monitored in our microbial communities displayed a conserved response to virus

lysate addition, showing similar increases or decreases in metabolite pools at all stations after 24h of incubation (Table 5.2). These metabolites with conserved responses to lysate addition represent metabolite groups mainly involved in nucleotide metabolism (~44% of conserved metabolites), amino acid metabolism (~31% of conserved metabolites), the pentose phosphate pathway (~13% of conserved metabolites), tricarboxylic acid cycle (~6% of conserved metabolites) and fatty acid biosynthesis (~6% of conserved metabolites). Of these metabolites, ~20% (glutamine, sedoheptulose-7-phosphate and thymidylate) were elevated (fold change ≥ 1.5) at all stations in response to virus lysate amendment and ~80% (12 metabolites; 3-(4-hydroxyphenyl)pyruvate, 3-methyl-2-oxobutanoic acid, homoserine, xanthurenic acid, succinate, 5-phospho-alpha-D-ribose 1-diphosphate, guanine, dihydroorotate, deoxyuridine, thymidine, guanosine diphosphate and lipoate) showed a decrease (fold change ≤ 0.66) in metabolite concentrations at all stations sampled. It should be noted that while these metabolites were highly discriminatory (fold change ≥ 1.5 ; fold change ≤ 0.66) between the lysate amended and unamended populations, statistically significant ($p \leq 0.05$) changes were only observed at discrete stations (Table 5.2). In contrast to the conserved responses of a large fraction of the metabolome to nutrient addition observed in the lysate amended communities, only two metabolites, glutamine (increased concentration) and 7-methylguanosine (decreased concentration), displayed a conserved response to C+N amendment at all stations sampled. These data further support the conclusions of the PCA: alterations in community metabolic profiles in response to virus lysate (and other nutrient) amendment appear to be community and/or environment specific.

It is also important to note that at all stations sampled, amendment of the bacterioplankton community with virus lysates resulted in a higher number of significantly ($p \leq$

0.05) altered intracellular metabolite concentrations representing more diverse metabolic pathways than the C+N controls. The exception was station 46, where a similar number of metabolic pathways were altered in response to lysate and C+N amendment (Figure 5.5 and 5.6). At the end of the 24 h incubation period, ~20, 11, 16 and 32% of metabolite concentrations were significantly different ($p \leq 0.05$ and ≥ 1.5 fold change) in lysate amended populations relative to the unamended controls at stations 22, 30, 40 and 46 respectively. In contrast to these changes, only 5, 4, 3 and 16% of metabolite concentrations were significantly different ($p \leq 0.05$ and ≥ 1.5 fold change) in C+N amended populations relative to the unamended controls at stations 22, 30, 40 and 46 respectively (Figure 5.5). Metabolite groups most significantly altered in response to lysate amendment were amino acid metabolism, glycolysis and TCA cycle intermediates and nucleotide metabolism intermediates (Figure 5.6a). Metabolite groups most significantly altered in response to C+N amendment were amino acid metabolism, glycolytic intermediates, TCA cycle intermediates and amino acid/nucleotide sugar metabolism intermediates (Figure 5.6b). Altogether, these observations clearly point to viral lysates as a complex labile nutrient source capable of supporting the diverse metabolic needs of most bacterioplankton populations.

Microbial community metabolic turnover and flux

To examine the metabolite turnover and metabolic flux of virus derived *Roseobacter* lysate in natural communities, complementary experiments were also performed using stable isotope-labeled carbon and nitrogen virus lysates. 50 μM ^{13}C and 10 μM ^{15}N fully labelled *Roseobacter*-derived virus lysate were added to natural bacterioplankton communities and incubated for a 12h period. Control communities supplemented with 50 μM ^{13}C -labelled sodium acetate and 10 μM ^{15}N -labelled ammonium chloride were maintained and sampled in parallel.

Incorporation of ^{13}C and ^{15}N label into 15 select metabolites representing nucleotide metabolism intermediates, tricarboxylic acid cycle components and amino acids were monitored via UPLC-HRMS at discrete timepoints during the 12h incubation. Measuring the metabolite turnover provides information about the rate at which a specific metabolite pool is converted to entirely new metabolites because of biosynthesis. The metabolic flux (the product of the turnover rate and metabolite pool size) provides information on the total amount of nutrients that pass through a specific compound, that is, the flux through them.

Incorporation of labelled ^{13}C or ^{15}N was observed for all metabolites monitored (Tables 5.2 and 5.3). Label incorporation into metabolites ranged from 1-64% of the total metabolite pool for citraconate and glutamate respectively by 12 hrs post lysate amendment. Four metabolites, aspartate, guanine, glutamate and malate, incorporated the most label from virus lysates among all metabolites monitored. In contrast to all other metabolites monitored, these metabolites had $\geq 10\%$ of their total metabolite pool labelled by 12 hrs post virus lysate amendment (Table 5.3, Figures 5.7-5.10). It is also important to note that only glutamate had more than 20% of its total metabolite pool incorporating both ^{13}C and ^{15}N label at all stations sampled 12 hrs post virus lysate amendment (Table 5.3, Figure 5.10). Calculations of metabolite turnover and fluxes for aspartate, guanine, glutamate and malate generally showed increases in metabolite turnover and fluxes in lysate amended communities relative to ^{13}C or ^{15}N controls at all stations sampled (Tables 5.4-5.6).

Measured turnover rates for aspartate were indistinguishable between viral lysate and control cultures for all stations; however, the calculated flux through aspartate in the viral lysate amended communities varied across stations due to differences in relative aspartate pools at each station (Table 5.5). Flux through aspartate was 70% greater at station 14, 40% decreased at

station 44 and indistinguishable from the controls at station 48 by the final timepoint 12h post amendment (Table 5.5).

Measured turnover rates for guanine also varied by station with increased guanine turnover observed at stations 2, 48 and 50 and decreased guanine turnover observed at stations 14 and 44 (Table 5.5). The calculated flux through guanine was however increased at all stations monitored due to increased relative guanine pools in the lysate amended communities relative to the controls, except for station 44, where a decrease in guanine flux was observed as a result of a decreased relative guanine pool at this station. Flux through guanine ranged from a 45% decrease at station 44 to an increase of more than 900% at station 50 after 12 h of incubation (Table 5.5).

Malate turnover rates were increased at 2 stations (station 44 and 50) and decreased at station 48 compared to the controls. These differences in turnover rates resulted in an ~400 and 700% increase in malate flux compared to controls at station 44 and 50, respectively, and an unchanged flux at station 48 relative to the controls (Table 5.6). Incorporation of labelled material into malate metabolite pools was not observed at station 2 and 14.

The turnover rates for glutamate N were mostly indistinguishable between the lysate amended and control communities for most of the stations sampled, except station 2 where turnover rates were increased ~70% in the lysate amended communities (Table 5.7). Glutamate N pools were also indistinguishable between the lysate amended and control treatments at station 48 and 50, increased at station 14 and decreased at stations 2 and 44 (Table 5.7). The relative flux of glutamate N was increased 12-80% at all stations except station 44 where a 62% decrease in glutamate N flux relative to the controls was observed (Table 5.7). In contrast to the indistinguishable glutamate N turnover rates, turnover rates for glutamate C were increased in the virus lysate amended communities relative to the ¹³C controls at all stations sampled (Table

5.7). Although the relative metabolite pools were decreased in the lysate amended communities at almost all stations sampled, the high turnover of glutamate C at all stations resulted in increased fluxes as smaller pools were being replenished at increased rates. Increases in glutamate C flux compared to controls ranged from 20% - 600% at all stations sampled. (Table 5.7).

Discussion

An estimated 10-20% of the bacterial population in the world's oceans is lysed by viruses each day (Suttle 1994), releasing labile dissolve organic matter that is metabolized by the surrounding bacterioplankton population. While qualitative assessments have been made of material released upon virus-mediated cell lysis (Ankrah *et al.* 2014, Middelboe and Jorgensen 2006, Shelford *et al.* 2012), we know relatively little how this material is metabolized by bacterioplankton populations and how this material affects community metabolism as a whole. Using virus lysates generated from the marine bacterium *Sulfitobacter* sp. CB2047, we investigated the effects of virus derived dissolved organic (v-DOM) matter on natural bacterioplankton community metabolism across a transect representing coastal and open ocean environments in the North Pacific ocean to provide insights into how virus derived dissolved organic matter is metabolized by natural bacterioplankton communities.

Our results from this study indicate that amendment of natural bacterioplankton communities with viral lysates significantly alters key central metabolism and biosynthetic pathways to a larger extent than communities amended with single substrate labile C+N sources.

Our results also indicate that although amendment of bacterioplankton communities generally results in station specific alterations to intracellular metabolite pools, ~14% of the metabolic changes that occur in bacterioplankton communities in response to virus lysate amendment are conserved across all stations sampled. Among the metabolites with conserved responses to virus lysate amendment, three metabolites glutamine, thymidylate (dTMP) and sedoheptulose 7-phosphate had elevated intracellular concentrations at all stations sampled by the final timepoint, 24h after virus lysate amendment. Twelve metabolites, 3-(4-hydroxyphenyl) pyruvate, 3-methyl-2-oxobutanoic acid, homoserine, xanthurenic acid, succinate, 5-phospho-alpha-D-ribose 1-diphosphate, guanine, dihydroorotate, deoxyuridine, thymidine, guanosine diphosphate and lipoate had decreased intracellular concentrations at all stations sampled by the final timepoint.

Glutamine, a precursor of glutamate, is an important entry point for nitrogen into microbial cells and is known to provide ~12% of cellular nitrogen requirements (Wohlhueter *et al.* 1973). Intracellular glutamine concentrations have also been demonstrated to serve as sensors for external nitrogen availability with decreased glutamine pools indicative of external nitrogen scarcity (Ikeda *et al.* 1996). The increased intracellular glutamine concentration in our virus lysate amendment communities is suggestive of nitrogen replete conditions in the lysate amended communities and provides evidence that virus lysates can provide all the N requirement of bacterioplankton communities. Additionally, glutamine plays an essential role in providing N sources for the synthesis of purine and pyrimidine rings during de novo nucleotide biosynthesis (Berg *et al.* 2012). The significant increases in cell concentrations observed in all virus amended communities highlight the contribution of glutamine to the increase in cell biomass in the lysate amended populations.

Thymidylate is a precursor to thymidine and thymine both important pyrimidine biosynthesis intermediates. The increase in thymidylate intracellular concentrations in lysate amended communities may be suggestive of an upregulation of nucleotide biosynthetic pathways in response to virus lysate amended, however the observation of decreased concentrations of other pyrimidine biosynthesis intermediates including, thymidine, deoxyuridine and dihydroorotate at all stations sampled does not support this observation. It is important to note that increases in intracellular metabolite concentrations could be a result of increased biosynthesis or decreased utilization of each metabolite and does not provide any information about the flux of metabolites within specific pathways.

Sedoheptulose 7-phosphate, a pentose phosphate pathway intermediate, is a precursor to the glycolytic intermediate fructose 6-phosphate and the purine biosynthesis intermediate 5-Phospho-alpha-D-ribose 1-diphosphate (PRPP) (Berg *et al.* 2012). Statistically significant ($p \leq 0.05$) increases in fructose 6-phosphate concentrations relative to the unamended controls were observed at 3 of the 4 stations sampled and this might be suggestive of an increased flux of sedoheptulose 7-phosphate for the production of fructose 6-phosphate to fuel lysate amended community glycolytic pathways. In contrast to the significantly increased fructose 6-phosphate metabolite pools, PRPP showed a consistent decrease in concentration relative to the uninfected controls at all stations sampled which might be suggestive of an increased flux of PRPP for the synthesis of new purine rings, however, the decreased concentration of guanine and guanosine diphosphate (GDP) both intermediates in purine biosynthesis observed at all stations sampled does not support this observation.

It is important to note that, a recent study characterizing *Sulfitobacter* derived viral lysates detected no glutamine in *Sulfitobacter* virus lysates despite increased intracellular

concentrations of this metabolite just prior to the onset of cell lysis (Ankrah *et al.* 2014). Additionally the same study reported decreased concentrations of thymidylate and sedoheptulose 7-phosphate in *Sulfitobacter* virus lysates despite their increased intracellular concentration just prior to cell lysis. The authors of the study attributed the absence or decrease in concentration of these metabolites to the fact that glutamine, thymidylate and sedoheptulose 7-phosphate were rapidly assimilated by members of the unlysed population, consequently depleting their concentrations in the viral lysates. The increased concentration of glutamine, thymidylate and sedoheptulose 7-phosphate observed in our community intracellular metabolomes further supports the preferential uptake and incorporation of specific metabolites from virus lysates hypothesis and reaffirms the importance of viral lysates as important sources of labile nutrients for natural bacterioplankton communities.

Following the measurement of metabolite pool concentrations in response to viral lysate amendment, stable isotope labeling studies using ^{13}C and ^{15}N labelled lysates were performed to determine whether the general alterations in metabolite concentrations were because of increases in biosynthesis or decreases in the utilization of each molecule. In harmony with our metabolite pool data, the uptake and metabolism of viral lysate metabolites was found to be mostly station specific although general trends were observed for most metabolites monitored.

Incorporation of labelled material was observed in almost all 15 metabolites monitored indicating an active flux of metabolites within diverse pathways, however, only four metabolites glutamate, aspartate, malate and guanine incorporated more than 10% of labelled material into their metabolite pools at the end of the 12h incubation period on virus lysates. Of these metabolites, the amino acids glutamate and aspartate incorporated the most label, incorporating up to ~78% and ~75% of labelled material into their metabolite pools respectively.

Glutamate accounts for over 50% of the total amino acid content of the microbial metabolite pools (Bennett *et al.* 2009, Tempest *et al.* 1970) and provides up to 88% of the cellular nitrogen requirement (Wohlhueter *et al.* 1973). Additionally, glutamate is an important osmolyte in microbes ensuring their survival across a wide range of environmental conditions (Csonka and Hanson 1991, Tempest *et al.* 1970). Measuring the incorporation of labelled ^{15}N and ^{13}C into glutamate indirectly provides information on the availability and uptake of two other metabolites, glutamine and 2-oxoglutarate, for which we do not see incorporation of label in lysate amended and control communities, and allows us to make inferences about alterations to pathways like the TCA cycle by bacterioplankton communities in response to lysate amendment. Two glutamate biosynthetic pathways exist in nature (Brown *et al.* 1972, Brown 1980), the glutamine synthetase /glutamate synthase pathway (GS/GOGAT), transfers an amide group from glutamine to 2-oxoglutarate to yield glutamate (Reitzer and Magasanik 1996) and glutamate dehydrogenase pathway (GDH), an alternate pathway usually utilized in nitrogen rich environments, forms glutamate by catalyzing the reductive amination of 2-oxoglutarate (Coulton and Kapoor 1973, Reitzer 2003). In both pathways, the carbon backbone of glutamate, 2-oxoglutarate, is derived from the tricarboxylic acid (TCA) cycle. Monitoring glutamate C and N biosynthesis is very important if we want to explore the metabolic intersection, connecting carbon with nitrogen metabolism. The relative increase in ^{13}C glutamate flux compared to controls observed in the lysate amended cultures clearly points to viral lysates as a rich source of 2-oxoglutarate. As we did not detect any intracellular ^{13}C labelled 2-oxoglutarate, the incorporation of ^{13}C into glutamate could only have come from labelled 2-oxoglutarate assimilated from the virus lysate. In fact 2-oxoglutarate was one of the metabolite hypothesized to be quickly taken up from viral lysates by unlysed cells (Ankrah *et al.* 2014). Similarly, the

relative increase in ^{15}N glutamate flux observed in the lysate amended cultures compared to the controls clearly points to viral lysates as a rich source of glutamine. As we did not see any intracellular ^{15}N labelled glutamine, the incorporation of ^{15}N into glutamine could mostly have come from ^{15}N labelled glutamine assimilated from the virus lysate. In fact, data from our metabolite pool studies shows an increased intracellular concentration of glutamine in lysate amended communities compared to controls after 24h of incubation. Additionally, Ankrah *et al.* hypothesized glutamine to be one of the metabolites rapidly taken up from virus lysates since it was not detected in *Sulfitobacter* lysates despite its significantly increased intracellular concentrations just prior to the onset of cell lysis.

Our metabolite flux data also shows incorporation of ~20% ^{15}N label in aspartate by the first hour after the start of incubation on viral lysates while less than 5% of the aspartate ^{13}C pool was labelled 12 hours after the start of incubation. Aspartate is formed by a transamination reaction involving the transfer of an amino group from glutamate to the TCA cycle intermediate oxaloacetate (Berg *et al.* 2012) The difference in labelling patterns for N and C aspartate observed in lysate amended microbial communities could be suggestive of a rapid uptake and labelling of glutamate from viral lysates and a slower uptake and metabolism of oxaloacetate from viral lysates. In fact, our metabolite flux data also show that malate, a precursor to oxaloacetate in the TCA cycle, is rapidly taken up and metabolized in the lysate amended communities as 9% of its total metabolite pool is ^{13}C labelled within a few minutes after lysate amendment at a subset of the stations sampled.

Substantial incorporation of labelled material into nucleotide biosynthetic pathway intermediates was not observed at any of our stations until 6 h after the start of incubation in our viral lysate amended communities. Although the relative flux of guanine, a purine biosynthesis

intermediate, was generally increased relative to the controls for most of stations sampled at all timepoints, an increase in the incorporation of ^{15}N label above 5% of the total guanine metabolite pool, was observed only after 6 hours of incubation for most stations sampled. However, by the final timepoint, 12 h after the start of incubation an average of 35% of the guanine pool was ^{15}N labelled at all stations and this significant increase in label incorporation also coincides with the onset of significant changes in cell concentration observed in the lysate amended microbial communities.

Altogether our flux data indicates that the first metabolites assimilated when microbial communities encounter viral lysates are amino acids and TCA cycle intermediates and these metabolites are used to meet the energy demands of the microbial community before being diverted to biosynthetic pathways to meet their replications needs. Although dissolved free amino acids are relatively poor sources of carbon and energy compared to other nutrient sources, such as glucose (Schut *et al.* 1995, Schut *et al.* 1997) they are ubiquitous in viral lysates and are important growth substrates for microbial communities. In fact, the main source of nitrogen for bacteria in oligotrophic ocean waters are dissolved free amino acids and free ammonia (Keil and Kirchman 1991). In summary, our intracellular metabolite pool and isotope-based flux measurements reaffirm the significance of viral lysates as important sources of labile nutrients in marine environments and provides a framework for establishing a sequence for the utilization and metabolism of virus lysates by natural bacterioplankton communities.

Acknowledgement

We are grateful to Dr. Zachary Johnson the chief scientist on the POWOW III research cruise and to Dr. Erik Zinser, cruise co-PI for help on board. We thank the captain and crew of R/V Kilo Moana for their help with sample collection and logistical support. We are grateful to Ming Leung for providing in situ NH_4 measurements. This work was supported by NSF grant OCE-1061352 to A.B, S.R.C. and S.W.W.

References

- Ankrah NYD, May AL, Middleton JL, Jones DR, Hadden MK, Gooding JR *et al.* (2014). Phage infection of an environmentally relevant marine bacterium alters host metabolism and lysate composition. *ISME J* **8**: 1089-1100.
- Bennett BD, Yuan J, Kimball EH, Rabinowitz JD (2008). Absolute quantitation of intracellular metabolite concentrations by an isotope ratio-based approach. *Nat Protocols* **3**: 1299-1311.
- Bennett BD, Kimball EH, Gao M, Osterhout R, Van Dien SJ, Rabinowitz JD (2009). Absolute metabolite concentrations and implied enzyme active site occupancy in *Escherichia coli*. *Nature chemical biology* **5**: 593-599.
- Berg JM, Tymoczko JL, Stryer L (2012). *Biochemistry*. W.H. Freeman: Basingstoke.
- Bratbak G, Jacobsen A, Heldal M (1998). Viral lysis of *Phaeocystis pouchetii* and bacterial secondary production. *Aquatic microbial ecology* **16**: 11-16.
- Breitbart M (2012). Marine viruses: truth or dare. *Annual Review of Marine Science* **4**: 425-448.
- Brown C, Macdonald-Brown DS, Stanley S (1972). Inorganic nitrogen metabolism in marine bacteria: Nitrogen assimilation in some marine pseudomon. *Journal of the Marine Biological Association of the United Kingdom* **52**: 793-804.
- Brown C (1980). Ammonia assimilation and utilization in bacteria and fungi. *Microorganisms and nitrogen sources New York: John Wiley and Sons p.*

- Brussaard C, Mari X, Van Bleijswijk J, Veldhuis M (2005). A mesocosm study of *Phaeocystis globosa* (Prymnesiophyceae) population dynamics: II. Significance for the microbial community. *Harmful algae* **4**: 875-893.
- Budinoff CR, Hollibaugh JT (2007). Ecophysiology of a Mono Lake Picocyanobacterium. *Limnology and Oceanography* **52**: 2484-2495.
- Coulton J, Kapoor M (1973). Studies on the kinetics and regulation of glutamate dehydrogenase of *Salmonella typhimurium*. *Canadian journal of microbiology* **19**: 439-450.
- Csonka LN, Hanson AD (1991). Prokaryotic osmoregulation: genetics and physiology. *Annual Reviews in Microbiology* **45**: 569-606.
- de Hoon MJL, Imoto S, Nolan J, Miyano S (2004). Open source clustering software. *Bioinformatics* **20**: 1453-1454.
- Fuhrman JA, Azam F (1980). Bacterioplankton secondary production estimates for coastal waters of British Columbia, Antarctica, and California. *Applied and environmental microbiology* **39**: 1085-1095.
- Gobler CJ, Hutchins DA, Fisher NS, Cosper EM, Sanudo-Wilhelmy SA (1997). Release and bioavailability of C, N, P, Se, and Fe following viral lysis of a marine chrysophyte. *Limnology and Oceanography*: 1492-1504.
- Haaber J, Middelboe M (2009). Viral lysis of *Phaeocystis pouchetii*: implications for algal population dynamics and heterotrophic C, N and P cycling. *The ISME journal* **3**: 430-441.

- Hammes F, Vital M, Egli T (2010). Critical evaluation of the volumetric “bottle effect” on microbial batch growth. *Applied and environmental microbiology* **76**: 1278-1281.
- Ikeda TP, Shauger AE, Kustu S (1996). *Salmonella typhimurium* Apparently Perceives External Nitrogen Limitation as Internal Glutamine Limitation. *Journal of Molecular Biology* **259**: 589-607.
- Keil RG, Kirchman DL (1991). Contribution of dissolved free amino acids and ammonium to the nitrogen requirement of heterotrophic bacterioplankton. *Marine Ecology-Progress Series* **73**: 1-10.
- Lønborg C, Middelboe M, Brussaard CP (2013). Viral lysis of *Micromonas pusilla*: impacts on dissolved organic matter production and composition. *Biogeochemistry* **116**: 231-240.
- Middelboe M, Jørgensen N, Kroer N (1996). Effects of viruses on nutrient turnover and growth efficiency of noninfected marine bacterioplankton. *Applied and Environmental Microbiology* **62**: 1991-1997.
- Middelboe M, Riemann L, Steward GF, Hansen V, Nybroe O (2003). Virus-induced transfer of organic carbon between marine bacteria in a model community. *Aquatic microbial ecology* **33**: 1-10.
- Middelboe M, Jørgensen NOG (2006). Viral lysis of bacteria: an important source of dissolved amino acids and cell wall compounds. *Journal of the Marine Biological Association of the United Kingdom* **86**: 605-612.
- Poorvin L, Rinta-Kanto JM, Hutchins DA, Wilhelm SW (2004). Viral Release of Iron and Its Bioavailability to Marine Plankton. *Limnology and Oceanography* **49**: 1734-1741.

- Rabinowitz JD, Kimball E (2007). Acidic acetonitrile for cellular metabolome extraction from *Escherichia coli*. *Analytical Chemistry* **79**: 6167-6173.
- Reitzer L (2003). Nitrogen assimilation and global regulation in *Escherichia coli*. *Annual Reviews in Microbiology* **57**: 155-176.
- Reitzer LJ, Magasanik B (1996). Ammonia assimilation and the biosynthesis of glutamine, glutamate, aspartate, asparagine, L-alanine, and D-alanine. *Escherichia coli and Salmonella: cellular and molecular biology, 2nd ed ASM Press, Washington, DC*: 391-407.
- Saldanha AJ (2004). Java Treeview-extensible visualization of microarray data. *Bioinformatics* **20**: 3246-3248.
- Schut F, Jansen M, Gomes TMP, Gottschal JC, Harder W, Prins RA (1995). Substrate uptake and utilization by a marine ultramicrobacterium. *Microbiology-Uk* **141**: 351-361.
- Schut F, Prins RA, Gottschal JC (1997). Oligotrophy and pelagic marine bacteria: Facts and fiction. *Aquatic Microbial Ecology* **12**: 177-202.
- Sheik AR, Brussaard CP, Lavik G, Lam P, Musat N, Krupke A *et al.* (2013). Responses of the coastal bacterial community to viral infection of the algae *Phaeocystis globosa*. *The ISME journal*.
- Shelford EJ, Middelboe M, Møller EF, Suttle CA (2012). Virus-driven nitrogen cycling enhances phytoplankton growth. *Aquatic Microbial Ecology* **66**: 41-46.

- Shelford EJ, Jørgensen NO, Rasmussen S, Suttle CA, Middelboe M (2014). Dissecting the role of viruses in marine nutrient cycling: bacterial uptake of D-and L-amino acids released by viral lysis. *Aquatic Microbial Ecology* **73**.
- Suttle CA (1994). The significance of viruses to mortality in aquatic microbial communities. *Microbial Ecology* **28**: 237-243.
- Suttle CA (2007). Marine viruses—major players in the global ecosystem. *Nature Reviews Microbiology* **5**: 801-812.
- Tempest D, Meers J, Brown C (1970). Influence of environment on the content and composition of microbial free amino acid pools. *Journal of general microbiology* **64**: 171-185.
- Tripp HJ, Kitner JB, Schwalbach MS, Dacey JW, Wilhelm LJ, Giovannoni SJ (2008). SAR11 marine bacteria require exogenous reduced sulphur for growth. *Nature* **452**: 741-744.
- Weinbauer MG, Peduzzi P (1995). Effect of virus-rich high molecular weight concentrates of seawater on the dynamics of dissolved amino acids and carbohydrates. *Marine ecology progress series Oldendorf* **127**: 245-253.
- Weinbauer MG, Bonilla-Findji O, Chan AM, Dolan JR, Short SM, Šimek K *et al.* (2011). Synechococcus growth in the ocean may depend on the lysis of heterotrophic bacteria. *Journal of plankton research* **33**: 1465-1476.
- Wilhelm SW, Suttle CA (1999). Viruses and Nutrient Cycles in the Sea - Viruses play critical roles in the structure and function of aquatic food webs. *BioScience* **49**: 781-788.
- Wohlhueter R, Schutt H, Holzer H (1973). Regulation of glutamine synthesis in vivo in *E. coli*. *The enzymes of glutamine metabolism Academic Press, Inc, New York*: 45-64.

Xia J, Mandal R, Sinelnikov IV, Broadhurst D, Wishart DS (2012). MetaboAnalyst 2.0—a comprehensive server for metabolomic data analysis. *Nucleic acids research* **40**: W127-W133.

Yuan J, Bennett BD, Rabinowitz JD (2008). Kinetic flux profiling for quantitation of cellular metabolic fluxes. *Nature protocols* **3**: 1328-1340.

Appendix

Tables

Table 5.1. Site description of sampling stations

| Station | Sampling time | SST (°C) | Depth (m) | Latitude | Longitude | NH ₄ (nM)* | ISUS Nitrate (5m)* | Type of metabolomics study |
|---------|---------------|----------|-----------|-----------|------------|-----------------------|--------------------|----------------------------|
| 22 | 4:00am | 20 | 3 | 33 59.943 | 145 00.028 | 1.67 | -0.21 | Metabolite pool |
| 30 | 11:00am | 14 | 2 | 46 01.636 | 138 16.087 | 98 | 7.7 | Metabolite pool |
| 40 | 4:00am | 17 | 4 | 33 10.686 | 130 48.883 | 0 | -1.03 | Metabolite pool |
| 46 | 2:00am | 18 | 2 | 29 49.984 | 124 00.027 | 10 | -0.72 | Metabolite pool |
| 2 | 4:00am | 23 | 3 | 22 44.999 | 158 00.021 | N/A | N/A | Stable-isotope flux |
| 14 | 2:00am | 11 | 2 | 46 41.327 | 157 59.900 | N/A | N/A | Stable-isotope flux |
| 44 | 2:00am | 18 | 2 | 29 47.993 | 126 36.498 | N/A | N/A | Stable-isotope flux |
| 48 | 2:00am | 18 | 2 | 29 14.998 | 122 20.013 | N/A | N/A | Stable-isotope flux |
| 50 | 6:30am | 15 | 15 | 33 05.025 | 118 40.042 | N/A | N/A | Stable-isotope flux |

SST- sea surface temperature

ISUS- in situ ultraviolet spectrophotometer

*Measurements taken from same station but not from same CTD cast as metabolomics samples.

Table 5.2. Metabolites with conserved responses across all stations 24 h after incubation on virus lysates

| Metabolite name | Fold change* | p-value | Fold change* | p-value | Fold change* | p-value | Fold change* | p-value |
|--|--------------|---------|--------------|---------|--------------|---------|--------------|---------|
| Thymidylate (dTMP) | 2.12 | 0.203 | 2.10 | 0.321 | 1.73 | 0.219 | 12.88 | 0.018 |
| Glutamine | 14.94 | 0.002 | 2.74 | 0.364 | 3.15 | 0.021 | 22.80 | 0.006 |
| Sedoheptulose-7-phosphate | 51.07 | 0.052 | 1.54 | 0.207 | 1.87 | 0.268 | 2241.13 | 0.054 |
| Dihydroorotate | 0.33 | 0.082 | 0.35 | 0.158 | 0.62 | 0.490 | 0.40 | 0.149 |
| 3-(4-Hydroxyphenyl)pyruvate | 0.43 | 0.082 | 0.48 | 0.076 | 0.62 | 0.165 | 0.51 | 0.103 |
| 3-Methyl-2-oxobutanoic acid | 0.61 | 0.001 | 0.55 | 0.014 | 0.60 | 0.010 | 0.41 | 0.097 |
| 5-Phospho-alpha-D-ribose 1-diphosphate | 0.41 | 0.013 | 0.49 | 0.083 | 0.55 | 0.029 | 0.49 | 0.003 |
| Deoxyuridine | 0.39 | 0.031 | 0.43 | 0.070 | 0.45 | 0.114 | 0.58 | 0.321 |
| GDP | 0.46 | 0.302 | 0.37 | 0.494 | 0.45 | 0.318 | 0.27 | 0.367 |
| Guanine | 0.32 | 0.053 | 0.46 | 0.067 | 0.56 | 0.005 | 0.48 | 0.030 |
| Homoserine | 0.46 | 0.054 | 0.55 | 0.135 | 0.57 | 0.118 | 0.46 | 0.107 |
| Lipoate | 0.31 | 0.173 | 0.42 | 0.030 | 0.62 | 0.288 | 0.48 | 0.182 |
| Succinate | 0.62 | 0.031 | 0.56 | 0.027 | 0.64 | 0.031 | 0.64 | 0.156 |
| Thymidine | 0.43 | 0.159 | 0.37 | 0.216 | 0.25 | 0.149 | 0.39 | 0.113 |
| Xanthurenic acid | 0.58 | 0.102 | 0.53 | 0.000 | 0.58 | 0.016 | 0.58 | 0.178 |

*Fold changes are relative to metabolite concentration levels measured in the unamended controls.

Table 5.3. %N label

| Station | Time (h) | Glutamate | | Aspartate | | Guanine | |
|---------|----------|-----------|-----------|-----------|-----------|---------|-----------|
| | | Lysate | 15N cntrl | Lysate | 15N cntrl | Lysate | 15N cntrl |
| 2 | 0 | 5±3 | 4±0 | NA | NA | NA | NA |
| | 1 | 40±3 | 31±3 | NA | NA | NA | NA |
| | 2 | 38±1 | 46±5 | NA | NA | NA | NA |
| | 4 | 62±3 | 54±2 | NA | NA | 2±1 | NA |
| | 6 | 66±5 | 53±10 | NA | NA | 66±2 | 8±1 |
| | 12 | 79±4 | 64±5 | NA | NA | 35±8 | 41±9 |
| 14 | 0 | 1±0 | 1±0 | 0±1 | 0±1 | NA | NA |
| | 1 | 14±1 | 11±0 | 19±2 | 17±2 | NA | NA |
| | 2 | 23±1 | 19±1 | 24±2 | 25±6 | NA | 0±0 |
| | 4 | 29±2 | 26±2 | 28±1 | 29±6 | NA | 3±2 |
| | 6 | 33±1 | 30±0 | 27±2 | 27±1 | 5±3 | 5±1 |
| | 12 | 38±3 | 33±1 | 34±5 | 31±5 | 15±1 | 16±6 |
| 44 | 0 | 7±2 | 4±1 | 0±1 | 0±0 | NA | NA |
| | 1 | 41±3 | 33±2 | 26±6 | 23±5 | 0±1 | NA |
| | 2 | 51±3 | 50±4 | 46±1 | 49±5 | 2±2 | 0±1 |
| | 4 | 63±4 | 60±2 | 51±8 | 61±2 | 5±4 | 2±2 |
| | 6 | 68±2 | 69±2 | 59±3 | 59±2 | 6±2 | 7±4 |
| | 12 | 78±1 | 78±5 | 62±5 | 59±4 | 35±2 | 39±1 |
| 48 | 0 | 4±1 | 3±1 | 1±2 | 0±0 | NA | NA |
| | 1 | 34±0 | 33±1 | 14±7 | 32±9 | NA | 0±0 |
| | 2 | 51±2 | 47±6 | 35±3 | 35±8 | 0±0 | 0±1 |
| | 4 | 64±1 | 62±2 | 34±1 | 59±2 | 1±0 | 2±0 |
| | 6 | 69±4 | 66±1 | 63±13 | 68±9 | 13±3 | 11±3 |
| | 12 | 75±2 | 73±3 | 75±17 | 51±8 | 52±2 | 42±7 |
| 50 | 0 | 1±0 | 2±0 | NA | 0±0 | NA | 0±0 |
| | 1 | 8±3 | 9±1 | NA | 5±1 | NA | 0±0 |
| | 2 | 17±7 | 21±1 | NA | 4±3 | 1±0 | 0±0 |
| | 4 | 24±5 | 20±1 | 10±3 | 15±5 | 1±1 | 0±0 |
| | 6 | 27±3 | 26±1 | NA | 16±8 | 4±3 | 1±0 |
| | 12 | 32±5 | 32±2 | NA | 5±4 | 14±4 | 3±0 |

Table 5.3. continued %N label

| Station | Time (h) | Acetylcarnitine | | Inosine | | Pyroglutamic acid | |
|---------|----------|-----------------|-----------|---------|-----------|-------------------|-----------|
| | | Lysate | 15N cntrl | Lysate | 15N cntrl | Lysate | 15N cntrl |
| 2 | 0 | 5±0 | 6±0 | 7±0 | 9±1 | NA | NA |
| | 1 | 8±3 | 5±1 | 4±2 | 3±2 | NA | NA |
| | 2 | 2±0 | NA | 2±1 | 5±2 | 0±0 | 0±0 |
| | 4 | 2±2 | 4±1 | 2±1 | 5±1 | 1±0 | 0±0 |
| | 6 | 9±2 | 5±2 | 1±1 | 0±0 | 2±1 | 1±1 |
| | 12 | 5±2 | 6±0 | 0±0 | 0±1 | 1±0 | 1±1 |
| 14 | 0 | NA | NA | NA | NA | 0±0 | 0±0 |
| | 1 | NA | NA | NA | NA | 5±1 | 3±1 |
| | 2 | NA | NA | NA | NA | 8±3 | 6±3 |
| | 4 | NA | NA | NA | NA | 5±1 | 5±1 |
| | 6 | NA | NA | NA | NA | 3±1 | 4±0 |
| | 12 | NA | NA | NA | NA | 3±1 | 4±1 |
| 44 | 0 | 4±1 | 5±1 | NA | NA | NA | NA |
| | 1 | 3±2 | 5±0 | NA | NA | 2±1 | 2±0 |
| | 2 | 3±1 | 4±0 | NA | NA | 2±1 | 3±1 |
| | 4 | NA | 3±0 | NA | NA | 3±1 | 5±1 |
| | 6 | NA | 3±2 | NA | NA | 6±2 | 4±2 |
| | 12 | NA | 4±1 | NA | NA | 5±3 | 5±2 |
| 48 | 0 | 1±2 | 2±1 | 7±1 | 6±1 | 0±0 | NA |
| | 1 | 3±1 | 2±0 | 6±1 | 6±1 | 5±1 | 5±1 |
| | 2 | 3±1 | 2±1 | 5±1 | 6±2 | 7±3 | 11±5 |
| | 4 | 0±1 | 2±1 | NA | 2±2 | 5±3 | 7±1 |
| | 6 | 4±2 | 3±1 | 2±2 | 0±1 | 9±3 | 9±4 |
| | 12 | 3±0 | 3±2 | NA | NA | 7±3.1 | 6±3 |
| 50 | 0 | 4±2 | 1±0 | NA | NA | NA | NA |
| | 1 | 3±1 | 3±1 | NA | NA | 1±1 | 3±1 |
| | 2 | 5±1 | 3±1 | NA | NA | 3±0 | 3±0 |
| | 4 | 5±1 | 4±1 | NA | NA | 3±1 | 2±0 |
| | 6 | 5±1 | 5±0 | NA | NA | 5±2 | 4±1 |
| | 12 | 4±1 | 3±1 | NA | NA | 3±1 | 4±1 |

Table 5.4. %C label

| Station | Time (h) | Glutamate | | Malate | | Aspartate | | Succinate | |
|---------|----------|-----------|-----------|--------|-----------|-----------|-----------|-----------|-----------|
| | | Lysate | 13C cntrl | Lysate | 13C cntrl | Lysate | 13C cntrl | Lysate | 13C cntrl |
| 2 | 0 | 4±0 | 4±1 | NA | NA | NA | NA | 1±0 | 0±1 |
| | 1 | 13±0 | 10±1 | NA | NA | NA | NA | 1±0 | 1±1 |
| | 2 | 23±3 | 9±4 | NA | NA | NA | NA | 1±0 | 2±0 |
| | 4 | 25±1 | 15±9 | NA | NA | 1±1 | NA | 1±0 | 1±1 |
| | 6 | 27±1 | 18±1 | NA | NA | 4±4 | NA | 1±1 | 2±0 |
| | 12 | 51±5 | 16±0 | NA | NA | 22±11 | NA | 2±1 | 1±0 |
| 14 | 0 | 2±0 | 2±0 | NA | NA | 1±0 | 2±1 | 2±1 | 1±1 |
| | 1 | 4±1 | 4±0 | NA | NA | 2±2 | 1±1 | 1±1 | 0±0 |
| | 2 | 7±0 | 5±0 | NA | NA | 2±0 | 2±1 | 1±0 | 1±0 |
| | 4 | 12±3 | 7±0 | NA | NA | 3±1 | 3±0 | 3±2 | 1±1 |
| | 6 | 15±1 | 8±0 | NA | NA | 5±2 | 3±2 | 3±1 | 4±2 |
| | 12 | 22±1 | 11±0 | NA | NA | 4±1 | 2±0 | 2±1 | 1±0 |
| 44 | 0 | 8±1 | 2±0 | 1±1 | 2±1 | NA | NA | 2±0 | 1±0 |
| | 1 | 27±1 | 8±1 | 1±0 | 2±1 | NA | NA | 2±0 | 2±0 |
| | 2 | 33±1 | 10±2 | 1±0 | 1±0 | NA | NA | 1±0 | 1±1 |
| | 4 | 37±4 | 15±3 | 2±1 | 2±1 | NA | NA | 1±0 | 2±0 |
| | 6 | 43±2 | 19±4 | 4±1 | 3±2 | 0±1 | NA | 2±1 | 4±1 |
| | 12 | 43±2 | 20±1 | 6±3 | 2±1 | 3±2 | NA | 1±1 | 1±1 |
| 48 | 0 | 9±1 | 3±1 | 6±4 | 1±0 | NA | NA | 1±0 | 2±0 |
| | 1 | 37±0 | 9±2 | 7±1 | 1±1 | NA | NA | 2±1 | 2±0 |
| | 2 | 38±1 | 12±1 | 8±1 | 2±2 | NA | NA | 2±0 | 2±0 |
| | 4 | 40±3 | 20±2 | 10±1 | 5±0 | NA | NA | 1±0 | 2±1 |
| | 6 | 57±4 | 22±2 | 7±3 | 5±2 | 4±2 | NA | 3±1 | 2±0 |
| | 12 | 64±1 | 21±1 | 10±4 | 6±0 | 8±2 | 6±6 | 5±1 | 3±0 |
| 50 | 0 | 4±1 | 2±0 | 9±2 | 2±0 | NA | NA | 2±0 | 1±0 |
| | 1 | 13±1 | 4±1 | 17±2 | 4±1 | NA | NA | 3±0 | 2±1 |
| | 2 | 19±5 | 7±1 | 20±0 | 7±1 | NA | NA | 5±2 | 2±1 |
| | 4 | 20±4 | 9±1 | 22±0 | 7±2 | NA | NA | 4±0 | 3±0 |
| | 6 | 25±4 | 11±2 | 22±1 | 8±1 | NA | NA | 4±1 | 4±1 |
| | 12 | 40±3 | 16±3 | 23±0 | 5±0 | NA | NA | 9±2 | 4±1 |

Table 5.4. continued %C label

| Station | Time (h) | Prephenate | | N-Acetyl-L-alanine | | Methylmalonic acid | | Hydroxyphenylacetic acid | |
|---------|----------|------------|-----------|--------------------|-----------|--------------------|-----------|--------------------------|-----------|
| | | Lysate | 13C cntrl | Lysate | 13C cntrl | Lysate | 13C cntrl | Lysate | 13C cntrl |
| 2 | 0 | 1±0 | 0±1 | 3±0 | 2±0 | 1±0 | 0±1 | NA | 1±1 |
| | 1 | 2±1 | NA | 3±0 | 1±1 | 1±0 | 1±1 | NA | 4±2 |
| | 2 | 0±1 | NA | 1±1 | 1±1 | 1±0 | 2±0 | 4±0 | 6±3 |
| | 4 | 3±1 | NA | 2±0 | 0±1 | 1±0 | 1±1 | 5±1 | 2±1 |
| | 6 | 2±2 | NA | 2±2 | 1±1 | 1±1 | 2±0 | 5±1 | 8±2 |
| | 12 | 2±2 | NA | 3±0 | 3±0 | 2±1 | 1±0 | 4±1 | 5±1 |
| 14 | 0 | 3±1 | 1±1 | 2±1 | 0±1 | 2±1 | 1±1 | 5±1 | 4±1 |
| | 1 | 3±2 | 2±1 | 3±0 | 2±1 | 1±1 | 0±0 | 5±3 | 3±2 |
| | 2 | 3±0 | 3±1 | 2±2 | 2±0 | 1±0 | 1±0 | 4±2 | 4±3 |
| | 4 | 4±1 | 5±1 | 1±1 | 2±1 | 3±2 | 1±0 | 7±3 | 3±3 |
| | 6 | 4±1 | 7±3 | 3±1 | 2±1 | 3±1 | 1±1 | 4±1 | 3±1 |
| | 12 | 3±1 | 4±2 | 3±2 | 2±1 | 0±0 | 1±0 | 3±1 | 5±2 |
| 44 | 0 | 4±1 | 7±1 | 2±1 | NA | 2±0 | 1±0 | 4±1 | 6±0 |
| | 1 | 4±1 | 6±1 | 2±1 | NA | 2±0 | 2±0 | 4±1 | 5±3 |
| | 2 | 4±1 | 4±0 | 2±1 | NA | 1±0 | 1±1 | 4±1 | 5±0 |
| | 4 | 4±1 | 4±1 | 2±1 | NA | 1±0 | 2±0 | 5±2 | 4±2 |
| | 6 | 4±1 | 3±1 | 1±1 | NA | 3±1 | 4±1 | 2±1 | 5±1 |
| | 12 | 5±1 | 4±0 | 1±1 | NA | 1±1 | 1±1 | 5±1 | 5±2 |
| 48 | 0 | 5±0 | 5±1 | 0±0 | 1±1 | 1±0 | 2±0 | 4±1 | 5±2 |
| | 1 | 6±1 | 5±1 | 1±1 | 1±1 | 2±1 | 2±0 | 5±2 | 5±1 |
| | 2 | 5±0 | 5±1 | 2±1 | 0±1 | 2±0 | 2±0 | 1±0 | 19±7 |
| | 4 | 4±0 | 6±1 | 1±1 | 1±2 | 1±0 | 2±1 | 4±0 | 14±8 |
| | 6 | 6±0 | 5±1 | 1±1 | 3±1 | 3±1 | 2±0 | 4±1 | 6±1 |
| | 12 | 5±1 | 4±1 | 1±2 | 1±1 | 5±1 | 3±0 | 4±1 | 16±10 |
| 50 | 0 | 3±2 | 0±1 | 1±1 | 0±1 | 2±0 | 1±0 | NA | NA |
| | 1 | 4±2 | 4±3 | 2±1 | 1±2 | 3±0 | 2±1 | NA | NA |
| | 2 | 4±2 | 6±2 | 2±2 | 1±1 | 5±2 | 2±1 | NA | NA |
| | 4 | 2±1 | 3±3 | 1±1 | 1±1 | 4±0 | 3±0 | NA | NA |
| | 6 | 3±1 | 2±2 | 1±1 | 0±1 | 5±0 | 4±1 | NA | NA |
| | 12 | 6±1 | 5±1 | 0±1 | 0±1 | 9±2 | 4±1 | NA | NA |

Table 5.4. continued %C label

| Station | Time (h) | Citraconic acid | | Pyroglutamic acid | | Cholic acid | | Phosphoenolpyruvate | |
|---------|----------|-----------------|-----------|-------------------|-----------|-------------|-----------|---------------------|-----------|
| | | Lysate | 13C cntrl | Lysate | 13C cntrl | Lysate | 13C cntrl | Lysate | 13C cntrl |
| 2 | 0 | 2±0 | 2±0 | 2±0 | 2±0 | 6±0 | 5±2 | NA | NA |
| | 1 | 1±0 | 2±1 | 2±0 | 2±1 | 8±2 | 3±1 | NA | NA |
| | 2 | 2±0 | 2±0 | 2±1 | 2±0 | 6±2 | 5±3 | NA | NA |
| | 4 | 2±0 | 2±0 | 2±0 | 1±1 | 5±1 | 0±1 | NA | NA |
| | 6 | 2±0 | 2±0 | 1±0 | 2±1 | 4±3 | 4±3 | NA | NA |
| | 12 | 1±0 | 2±0 | 2±1 | 2±0 | 4±2 | 6±3 | NA | NA |
| 14 | 0 | 1±0 | 1±0 | 2±0 | 1±0 | 9±1 | 10±1 | NA | NA |
| | 1 | 1±0 | 1±0 | 2±0 | 2±0 | 9±1 | 10±1 | NA | NA |
| | 2 | 1±0 | 1±0 | 2±0 | 2±0 | 10±1 | 9±1 | NA | NA |
| | 4 | 1±0 | 1±0 | 3±2 | 2±0 | 9±1 | 10±1 | NA | NA |
| | 6 | 1±0 | 1±0 | 2±0 | 2±0 | 10±1 | 9±0 | NA | NA |
| | 12 | 1±0 | 1±0 | 2±0 | 2±0 | 8±0 | 10±1 | NA | NA |
| 44 | 0 | 2±0 | 1±0 | 2±0 | 2±0 | 9±1 | 9±0 | 46±9 | NA |
| | 1 | 2±1 | 2±0 | 2±0 | 5±2 | 9±0 | 9±0 | 40±16 | 21±3 |
| | 2 | 2±0 | 1±0 | 2±0 | 3±1 | 9±0 | 9±0 | 29±3 | 20±1 |
| | 4 | 1±0 | 1±0 | 2±0 | 3±1 | 9±1 | 9±0 | 39±7 | 20±9 |
| | 6 | 2±1 | 1±0 | 3±1 | 3±2 | 9±0 | 8±0 | 33±1 | 11±0 |
| | 12 | 2±1 | 2±0 | 3±0 | 5±3 | 10±0 | 8±0 | 11±9 | 34±5 |
| 48 | 0 | 2±1 | 2±0 | 2±0.8 | 2±0 | 10±1 | 10±1 | NA | 23±6 |
| | 1 | 2±1 | 2±1 | 2±0.4 | 2±0 | 9±0 | 9±0 | NA | 22±0 |
| | 2 | 2±0 | 1±1 | 3±0.9 | 3±0 | 8±1 | 9±0 | 36±13 | 36±4 |
| | 4 | 1±1 | 1±1 | 2±0.5 | 2±0 | 10±1 | 10±0 | 32±18 | 38±0 |
| | 6 | 1±0 | 2±0 | 2±0.2 | 2±1 | 8±1 | 9±0 | 38±5 | 29±5 |
| | 12 | 1±0 | 1±0 | 3±0.2 | 2±0 | 10±0 | 10±0 | 43±6 | 36±2 |
| 50 | 0 | 1±1 | 2±1 | 2±0.4 | 2±0 | 9±1 | 9±0 | NA | NA |
| | 1 | 1±1 | 1±0 | 3±0.2 | 2±0 | 8±1 | 8±1 | NA | NA |
| | 2 | 0±1 | 2±1 | 2±0.5 | 3±1 | 8±1 | 9±1 | NA | NA |
| | 4 | 1±1 | 2±1 | 2±0.5 | 2±0 | 9±0 | 9±0 | NA | NA |
| | 6 | 2±1 | 2±1 | 3±0.9 | 2±0 | 9±1 | 9±1 | NA | NA |
| | 12 | 1±2 | NA | 2±0.4 | 2±0 | 8±1 | 8±1 | NA | NA |

Table 5.5. Relative flux measurements of aspartate and guanine

| Station | Time | Aspartate N | | | Guanine N | | |
|---------|------|----------------------------|--------------------------------|----------------------------|----------------------------|--------------------------------|----------------------------|
| | | Relative pool ^a | Relative turnover ^a | Relative flux ^b | Relative pool ^a | Relative turnover ^a | Relative flux ^b |
| 2 | 0 | NA | NA | NA | NA | NA | NA |
| | 1 | NA | NA | NA | NA | NA | NA |
| | 2 | NA | NA | NA | NA | NA | NA |
| | 4 | NA | NA | NA | 6.11±0.33 | 1.62±0 | 9.93±0 |
| | 6 | NA | NA | NA | 3.08±1.68 | 1.62±0 | 5±0 |
| | 12 | NA | NA | NA | 1.20±0.29 | 1.62±0 | 1.96±0 |
| 14 | 0 | 1.50±0.82 | 1.11±0 | 1.68±0 | 1.15±0.37 | 0.93±0 | 1.08±0 |
| | 1 | 1.76±1.93 | 1.11±0 | 1.97±0 | 1.43±0.92 | 0.93±0 | 1.34±0 |
| | 2 | 1.61±1.38 | 1.11±0 | 1.8±0 | 1.35±0.91 | 0.93±0 | 1.26±0 |
| | 4 | 1.57±0.34 | 1.11±0 | 1.76±0 | 1.44±0.36 | 0.93±0 | 1.34±0 |
| | 6 | 0.94±0.10 | 1.11±0 | 1.06±0 | 0.96±0.23 | 0.93±0 | 0.9±0 |
| | 12 | 1.53±1.02 | 1.11±0 | 1.71±0 | 1.31±0.89 | 0.93±0 | 1.22±0 |
| 44 | 0 | 1.71±1.70 | 0.93±0 | 1.61±0 | 1.10±0.42 | 0.89±0 | 0.98±0 |
| | 1 | 1.27±0.37 | 0.93±0 | 1.2±0 | 0.91±0.10 | 0.89±0 | 0.81±0 |
| | 2 | 0.75±0.41 | 0.93±0 | 0.71±0 | 0.81±0.15 | 0.89±0 | 0.72±0 |
| | 4 | 0.67±0.13 | 0.93±0 | 0.63±0 | 0.58±0.11 | 0.89±0 | 0.51±0 |
| | 6 | 0.79±0.39 | 0.93±0 | 0.74±0 | 0.94±0.37 | 0.89±0 | 0.83±0 |
| | 12 | 0.66±0.19 | 0.93±0 | 0.62±0 | 0.62±0.08 | 0.89±0 | 0.55±0 |
| 48 | 0 | 0.69±0.57 | 1.22±0 | 0.85±0 | NA | NA | NA |
| | 1 | 1.24±0.37 | 1.22±0 | 1.51±0 | NA | NA | NA |
| | 2 | 1.41±0.55 | 1.22±0 | 1.73±0 | 0.95±0.06 | 1.24±0 | 1.19±0 |
| | 4 | 0.09±0.11 | 1.22±0 | 0.11±0 | 0.66±0.38 | 1.24±0 | 0.83±0 |
| | 6 | 4.60±4.20 | 1.22±0 | 5.61±0 | 1.24±0.27 | 1.24±0 | 1.55±0 |
| | 12 | 0.85±0.56 | 1.22±0 | 1.04±0 | 1.25±0.17 | 1.24±0 | 1.57±0 |
| 50 | 0 | NA | NA | NA | 0.50±0.30 | 4.09±0 | 2.05±0 |
| | 1 | NA | NA | NA | 2.46±2.74 | 4.09±0 | 10.1±0 |
| | 2 | NA | NA | NA | 0.88±0.58 | 4.09±0 | 3.63±0 |
| | 4 | NA | NA | NA | 1.82±2.18 | 4.09±0 | 7.47±0 |
| | 6 | NA | NA | NA | 0.70±0.66 | 4.09±0 | 2.87±0 |
| | 12 | NA | NA | NA | 2.35±1.47 | 4.09±0 | 9.63±0 |

^aRelative pool and turnover were calculated by dividing the measured values from the lysate amended by that of the control. ^bRelative flux was calculated as the product of the relative pool and turnover.

In each case, s.d. values were determined for measured values and then propagated through the calculations as appropriate for the mathematical operation being performed.

Table 5.6. Relative flux measurements of malate

| Malate C | | | | | |
|-----------------|-------------|----------------------------------|--------------------------------------|----------------------------------|-------|
| Station | Time | Relative pool^a | Relative turnover^a | Relative flux^b | |
| 44 | 0 | 2.24±2.04 | 9±0 | 20.24±0 | |
| | 1 | 0.66±0.16 | 9±0 | 6±0 | |
| | 2 | 0.69±0.05 | 9±0 | 6.27±0 | |
| | 4 | 0.28±0.13 | 9±0 | 2.57±0 | |
| | 6 | 0.75±0.26 | 9±0 | 6.82±0 | |
| | 12 | 0.45±0.15 | 9±0 | 4.12±0 | |
| | 48 | 0 | 0.33±0.33 | 0.62±0 | 0.2±0 |
| 1 | | 0.88±0.76 | 0.62±0 | 0.55±0 | |
| 2 | | 1.56±1.43 | 0.62±0 | 0.98±0 | |
| 4 | | 0.36±0.47 | 0.62±0 | 0.22±0 | |
| 6 | | 0.60±0.04 | 0.62±0 | 0.38±0 | |
| 12 | | 1.60±0.44 | 0.62±0 | 1±0 | |
| 50 | | 0 | 1.40±0.60 | 5.4±0 | 7.6±0 |
| | 1 | 0.57±0.50 | 5.4±0 | 3.09±0 | |
| | 2 | 0.42±0.50 | 5.4±0 | 2.32±0 | |
| | 4 | 1.95±1.73 | 5.4±0 | 10.6±0 | |
| | 6 | 1.25±0.67 | 5.4±0 | 6.79±0 | |
| | 12 | NA | NA | NA | |

^aRelative pool and turnover were calculated by dividing the measured values from the lysate amended by that of the control. ^bRelative flux was calculated as the product of the relative pool and turnover.

In each case, s.d. values were determined for measured values and then propagated through the calculations as appropriate for the mathematical operation being performed.

Table 5.7. Relative flux measurements of glutamate N and C

| Station | Time | Glutamate N | | | Glutamate C | | |
|---------|------|----------------------------|--------------------------------|----------------------------|----------------------------|--------------------------------|----------------------------|
| | | Relative pool ^a | Relative turnover ^a | Relative flux ^b | Relative pool ^a | Relative turnover ^a | Relative flux ^b |
| 2 | 0 | 1.61±0.07 | 1.67±0 | 2.7±0 | 0.35±0.61 | 4.46±0 | 1.57±0 |
| | 1 | 0.41±0.59 | 1.67±0 | 0.7±0 | 0.52±0.14 | 4.46±0 | 2.34±0 |
| | 2 | 0.87±0.77 | 1.67±0 | 1.46±0 | 1.11±1.22 | 4.46±0 | 4.97±0 |
| | 4 | 0.90±0.21 | 1.67±0 | 1.52±0 | 0.79±0.41 | 4.46±0 | 3.57±0 |
| | 6 | 1.22±0.08 | 1.67±0 | 2.04±0 | 0.63±0.10 | 4.46±0 | 2.82±0 |
| | 12 | 0.84±0.20 | 1.67±0 | 1.42±0 | 0.68±0.14 | 4.46±0 | 3.07±0 |
| 14 | 0 | 1.20±0.57 | 1.21±0 | 1.45±0 | 1.53±0.88 | 2.56±0 | 3.94±0 |
| | 1 | 1.39±1.02 | 1.21±0 | 1.68±0 | 1.66±1.21 | 2.56±0 | 4.27±0 |
| | 2 | 1.65±0.88 | 1.21±0 | 2±0 | 0.99±0.22 | 2.56±0 | 2.55±0 |
| | 4 | 1.85±0.33 | 1.21±0 | 2.24±0 | 0.75±0.46 | 2.56±0 | 1.94±0 |
| | 6 | 1.11±0.32 | 1.21±0 | 1.35±0 | 1.43±0.90 | 2.56±0 | 3.68±0 |
| | 12 | 1.48±0.93 | 1.21±0 | 1.8±0 | 0.68±0.22 | 2.56±0 | 1.76±0 |
| 44 | 0 | 0.79±0.25 | 0.94±0 | 0.75±0 | 0.37±0.10 | 2.31±0 | 0.85±0 |
| | 1 | 1.13±0.06 | 0.94±0 | 1.07±0 | 0.19±0.07 | 2.31±0 | 0.46±0 |
| | 2 | 0.94±0.25 | 0.94±0 | 0.89±0 | 0.43±0.27 | 2.31±0 | 0.99±0 |
| | 4 | 0.62±0.14 | 0.94±0 | 0.59±0 | 0.29±0.13 | 2.31±0 | 0.68±0 |
| | 6 | 0.67±0.35 | 0.94±0 | 0.63±0 | 0.41±0.17 | 2.31±0 | 0.97±0 |
| | 12 | 0.40±0.09 | 0.94±0 | 0.38±0 | 0.51±0.11 | 2.31±0 | 1.18±0 |
| 48 | 0 | 0.67±0.16 | 1.12±0 | 0.75±0 | 0.50±0.09 | 4.53±0 | 2.26±0 |
| | 1 | 0.72±0.29 | 1.12±0 | 0.8±0 | 0.51±0.16 | 4.53±0 | 2.32±0 |
| | 2 | 1.04±0.36 | 1.12±0 | 1.17±0 | 0.56±0.20 | 4.53±0 | 2.55±0 |
| | 4 | 0.47±0.16 | 1.12±0 | 0.53±0 | 0.57±0.36 | 4.53±0 | 2.58±0 |
| | 6 | 1.14±0.28 | 1.12±0 | 1.28±0 | 0.86±0.59 | 4.53±0 | 3.9±0 |
| | 12 | 1.02±0.32 | 1.12±0 | 1.15±0 | 1.38±0.44 | 4.53±0 | 6.29±0 |
| 50 | 0 | 0.79±0.11 | 1.09±0 | 0.86±0 | 0.84±0.05 | 3.01±0 | 2.55±0 |
| | 1 | 1.23±0.57 | 1.09±0 | 1.35±0 | 0.71±0.44 | 3.01±0 | 2.15±0 |
| | 2 | 1.02±0.60 | 1.09±0 | 1.12±0 | 0.79±0.22 | 3.01±0 | 2.39±0 |
| | 4 | 1.16±0.79 | 1.09±0 | 1.27±0 | 1.11±0.29 | 3.01±0 | 3.36±0 |
| | 6 | 0.73±0.64 | 1.09±0 | 0.8±0 | 0.89±0.11 | 3.01±0 | 2.7±0 |
| | 12 | 1.02±0.21 | 1.09±0 | 1.12±0 | 1.20±0.49 | 3.01±0 | 3.63±0 |

^aRelative pool and turnover were calculated by dividing the measured values from the lysate amended by that of the control. ^bRelative flux was calculated as the product of the relative pool and turnover.

In each case, s.d. values were determined for measured values and then propagated through the calculations as appropriate for the mathematical operation being performed.

Figures

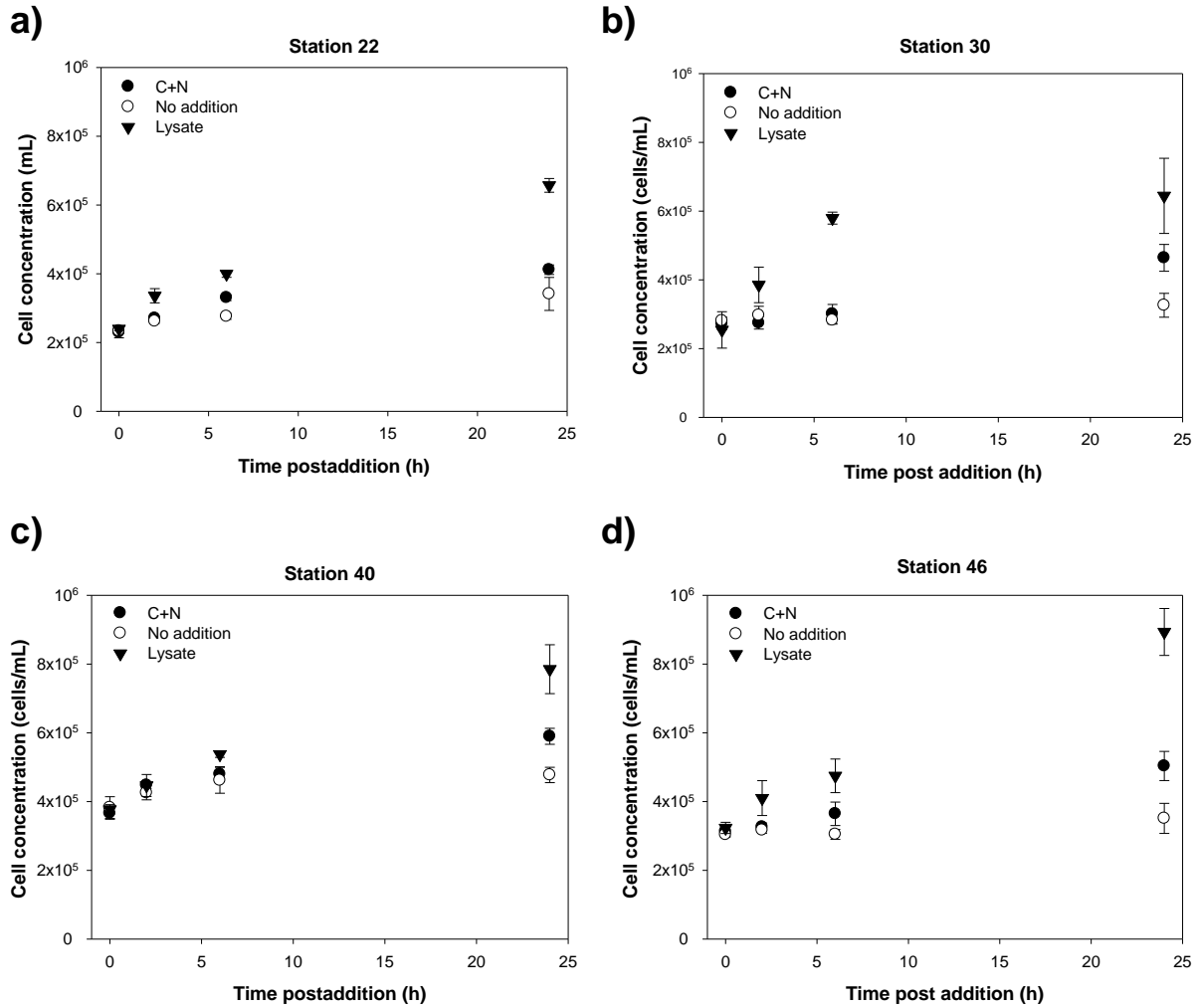


Figure 5.1. Changes in microbial abundance at each sampling station. Cell counts were determined by flow cytometry. Values reflect the average of triplicate biological replicates. Error bars represent the standard error of the mean and are obscured by the data markers, in some cases.

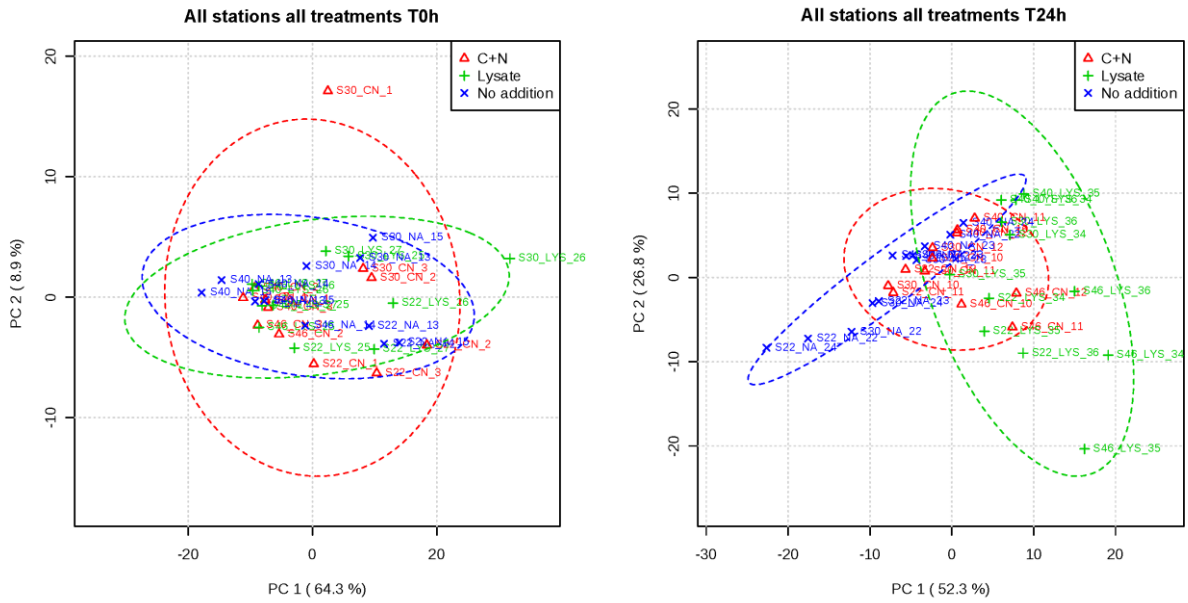


Figure 5.2. Principal component analysis (PCA) scores plots of community metabolite profiles for all treatments at 0 and 24 h of incubation. Metabolite ion counts were normalized to cell counts. Circles represent 95% confidence region. Sample key: (station number_treatment_sample ID). ‘C+ N’ = C+N amended, ‘LYS’ = lysate amended, ‘NA’ = No addition controls.

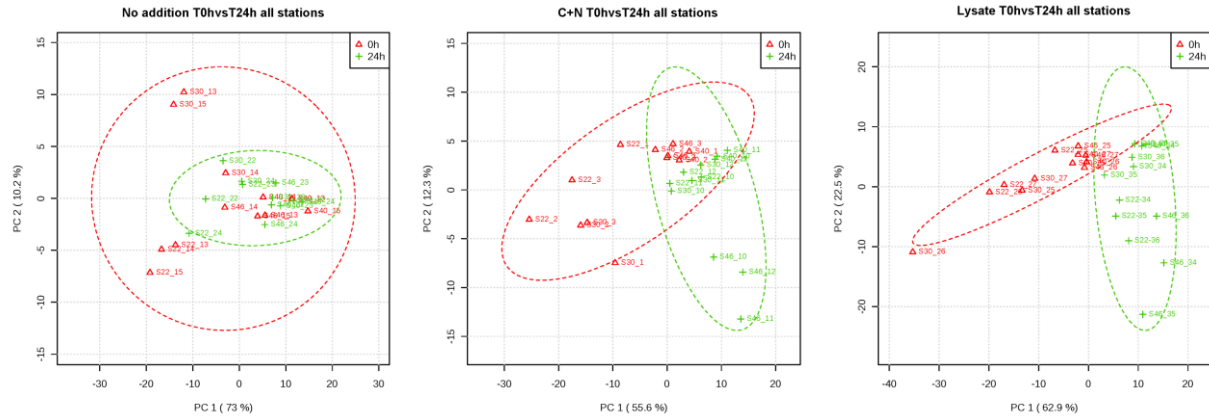


Figure 5.3. Principal component analysis (PCA) scores plots of community metabolite profiles displaying variation within treatments at 0 and 24 h of sample collection. Metabolite ion counts were normalized to cell counts. Circles represent 95% confidence region. Sample key: (station number_sample ID).

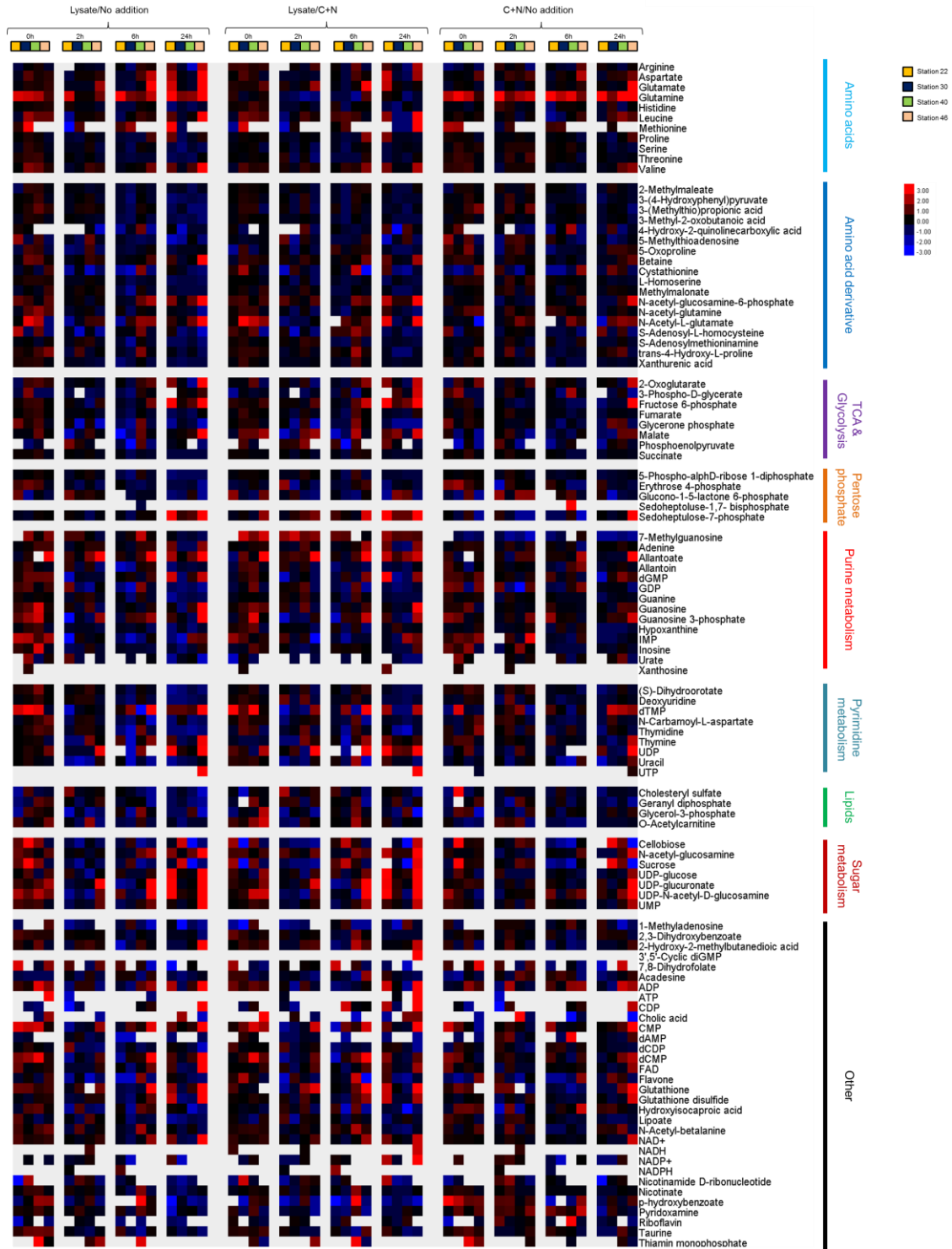


Figure 5.4. Heatmap of intracellular metabolites of nutrient amended and non-amended microbial communities. Metabolite concentrations are normalized to bacterial cell number and expressed relative to levels measured in the amended and non-amended communities at the corresponding time point. Ratios are log₂ transformed. Increases in intracellular metabolite concentrations are shown in red and decrease in blue. Columns correspond to hours post amendment, rows represent specific metabolites. Values are averages of triplicate biological replicates.

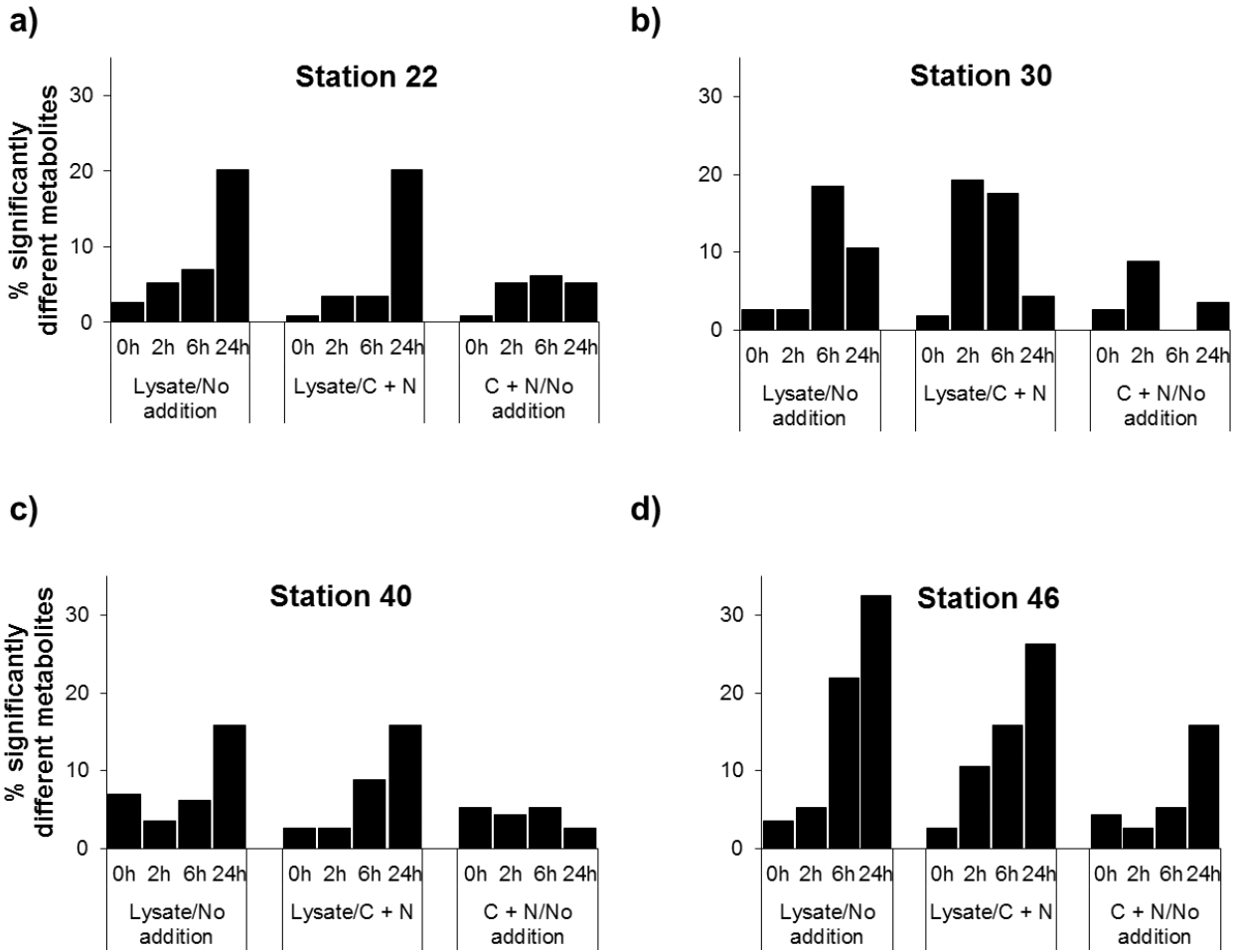
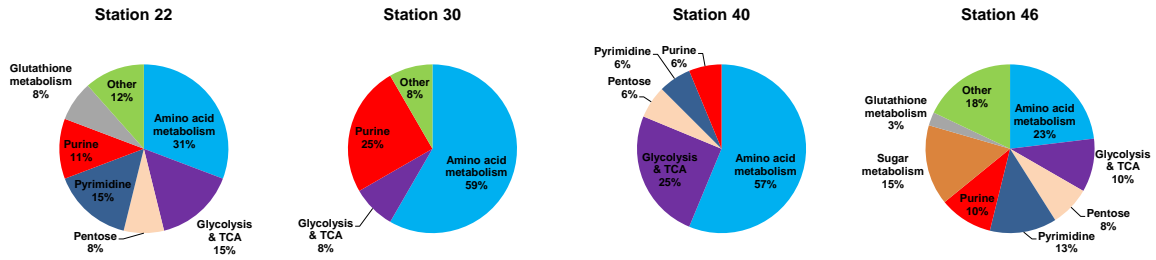


Figure 5.5. Variation in intracellular metabolite concentrations between lysate amended and C+N amended populations during the 24h incubation period shown in Figure 2. Fold changes are relative to metabolite concentration levels measured in the unamended and C+N amended communities. Fold changes are calculated from averages of three biological replicates. Significance is defined as fold changes ≥ 1.5 and $p \leq 0.05$.

a



b

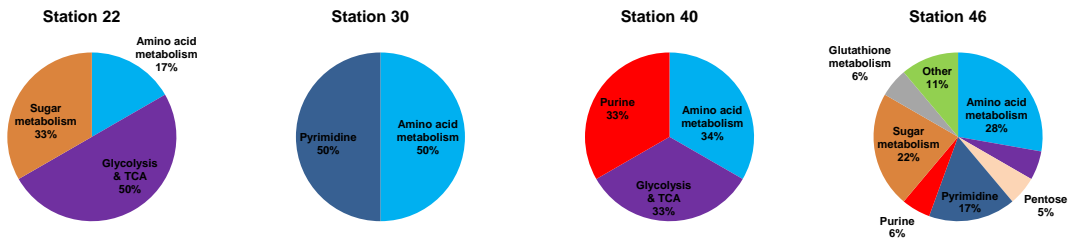


Figure 5. 6. Metabolic pathways significantly altered in (a) lysate amended communities (b) C+N amended communities. Significance is defined as fold changes ≥ 1.5 and $p \leq 0.05$.

Malate ^{13}C incorporation

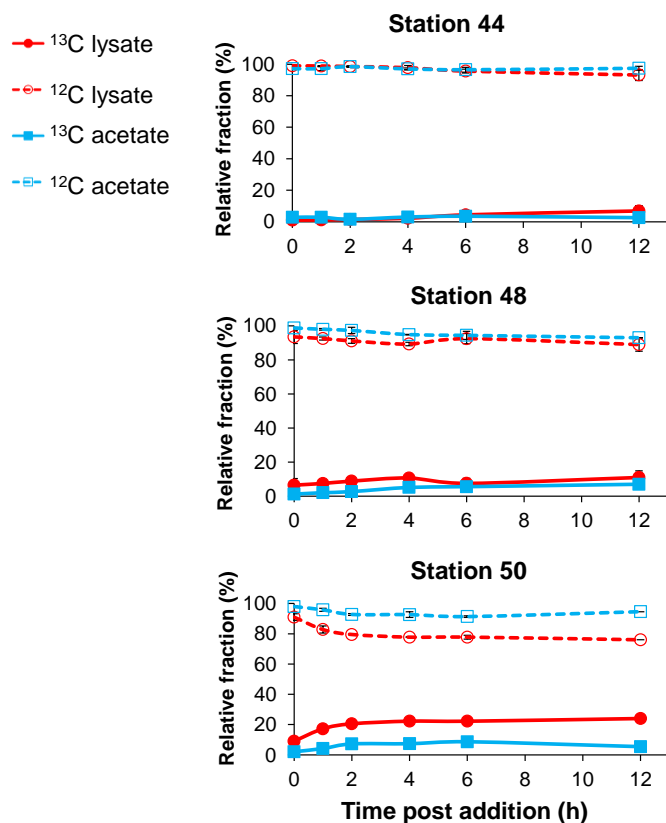


Figure 5.7. Incorporation of ^{13}C label into bacterioplankton community malate pools. The graphs show the disappearance of unlabeled metabolites for lysate amended and control populations as well as the appearance of fully ^{13}C -labeled metabolites in lysate amended and control populations. Error bars represent the standard error of the mean and are obscured by the data markers, in some cases.

Guanine ¹⁵N incorporation

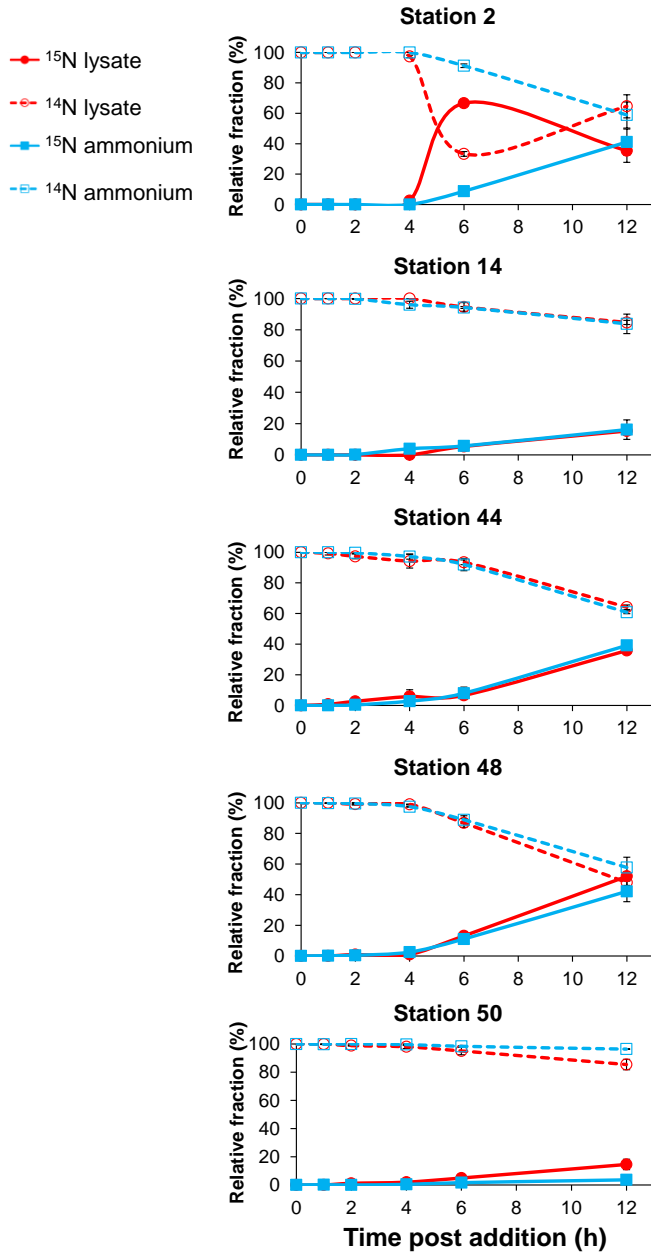


Figure 5.8. Incorporation of ¹⁵N label into bacterioplankton community guanine pools. The graphs show the disappearance of unlabeled metabolites for lysate amended and control populations as well as the appearance of fully ¹⁵N -labeled metabolites in lysate amended and control populations. Error bars represent the standard error of the mean and are obscured by the data markers, in some cases.

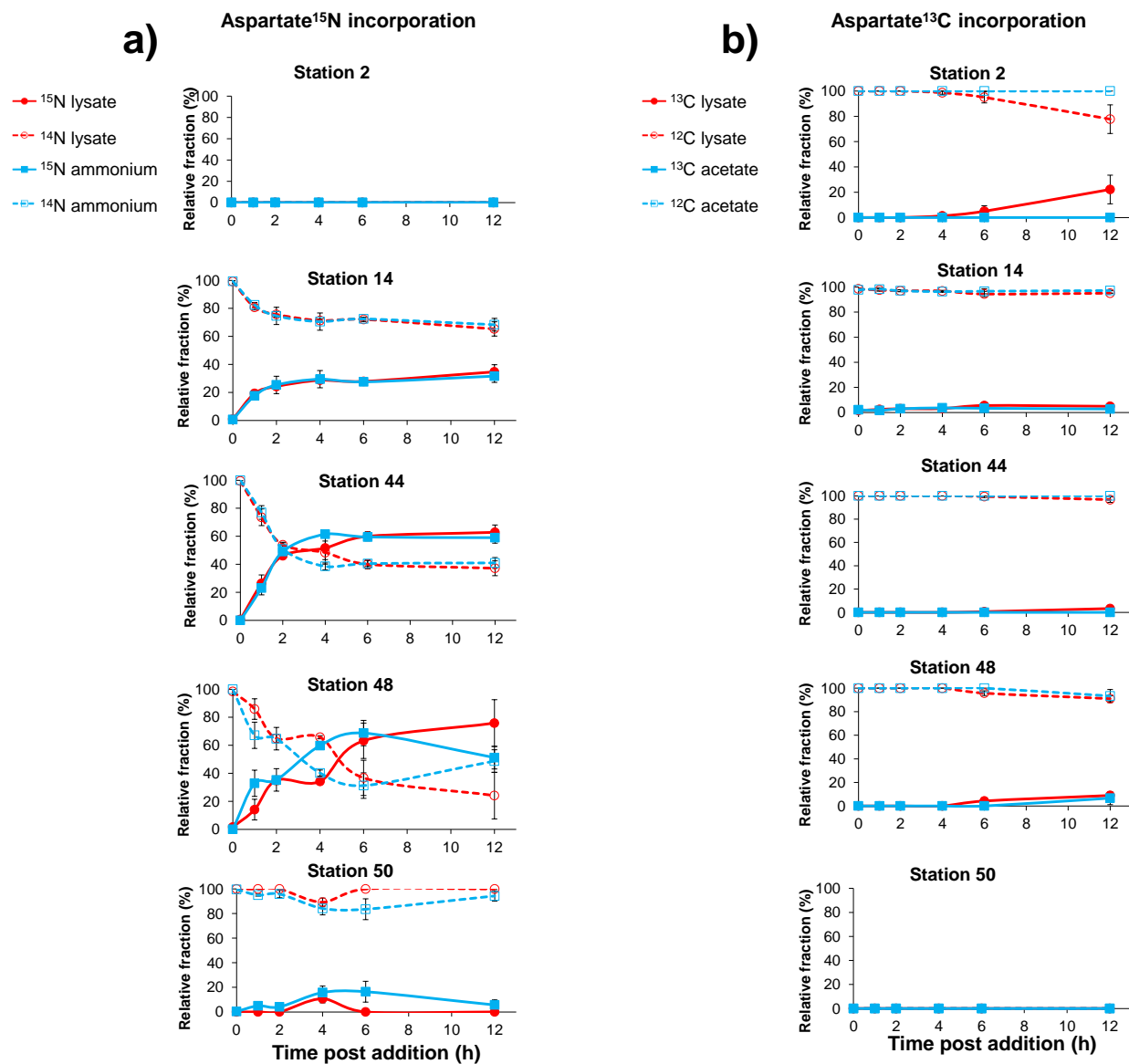


Figure 5.9. Incorporation of (a) ¹⁵N and (b) ¹³C label into bacterioplankton community aspartate pools. The graphs show the disappearance of unlabeled metabolites for lysate amended and control populations as well as the appearance of fully ¹⁵N and ¹³C-labeled metabolites in lysate amended and control populations. Error bars represent the standard error of the mean and are obscured by the data markers, in some cases.

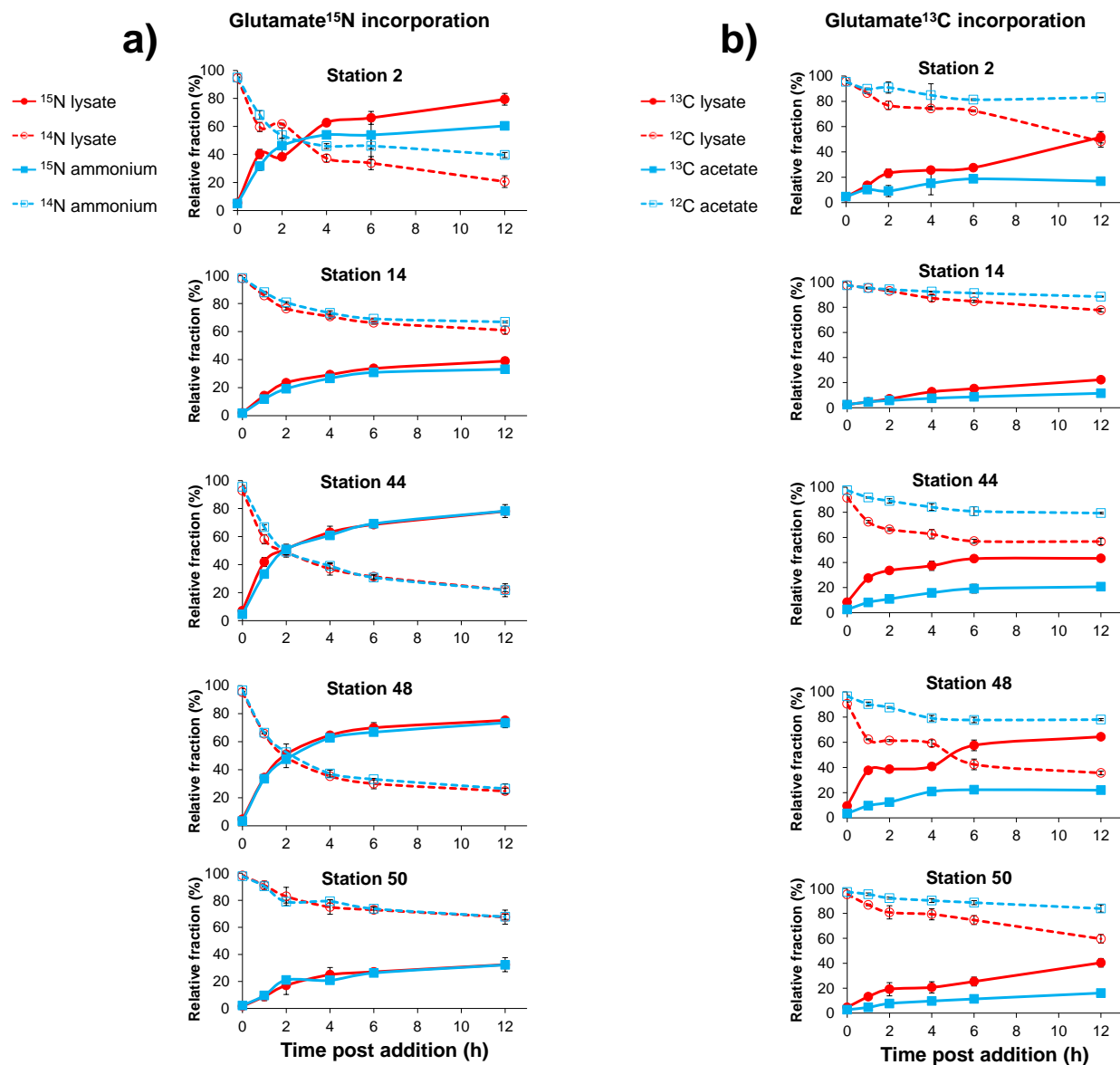


Figure 5.10. Incorporation of (a) ^{15}N and (b) ^{13}C label into bacterioplankton community glutamate pools. The graphs show the disappearance of unlabeled metabolites for lysate amended and control populations as well as the appearance of fully ^{15}N and ^{13}C -labeled metabolites in lysate amended and control populations. Error bars represent the standard error of the mean and are obscured by the data markers, in some cases.

Chapter 6

Conclusions

Viruses are an important component of aquatic food webs that contribute significantly to the mortality of marine microorganisms and consequently alter species composition and influence the flow of carbon, nitrogen and other nutrients within an ecosystem (Breitbart 2012, Suttle 2007, Weitz and Wilhelm 2012). Despite the growing recognition of the impact of viral activity on marine biogeochemical cycles and regulating microbial species composition, other aspects of viral activity in natural systems, such as the extent to which virus infection reshapes host metabolism and the uptake and metabolism of virus lysis material by natural bacterioplankton communities, remain poorly understood. For this dissertation, we developed a model host-phage system using the bacterium *Sulfitobacter* sp. 2047 and its infecting phages, Φ CB2047-A and Φ CB2047-B, to gain insights into the effect virus infections have on host cell metabolism and the quality of dissolved organic matter released upon virus-mediated cell lysis. Additionally, we tracked the uptake and metabolism of viral lysis products by bacterioplankton communities to gain insights into the fate of virus lysis products in natural systems.

Prior to examining the effect of virus infection on host metabolism and lysate quality, a genomic analysis of *Sulfitobacter* sp. 2047 revealed it was lysogenized by a prophage (Φ NYA). With no previous study documenting the effect of superinfection (infection of an already infected cell with another phage) on *Roseobacter* lysogens it was essential to better characterize my host-phage system before embarking on any further studies. This detour provided valuable insights into the biological factors that affect prophage conversion and the transfer of genetic material in the marine environment. From this study, we showed that superinfection of *Sulfitobacter* lysogens significantly increases resident prophage induction by as much as 24-fold. We also provided data suggestive of a RecA-mediated role in *Sulfitobacter* prophage induction, however, we did not provide conclusive evidence to support this observation. Future studies using

superinfected *Sulfitobacter* *lexA* and *recA* mutants and measuring changes in LexA and RecA protein concentration will provide conclusive experimental evidence for the mechanism of prophage induction in *Sulfitobacter* lysogens. Furthermore, my induction studies did not include assays to characterize potential growth costs associated with the establishment of lysogeny in *Sulfitobacter* strains. Experiments growing *Sulfitobacter* lysogens on various minimal and rich media across a temperature gradient will help address this issue.

In Chapter 4, we examined the extent to which virus infection reshapes host cell metabolism and the effect of this alteration on cellular organic matter released following viral lysis. Prior to this study, very few studies had investigated the effects of virus infection on environmentally relevant marine host-phage systems (e.g., Wikner *et al.* 1993) and most of our knowledge on how virus infection reshapes host metabolism were adapted from studies using *E. coli* as a model organism (e.g., Calendar 2006, Kazmierczak and Rothman-Denes 2006, Miller *et al.* 2003, Poranen *et al.* 2006, Putnam *et al.* 1952). We also knew very little on the quality of material released upon virus-mediated cell lysis and how this material influences natural bacterioplankton metabolism and ocean biogeochemistry. Most studies on this topic only characterize bulk properties or specific compound classes found in virus lysates (Bratbak *et al.* 1998, Brussaard *et al.* 2008, Gobler *et al.* 1997, Haaber and Middelboe 2009, Lønborg *et al.* 2013, Middelboe and Lyck 2002, Riemann and Middelboe 2002, Shelford *et al.* 2012, Shelford *et al.* 2014). My study provided a more qualitative and quantitative description of the material found in virus derived lysates from an environmentally relevant clade of marine bacteria and provided a framework and the necessary methodology for similar studies to be undertaken in other relevant marine host-phage models. Although we use an environmentally relevant host-phage model in this study, we do not provide relevant controls to discriminate between prophage,

Φ NYA, and superinfecting phage, Φ CB2047-B, contributions in altering host metabolism. A similar study using a *Sulfitobacter* non-lysogen as a host organism may help clarify this issue. However, it is also important to note that with an estimated 50% of marine bacterial isolates known to contain prophages (Paul 2008), the host-phage system used in this study and the complexity of this infection process may actually be reflective of events that are common in nature.

Finally, in Chapter 5, we monitored the uptake and metabolism of virus derived organic matter in marine surface water microbial communities by comparing the uptake and metabolism of viral lysates at various sampling locations in the North Pacific. Prior to this study, efforts to characterize the effect virus DOM on bacterioplankton communities in natural systems mostly focused on the impact of virus lysates on natural bacterioplankton abundance and diversity or monitored the uptake and/or metabolism of bulk virus DOM by tracking specific elements, principally total C, N and P, or measured uptake rates of certain compound classes, e.g. amino acids (Haaber and Middelboe 2009, Middelboe *et al.* 2003, Sheik *et al.* 2013, Shelford *et al.* 2014). These prior studies, though very informative, did not provide a global assessment of the impact of virus activity on natural bacterioplankton metabolism and were mostly performed at single locations without acknowledging the impact environmental parameters such as temperature and nutrient availability may have on virus lysate metabolism. Measuring the uptake and metabolism of viral lysates across various temperature gradients and nutrient regimes is essential to accurately create models to help us to predict how changes in environmental conditions will affect the metabolism of viral lysates by natural bacterioplankton communities and how these alterations in community metabolism will affect ecosystem function. To that end, we monitored global metabolic changes and nutrient turnover in natural bacterioplankton

communities amended with virus lysates across various temperature and nutrient gradients at nine locations in the North Pacific. While the data from my study provides detail on the overall metabolism and specific biochemical pathways involved in the transformation of viral lysis-derived cellular components by bacterioplankton populations under different temperature and nutrient regimes, the variability in community species composition associated with each sampling station presented a challenge in my attempts to decipher the role environmental factors, such as temperature and nutrient availability, have on virus lysate metabolism. Future studies using microbial communities with similar species composition (ideally from the same site) incubated under different temperature and nutrient gradients will further help clarify the effects physical factors have on the metabolism of viral lysates in natural bacterioplankton communities.

References

- Bratbak G, Jacobsen A, Heldal M (1998). Viral lysis of *Phaeocystis pouchetii* and bacterial secondary production. *Aquatic microbial ecology* **16**: 11-16.
- Breitbart M (2012). Marine viruses: truth or dare. *Annual Review of Marine Science* **4**: 425-448.
- Brussaard CPD, Wilhelm SW, Thingstad F, Weinbauer MG, Bratbak G, Heldal M *et al.* (2008). Global-scale processes with a nanoscale drive: the role of marine viruses. *ISME J* **2**: 575-578.
- Buchan A, Gonzalez JM, Moran MA (2005). Overview of the marine Roseobacter lineage. *Applied and Environmental Microbiology* **71**: 5665-5677.
- Buchan A, LeCleir GR, Gulvik CA, Gonzalez JM (2014). Master recyclers: features and functions of bacteria associated with phytoplankton blooms. *Nat Rev Micro* **12**: 686-698.
- Calendar R (2006). *The Bacteriophages*. Oxford University Press: New York.
- Gobler CJ, Hutchins DA, Fisher NS, Cosper EM, Sanudo-Wilhelmy SA (1997). Release and bioavailability of C, N, P, Se, and Fe following viral lysis of a marine chrysophyte. *Limnology and Oceanography*: 1492-1504.
- Haaber J, Middelboe M (2009). Viral lysis of *Phaeocystis pouchetii*: implications for algal population dynamics and heterotrophic C, N and P cycling. *The ISME journal* **3**: 430-441.
- Kazmierczak KM, Rothman-Denes LB (2006). Bacteriophage N4. In: Calendar R (ed). *The Bacteriophages*. Oxford University Press: New York. pp 302-314.

- Lønborg C, Middelboe M, Brussaard CP (2013). Viral lysis of *Micromonas pusilla*: impacts on dissolved organic matter production and composition. *Biogeochemistry* **116**: 231-240.
- Middelboe M, Lyck PG (2002). Regeneration of dissolved organic matter by viral lysis in marine microbial communities. *Aquatic Microbial Ecology* **27**: 187-194.
- Miller ES, Kutter E, Mosig G, Arisaka F, Kunisawa T, Ruger W (2003). Bacteriophage T4 genome. *Microbiology and Molecular Biology Reviews* **67**: 86-+.
- Poranen MM, Ravantti JJ, Grahn AM, Gupta R, Auvinen P, Bamford DH (2006). Global changes in cellular gene expression during bacteriophage PRD1 infection. *J Virol* **80**: 8081-8088.
- Putnam FW, Miller D, Palm L, Evans EA (1952). Biochemical studies of virus reproduction X Precursors of bacteriophage T7. *Journal of Biological Chemistry* **199**: 177-191.
- Riemann L, Middelboe M (2002). Viral lysis of marine bacterioplankton: Implications for organic matter cycling and bacterial clonal composition. *Ophelia* **56**: 57-68.
- Sheik AR, Brussaard CP, Lavik G, Lam P, Musat N, Krupke A *et al.* (2013). Responses of the coastal bacterial community to viral infection of the algae *Phaeocystis globosa*. *The ISME journal*.
- Shelford EJ, Middelboe M, Møller EF, Suttle CA (2012). Virus-driven nitrogen cycling enhances phytoplankton growth. *Aquatic Microbial Ecology* **66**: 41-46.
- Shelford EJ, Jørgensen NO, Rasmussen S, Suttle CA, Middelboe M (2014). Dissecting the role of viruses in marine nutrient cycling: bacterial uptake of D- and L-amino acids released by viral lysis. *Aquatic Microbial Ecology* **73**.

- Suttle CA (1994). The significance of viruses to mortality in aquatic microbial communities. *Microbial Ecology* **28**: 237-243.
- Suttle CA (2007). Marine viruses—major players in the global ecosystem. *Nature Reviews Microbiology* **5**: 801-812.
- Weitz JS, Wilhelm SW (2012). Ocean viruses and their effects on microbial communities and biogeochemical cycles. *FI000 biology reports* **4**.
- Wikner J, Vallino JJ, Steward GF, Smith DC, Azam F (1993). Nucleic acids from the host bacterium as a major source of nucleotides for three marine bacteriophages. *FEMS microbiology ecology* **12**: 237-248.

Vita

Nana Y.K. Ankrah was born in Accra, Ghana. He attended Achimota High School where he graduated in 2003. After graduation from high school, Nana worked as a production assistant for a local TV station, a job he dearly enjoyed since it exposed him new techniques in photography, videography and stage setting; of course the free food on set and meeting local celebrities as part of the job didn't hurt either. After working a few months in this overly awesome job, Nana enrolled at the University of Ghana to pursue a degree in Biological Sciences. He graduated *summa cum laude* with a Bachelor of Science degree with a focus in Oceanography and Fisheries in 2008. While in college, Nana volunteered on a couple of Earthwatch Institute conservation projects and also did internships on commercial and research fish farms, both experiences he enjoyed immensely. After graduating from college, and while applying to graduate school programs, Nana worked for a local conservation group, Nature Conservation Research Council, as a research assistant on various conservation projects ranging from manatee conservation projects to cocoa farming and biodiversity projects, all of which, again, he enjoyed immensely. Nana enrolled in the Microbiology doctoral program at the University of Tennessee where he received his Ph.D. in May 2015.